



---

National Technical University of Athens  
School of Naval Architecture and Marine engineering  
Division of Marine Structures  
Shipbuilding Technology laboratory

Diploma Thesis

Structural optimization of stiffened panels found in ship  
structures by employing Genetic Algorithms and FEA

Panagiotis Sakkoulis

Thesis supervisor: Konstantinos N. Anyfantis, Assistant professor

ATHENS, FEBRUARY 2022

This page has been intentionally left blank.

## **Acknowledgements**

The elaboration and presentation of this thesis mark the end of my studies at the school of Naval Architecture and Marine Engineering of NTUA. This academic journey has offered me many experiences and life lessons which have sculpted my way of thinking and have influenced my approach to life in general. At the same time a new chapter starts in my life, which could not find me more driven and content. As this is the last page I am writing for the elaboration of my thesis, I feel the need to warmly thank those who contributed substantially and morally to its completion.

First of all, I would like to express my gratitude towards my thesis supervisor, Assistant Professor of NTUA, Mr. Konstantinos Anyfantis who gave me the opportunity to deal with an extremely interesting topic. Without his scientific guidance, support and direction the completion of this work would not have been possible. His knowledge on the subject, which he generously imparted to me, as well as his insightful feedback pushed me to sharpen my thinking and brought my work to a higher level. But most importantly, his patience and willingness to provide assistance at all times proved invaluable during the course of this thesis.

I would also like to thank the PhD candidate Nikolaos Silionis for his assistance at crucial times and also for his insight in ANSYS, without which the completion of this dissertation would be much harder. I will never forget our fruitful conversations about science and real life.

To my family, for their unconditional support throughout my studies, for their patience and belief in me, I extend my deepest thanks. Without their tremendous understanding and encouragement, it would be impossible for me to complete this undertaking.

Finally, I would like to thank all my friends, who supported me but also provided stimulating discussions as well as happy distractions to rest my mind during this journey.

## Περίληψη

Η ανθρωπότητα πάντα αναζητεί την καλύτερη δυνατή λύση προκειμένου να λύσει τα προβλήματά της, με απώτερο σκοπό να εξοικονομήσει διαθέσιμους πόρους, χρόνο ή συνολικά να βελτιώσει την ποιότητα ζωής της. Σε αυτό το πλαίσιο, εφαρμόζεται η βελτιστοποίηση κατασκευών, στόχος της οποίας είναι να κάνει ένα σύνολο υλικών να υποστηρίξει φορτία με το βέλτιστο τρόπο· όπου ο όρος ‘βέλτιστος’ μεταφράζεται διαφορετικά ανάλογα με το κάθε πρόβλημα. Η διπλωματική αυτή εργασία αντλεί έμπνευση από αυτήν την ιδέα και στοχεύει να παράσχει μια αρχική εναλλακτική προσέγγιση για το σχεδιασμό ενισχυμένων ελασμάτων που χρησιμοποιούνται συχνά σε ναυπηγικές κατασκευές.

Ο στόχος του σχεδιασμού ενός συνόλου δομικών μελών με τον καλύτερο τρόπο συνοψίζεται τελικά στη μεγιστοποίηση ή την ελαχιστοποίηση μιας ή περισσοτέρων μεταβλητών, που περιγράφουν το πρόβλημα με σαφήνεια. Σε αυτή την εργασία, ο κύριος στόχος είναι να αναπτυχθεί μια αλγοριθμική διαδικασία, η οποία θα βρίσκει τον καλύτερο δυνατό σχεδιασμό για ένα ενισχυμένο έλασμα ελαχιστοποιώντας τη μάζα του ενώ παράλληλα πληρούνται συγκεκριμένα κριτήρια αντοχής. Τα αρχικά διαθέσιμα δεδομένα για αυτό το πρόβλημα βελτιστοποίησης θα είναι η φόρτιση του ελάσματος καθώς και το μήκος των δύο πλευρών του.

Αρχικά, χρησιμοποιώντας το εμπορικό λογισμικό ANSYS 19.2 αναπτύχθηκε ένα μοντέλο πεπερασμένων στοιχείων ενός ενισχυμένου ελάσματος, ως προαπαιτούμενο βήμα πριν από την εισαγωγή των αποτελεσμάτων στο βελτιστοποιητή, που παρέχεται από το ANSYS Workbench 19.2. Όσον αφορά στη μέθοδο βελτιστοποίησης, που επιλέχθηκε, λόγω της διακριτής φύσης του προβλήματος, αναπόφευκτα εφαρμόστηκε μια μεταερευτική μέθοδος και συγκεκριμένα οι Γενετικοί Αλγόριθμοι. Τέλος, οι καλύτερες λύσεις, τις οποίες έδωσε ο βελτιστοποιητής, επιθεωρήθηκαν οπτικά μέσω του εικονικού περιβάλλοντος του ANSYS και εξήχθησαν μερικά συμπεράσματα σχετικά με τα μοτίβα των αποτελεσμάτων.

## **Abstract**

Humanity always seeks for the best available solution to solve its problems, with the ultimate purpose to save available resources, time or all in all improve its quality of life. Within this scope, structural optimization is applied, whose goal is to make an assemblage of materials sustain loads in the best way; where the term best is translated differently according to each individual problem. This thesis draws inspiration from this concept and aims to provide an initial alternative approach for designing stiffened panels which are often found in naval structures.

The objective of designing a set of structural members in the best way eventually summarizes into maximizing or minimizing one or more variables which describe the problem clearly. In this work, the main objective is to develop an algorithmic process that will find the best possible design for a cross stiffened panel by minimizing its mass while meeting specified strength criteria. The initial available data for this optimization problem will be the loading and the length of the two sides of the panel.

Firstly, using the commercial FE software ANSYS 19.2, a FE model of a cross stiffened panel was developed, as a necessary step before entering the results into the optimizer provided by ANSYS Workbench 19.2. As for the optimization method chosen, due to the discrete nature of the problem at hand, a metaheuristic method and specifically Genetic Algorithms was inevitably implemented. Finally, the best solutions provided by the optimizer, were visually inspected through the virtual environment of ANSYS and several conclusions regarding the patterns of the results were drawn.

This page has been intentionally left blank.

# Table of Contents

<b>List of figures.....</b>	<b>8</b>
<b>List of tables.....</b>	<b>11</b>
<b>1 Introduction.....</b>	<b>13</b>
1.1 Structural Optimization in Shipbuilding .....	13
1.2 Stiffened panels.....	15
1.3 Thesis structure .....	18
<b>2 Theoretical Background.....</b>	<b>19</b>
2.1 Introduction.....	19
2.2 Basic Concepts of Finite Element Analysis .....	19
2.2.1 The Finite Element Method .....	19
2.2.2 Subdivision of the structure .....	20
2.2.3 Finite Elements used in this work .....	23
2.2.4 Model Verification and Validation .....	26
2.3 Structural Optimization: An overview .....	28
2.3.1 Basic Concepts of Optimization.....	28
2.3.2 Fundamental Concepts of Structural Optimization.....	31
2.4 Genetic Algorithms: An overview .....	34
<b>3 Development of the FE model.....</b>	<b>45</b>
3.1 Introduction.....	45
3.2 Panels modeled and loading scenarios.....	45
3.3 The FE model.....	52
3.4 Algorithmic Process.....	56
<b>4 Indicative results .....</b>	<b>61</b>
4.1 Introduction.....	61
4.2 Results presentation .....	61
<b>5 Conclusions and Future Work.....</b>	<b>88</b>
5.1 Conclusions.....	88
5.2 Suggestions for Future works .....	89
<b>6 References.....</b>	<b>90</b>

## List of figures

Figure 1.1 Variety of solutions towards decarbonization of international shipping .....	14
Figure 1.2: Simplest form of a cross-stiffened panel .....	15
Figure 1.3: Inside of a fuselage .....	16
Figure 1.4: Typical cross-sections of stiffeners .....	16
Figure 1.5: Buckling failure modes for stiffened panels .....	17
Figure 2.1 Beam modeled by 9-node Rectangular Elements .....	20
Figure 2.2 Two-dimensional model of a gear tooth comprised of triangular elements .....	21
Figure 2.3 Nodal displacements of CST element .....	22
Figure 2.4 Representation of a beam element with given geometrical properties. ....	23
Figure 2.5: 2-node beam element and Typical Nodal Degrees of Freedom. ....	24
Figure 2.6: Basic shell element with local six degrees of freedom at a node .....	25
Figure 2.7: (a) A 20-node isoparametric solid element. (b) Reduction to an 8-node shell element. (c) DOF's at node b. ....	26
Figure 2.8: Mesh grading near the point of application of a concentrated load .....	27
Figure 2.9: Equivalent nodal point loads. ....	27
Figure 2.10: Representation of the decision variable space and the corresponding objective space. ...	30
Figure 2.11: Structural Optimization problem. Find the structure which best transmits the load F to the support. ....	31
Figure 2.12: A sizing structural optimization problem. Change in the size of the cross-sectional area of truss members can be observed. ....	32
Figure 2.13: A shape optimization problem. Find the function $\eta(x)$ , describing the shape of the beam-like structure. ....	33
Figure 2.14: Topology optimization of a truss. Bars are removed by letting cross-sectional areas take the value zero. ....	33
Figure 2.15: Two-dimensional topology optimization. The box in the above picture is to be filled 50% by material and the question is what is the proper material distribution for optimal performance under loads and boundary conditions. The result is shown in the 2nd. ....	34
Figure 2.16: Basic terminology of GAs. ....	35
Figure 2.17: A flowchart of the working principle of a GA. ....	36
Figure 2.18: Roulette Wheel Selection for reproduction in GAs. ....	38
Figure 2.19: Stochastic Universal Sampling Method for reproduction in GAs. ....	39
Figure 2.20: Tournament Selection method for reproduction in GAs .....	39
Figure 2.21: Very close fitness values of individuals in a GA .....	40
Figure 2.22: Example of One-point crossover .....	41
Figure 2.23: Example of Multi-point crossover .....	41
Figure 2.24: Example of Uniform crossover .....	41
Figure 2.25: Example of a Bit Flip Mutation .....	42
Figure 2.26: Example of a Swap Mutation .....	42
Figure 2.27: Example of a Scramble Mutation .....	42
Figure 2.28: Example of an Inversion Mutation .....	42
Figure 2.29: Example of a Fitness Based Survival Selection .....	43
Figure 2.30: Example of an Age Based Survival Selection .....	44
Figure 3.1: Stiffened panel between 2 neighboring girders and floors at a bulk carrier's hold. ....	46
Figure 3.2: CS panel from the car deck of a passenger ship .....	47
Figure 3.3: Ship static loads, Shear Force and Bending Moment Distributions .....	48
Figure 3.4: Bending stress distribution of a midship section. ....	49



Figure 3.5: Compound loading on an unstiffened panel.....	49
Figure 3.6: Creation of the cross-stiffened panel in “tile-wise” fashion.....	52
Figure 3.7: 2D model of a cross stiffened panel created in “tile-wise” fashion.....	53
Figure 3.8: T section along with its 5 parameters.....	54
Figure 3.9: Uneven pulling of the plate in case DOFs of side are not coupled.....	55
Figure 3.10: Solid element model with all the loads and boundary conditions applied.....	55
Figure 3.11: Criteria for net thickness of stiffeners.....	58
Figure 3.12: Values of Slenderness coefficients for each case.....	59
Figure 3.13: Flowchart of algorithmic process.....	60
Figure 4.1: Contour plot of Von Mises Stress at Shell Elements. Small stiffened panel. Loading case: Pressure Only // LOW.....	62
Figure 4.2: Contour plot of Sx Stress at Beam Elements (Transverses). Small stiffened panel. Loading case: Pressure Only // LOW.....	62
Figure 4.3: Contour plot of vertical displacement Uz. Small stiffened panel. Loading case: Pressure Only // LOW.....	63
Figure 4.4: Contour plot of Von Mises Stress at Shell Elements. Small stiffened panel. Loading case: Pressure Only // MEDIUM.....	64
Figure 4.5: Contour plot of Sx Stress at Beam Elements (Transverses). Small stiffened panel. Loading case: Pressure Only // MEDIUM.....	64
Figure 4.6: Contour plot of vertical Displacement (Uz). Small stiffened panel. Loading case: Pressure Only // MEDIUM.....	65
Figure 4.7: Contour plot of Von Mises Stress at Shell Elements. Small stiffened panel. Loading case: Pressure Only // HIGH.....	66
Figure 4.8: Contour plot of Sx Stress at Beam Elements (Longitudinals). Small stiffened panel. Loading case: Pressure Only // HIGH.....	66
Figure 4.9: Contour plot of Sx Stress at Beam Elements (Transverses). Small stiffened panel. Loading case: Pressure Only // HIGH.....	67
Figure 4.10: Contour plot of vertical Displacement (Uz). Small stiffened panel. Loading case: Pressure Only // HIGH.....	67
Figure 4.11: Contour plot of Von Mises Stress at Shell Elements. Small stiffened panel. Loading case: Pressure // LOW.....	68
Figure 4.12: Contour plot of Sx Stress at Beam Elements (Longitudinals). Small stiffened panel. Loading case: Pressure and Stress // LOW.....	69
Figure 4.13: Contour plot of vertical Displacement (Uz). Small stiffened panel. Loading case: Pressure and Stress // LOW.....	69
Figure 4.14: Contour plot of Von Mises Stress at Shell Elements. Small stiffened panel. Loading case: “Pressure and Stress // MEDIUM”.....	70
Figure 4.15: Contour plot of Sx Stress at Beam Elements (Longitudinals). Small stiffened panel. Loading case: Pressure and Stress // MEDIUM.....	71
Figure 4.16: Contour plot of vertical Displacement (Uz). Small stiffened panel. Loading case: Pressure and Stress // MEDIUM.....	71
Figure 4.17: Contour plot of Von Mises Stress at Shell Elements. Small stiffened panel. Loading case: Pressure and Stress // HIGH.....	72
Figure 4.18: Contour plot of Sx Stress at Beam Elements (Longitudinals). Small stiffened panel. Loading case: Pressure and Stress // HIGH.....	73
Figure 4.19: Contour plot of Sx Stress at Beam Elements (Transverses). Small stiffened panel. Loading case: Pressure and Stress // HIGH.....	73
Figure 4.20: Contour plot of vertical Displacement (Uz). Small stiffened panel. Loading case: Pressure and Stress // HIGH.....	74
Figure 4.21: Contour plot of Von Mises Stress at Shell Elements. Car Deck. Loading case: Pressure only // LOW.....	75

Figure 4.22: Contour plot of Sx Stress at Beam Elements (Transverses). Car Deck. Loading case: Pressure only// LOW.....	75
Figure 4.23: Contour plot of vertical Displacement (Uz). Car Deck. Loading case: Pressure only// LOW .....	76
Figure 4.24: Contour plot of Von Mises Stress at Shell Elements. Car Deck. Loading case: Pressure only // MEDIUM.....	77
Figure 4.25: Contour plot of Sx Stress at Beam Elements (Longitudinals). Car Deck. Loading case: Pressure only// MEDIUM .....	77
Figure 4.26: Contour plot of Sx Stress at Beam Elements (Transverses). Car Deck. Loading case: Pressure only// MEDIUM.....	78
Figure 4.27: Contour plot of vertical Displacement (Uz). Car Deck. Loading case: Pressure only// MEDIUM.....	78
Figure 4.28: Contour plot of Von Mises Stress at Shell Elements. Car Deck. Loading case: Pressure only // HIGH .....	79
Figure 4.29: Contour plot of Sx Stress at Beam Elements (Longitudinals). Car Deck. Loading case: Pressure only// HIGH.....	80
Figure 4.30: Contour plot of Sx Stress at Beam Elements (Transverses). Car Deck. Loading case: Pressure only// HIGH.....	80
Figure 4.31: Contour plot of vertical Displacement (Uz). Car Deck. Loading case: Pressure only// HIGH .....	81
Figure 4.32: Contour plot of Von Mises Stress at Shell Elements. Car Deck. Loading case: Pressure and Stress // LOW .....	82
Figure 4.33: Contour plot of Sx Stress at Beam Elements (Transverses). Car Deck. Loading case: Pressure and Stress // LOW .....	82
Figure 4.34: Contour plot of vertical Displacement (Uz). Car Deck. Loading case: Pressure and Stress // LOW .....	83
Figure 4.35: Contour plot of Von Mises Stress at Shell Elements. Car Deck. Loading case: Pressure and Stress // MEDIUM .....	84
Figure 4.36: Contour plot of Sx Stress at Beam Elements (Longitudinals). Car Deck. Loading case: Pressure and Stress // MEDIUM.....	84
Figure 4.37: Contour plot of Sx Stress at Beam Elements (Transverses). Car Deck. Loading case: Pressure and Stress // MEDIUM.....	85
Figure 4.38: Contour plot of vertical Displacement (Uz). Car Deck. Loading case: Pressure and Stress // MEDIUM.....	85
Figure 4.39: Contour plot of Von Mises Stress at Shell Elements. Car Deck. Loading case: Pressure and Stress // HIGH.....	86
Figure 4.40: Contour plot of Sx Stress at Beam Elements (Transverses). Car Deck. Loading case: Pressure and Stress // HIGH .....	87
Figure 4.41: Contour plot of vertical Displacement (Uz). Car Deck. Loading case: Pressure and Stress // HIGH .....	87

## List of tables

Table 2.1: Example of a Rank Selection in GAs .....	40
Table 3.1: Dimensions of the sides of the two panels modeled .....	47
Table 3.2: The 3 Levels of intensity for the loading of the panels.....	50
Table 3.3: Design variables and their ranges of value .....	56
Table 3.4: Constraints and their ranges of value.....	57
Table 4.1: Candidate points for Small stiffened panel. Loading case: Pressure only // LOW .....	61
Table 4.2: Candidate points for Small stiffened panel. Loading case: Pressure only // MEDIUM .....	63
Table 4.3: Candidate points for Small stiffened panel. Loading case: Pressure only // HIGH.....	65
Table 4.4: Candidate points for Small stiffened panel. Loading case: Pressure and Stress // LOW.....	68
Table 4.5: Candidate points for Small stiffened panel. Loading case: Pressure and Stress // MEDIUM .....	70
Table 4.6: Candidate points for Small stiffened panel. Loading case: Pressure and Stress // HIGH....	72
Table 4.7: Candidate points for Car Deck. Loading case: Pressure only// LOW .....	74
Table 4.8: Candidate points for Car Deck. Loading case: Pressure only// MEDIUM.....	76
Table 4.9: Candidate points for Car Deck. Loading case: Pressure only// HIGH.....	79
Table 4.10: Candidate points for Car Deck. Loading case: Pressure and Stress// LOW .....	81
Table 4.11: Candidate points for Car Deck. Loading case: Pressure and Stress// MEDIUM.....	83
Table 4.12: Candidate points for Car Deck. Loading case: Pressure and Stress// HIGH .....	86

This page is intentionally left blank.

# 1 Introduction

## 1.1 Structural Optimization in Shipbuilding

Throughout history, shipping has played a central role in transportation and trade. Even today, ships transport more than 80% of world trade volume and about 70% of trade value. This remarkable expansion of world trade and manufacturing over the past 50 years with distributed manufacturing, just-in-time delivery, and other features of the modern world was possible only with a reliable and dependable shipping network distributing all kinds of goods throughout the world, from basic commodities and semi-products to finished goods.

In the past, ship structural design was largely empirical, based on accumulated experience and ship performance and expressed in the form of structural design codes or “rules” published by various ship classification societies. These rules provided simplified and easily applicable formulas for structural dimensions, or scantlings, of the panels of a ship. This approach saves time in the design process and, although much evolved, is still the basis for the preliminary structural design of most ships.

However, there are several disadvantages and risks to a completely “rulebook” approach to design. Firstly, the modes of structural failure are numerous, complex and most importantly they interact with each other. Approaching structural design with prescribed and simplified formulas the margin against failure remains unknown. Thus, the boundaries between structural adequacy and overcapacity remain remote and vague. In other words, such formulas, in their effort to generalize structural behavior, cannot give a truly efficient design. In some cases, the overestimation of need for steel may represent a significant cost penalty which will burden the ship owner throughout the life of the ship. That significant cost basically translates into two aspects: a) the extra cost for material acquisition initially and b) the ongoing extra cost for fuel consumption for transferring unneeded amounts of steel rather than extra payload which is also lucrative.

In addition to this, the aspect of overconsumption of fuel due to overestimating the scantlings of the panels used in a ship (or aircraft also) should not be taken lightly. In fact, IMO has set certain measures in order to reduce carbon intensity of all ships. More specifically, the initial GHG (i.e. Green House Gases) strategy of IMO envisages in particular a reduction in carbon intensity of international shipping (to reduce CO<sub>2</sub> emissions per transport work), as an average across international shipping, by at least 40% by 2030, pursuing efforts towards 70% by 2050, compared to 2008; and that total annual GHG emissions from international shipping should be reduced by at least 50% by 2050 compared to 2008. In addition, it is emphasized that work should be done towards phasing out GHG emissions from shipping entirely as soon as possible this century [12]. Of course, someone could argue that this is not a problem which structural engineers should be bothered with and only engineers specialized in energy efficiency should be responsible for solving it. However, as humanity is on the verge of an actual climate crisis which may eventually lead to an irreparable climate change, every effort possible should be made in order to reduce the carbon foot print of national shipping in the planet and structural optimization is definitely a mean to reach this goal.

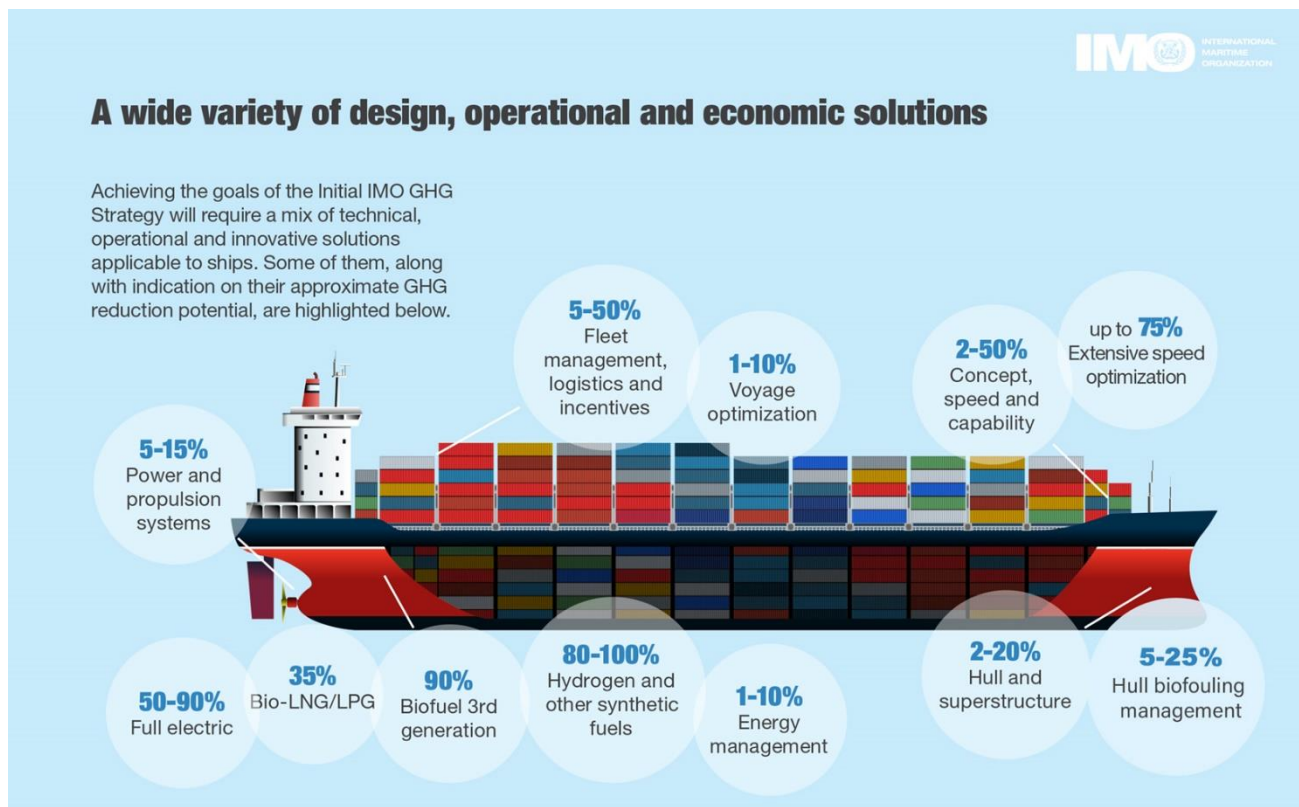


Figure 1.1 Variety of solutions towards decarbonization of international shipping [12]

The second reason for which a “rulebook” approach towards design is not a good idea is that the sole purpose of these formulas is that the structures avoid structural failure at all cost, as much of course as this can be predicted. However, this can be achieved in many ways and the particular implied in the formulas does not necessarily suit potential specific goals of the ship owner regarding the life span of the vessel or its particular purpose or economic environment. A rational design process must be capable of setting an objective, of actively moving toward it, and of achieving it to the fullest extent possible.

Finally, one must never forget that these formulas involve several assumptions which aim to simplify the problem at hand and for that reason they can be used within certain limits. Outside of their range of validity, they may be inaccurate to some degree which is unknown. Besides, throughout the history of structural design, there are quite a few examples of structural failures -in ships, bridges and aircraft despite the fact that a standard, time-honored method or formula was used.

For these reasons, there has been a general trend towards a more “rationally-based” structural design ever since the last twenty years of the previous century, approximately. The characteristics of this kind of design are that it is directly and entirely based on structural theory and uses computer-based methods of structural analysis and optimization in order to achieve an optimum structure; where the term “optimum” is measured via specific metrics selected by the designer. Therefore, a complete rationally-based design requires a detailed and accurate analysis of all factors related with safety and performance of the structure throughout its life and a synthesis of this information, along with objective the structure is intended to achieve. The goal is to find the design which best achieves this objective and at the same time ensures adequate safety. As expected, this procedure involves far more calculations than conventional methods and can only be achieved thanks to the computational power of computers.

Moreover, the rationally-based approach is not a fully automated process, that resembles a “black box” where the designer simply enters the input data and the exported result is a finished product. Such a rigid approach to designing, would require that all design decisions -objectives, criteria, priorities,

constraints- have to be made before the designing process commences and any subsequent potential modifications are out of discussion. On the contrary, the designing process must be interactive so as the designer is aware of the influence of every objective that is being accomplished at each stage of construction process. Therefore, in light of intermediate results, the designer can interrupt the designing process at discrete stages, search for more information, adjust certain things -with regards to the objectives, criteria and constraints- and possibly skip some steps, if he deems that they are not relevant at the time.

To conclude this introductory paragraph, rationally-based design in conjunction with structural optimization, gives the designer much more oversight of the designing process, the capability to intervene and change things while the process is ongoing and overall adds efficiency to the whole procedure. However, it does require a basic knowledge of structural analysis, fundamentals of finite element analysis and optimization methods and some programming skills. Given these requirements, the deciding factor in choosing the rationally-based approach is whether and to what extent a product and/or its performance (economic, operational or both) is intended that goes beyond what the rule-based approach has to offer. The latter is simpler, but certainly not optimal and nonadaptable. Therefore, the two approaches are complementary, and a good and experienced designer will use whichever is more appropriate for a given problem.

## 1.2 Stiffened panels

Stiffened panels are one of the most commonly used structural parts in distinct fields of engineering such as aerospace and shipping. In aircrafts, the inside of the fuselage (outer shell) could be identified as a curved stiffened panel, as it is shown in Figure 1.3. Similarly, vessels are comprised of numerous stiffened panels, some plane and some curved, which constitute the side and bottom shell, the decks and the bulkheads. While some of them are stiffened only in one direction, most of them are cross-stiffened.

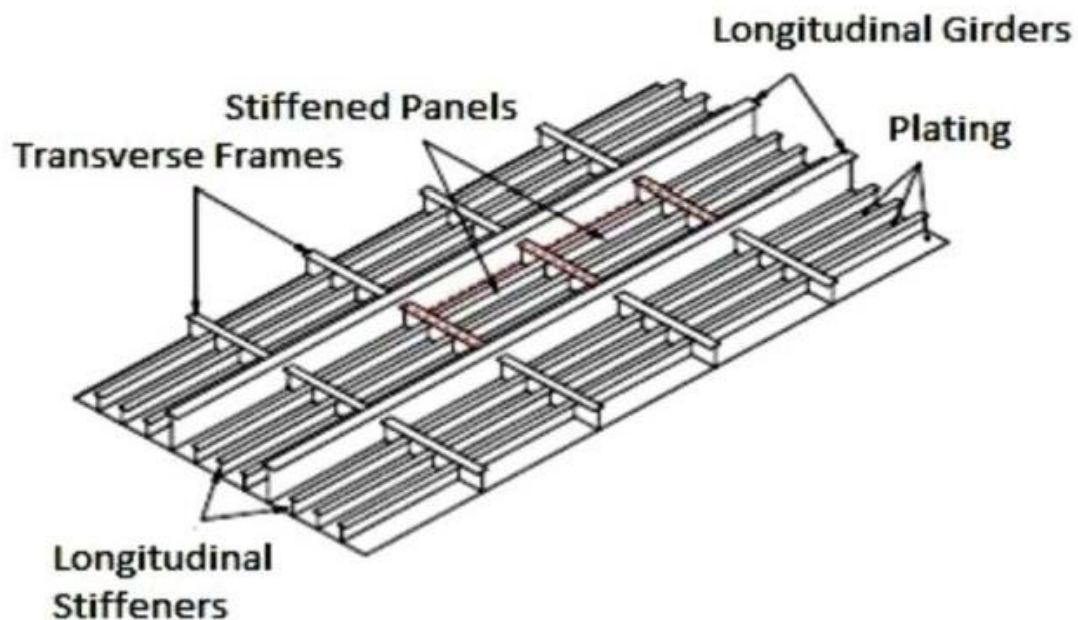


Figure 1.2: Simplest form of a cross-stiffened panel [18]

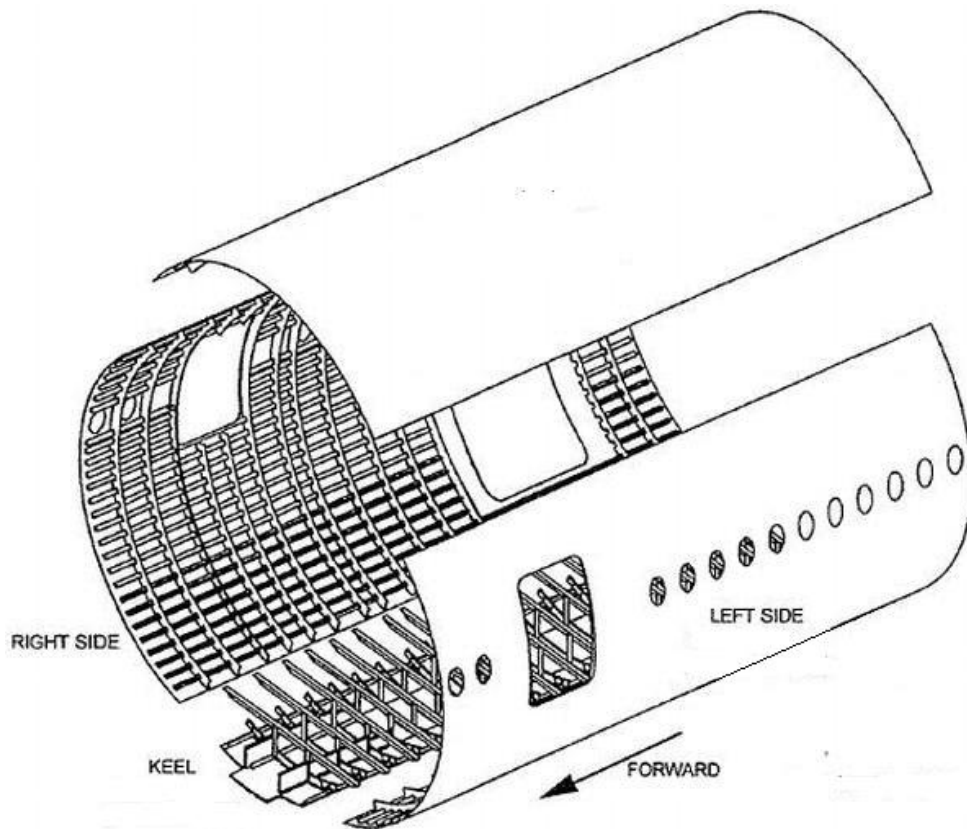


Figure 1.3: Inside of a fuselage[8]

The stiffeners attached to the panels are required to increase the panel's stiffness against axial and bending loads. Thus, with that configuration of material, a higher ratio of strength to weight is achieved, which is the desirable especially in fields such as aerospace and shipping because of the predominant economic significance of structural weight, and hence structural efficiency. In practice, companies mostly use a specific set of stiffener shapes most of which are depicted in Figure 1.4.

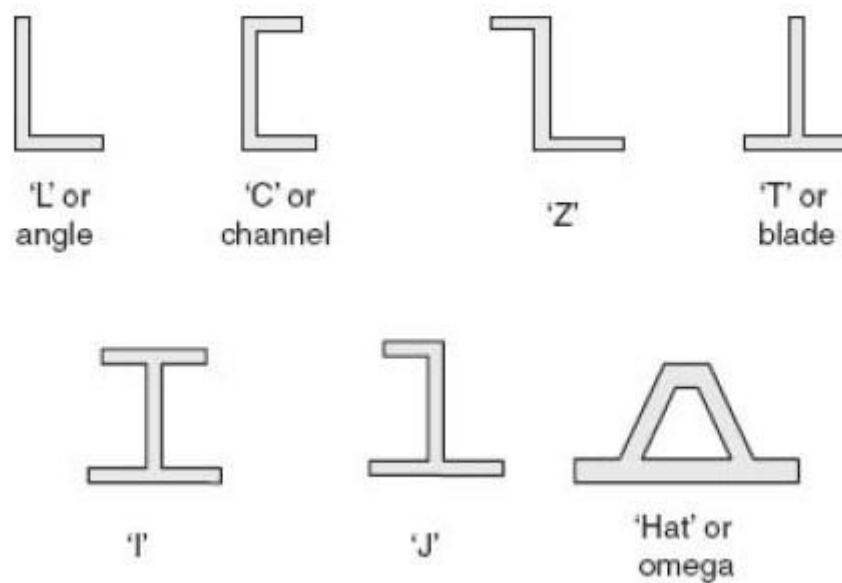


Figure 1.4: Typical cross-sections of stiffeners



Compressive loads are the origin for more failure modes than tensional loads. Therefore, stiffened panels in compression form the basis for this section and research in general. Since all the structural subsets that are comprised of stiffened panels are not supposed to fail in loading scenario, there are several failure modes that have to be accounted for. These can be attributed due to failure of the stiffener, panel or a combination of both. Figure 1.5 provides a visual representation of those failure modes while the list below provides a general description of each case.

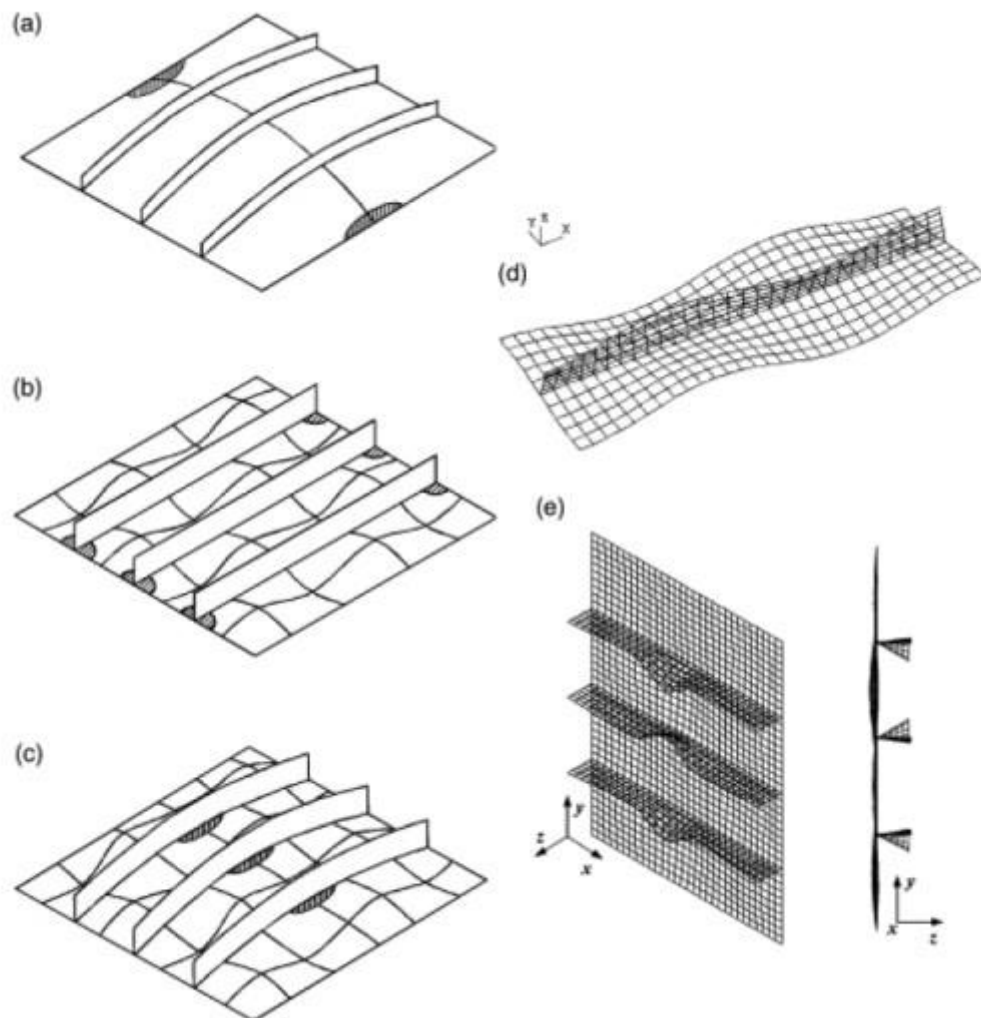


Figure 1.5: Buckling failure modes for stiffened panels [15]

1. **Stress failure:** Failure of the panel induced by a stress exceeding the stress limit, which is usually the yield or even the ultimate stress depending if plastic deformation is allowed.
2. **Buckling failure modes** (Figure 1.5)
  - a *Global buckling:* Buckling of the panel and stiffeners in a combined mode. This buckling mode appears more frequently when the stiffness of the panel is relatively larger than that of the stiffeners.
  - b *Panel buckling:* Local buckling of the part of the panel between stiffeners and/or boundary.

- c *Beam-Column buckling*: Column buckling of the stiffeners. Can result in global buckling or just happen in combination with another panel buckling mode. This buckling mode is including the failure of both the stiffener and the effective panel width.
- d *Local buckling*: Stiffener induced failure mode by local buckling of the web.
- e *Flexural torsional buckling*: Buckling mode similar to the local buckling of the stiffener's web. However, when 'tripping' occurs the plate loses its effective stiffness, which results in a global buckling mode.

Although the primal purpose of this work will not be the study of failure modes of stiffened panels, they ought to be mentioned so that the reader has a more complete view of the subject.

### 1.3 Thesis structure

At the core of this work, is the development of a Finite Element-based model of a cross-stiffened panel subjected to both bending and axial loads, which is often the case in naval structures. Three types of stiffeners were included - flat bar, T and L as these are the most often used in today's vessels. From the basic model, two cases of cross-stiffened panels were chosen to be simulated. The first one is a subset often found in the double bottom of bulk carriers. The second one resembles to a car deck which is often found in passenger ships. For each case, 3 levels of loading intensities (e.g. low, medium and high) were simulated where each level included two loading scenarios a) exertion of uniform vertical pressure on the unstiffened side of the panel and b) exertion of both uniform vertical pressure on the unstiffened side of the panel and tensile stress parallel to its longitudinal axis. Thus, in total 6 loading scenarios for each case. Afterwards, these 12 simulation cases were inserted into the built-in optimizer of ANSYS Workbench 19.2 so that the optimum configuration of stiffeners onto the panel and scantlings is found. The optimizer selected were Genetic Algorithms.

This thesis was organized as follows. In Chapter 2, the necessary theoretical background for the methods employed herein is provided. In Chapter 3, the algorithmic procedure which was developed in this work is presented. More specifically, in this Chapter the development of the FE-based model is discussed in more detail along with the formulation of the optimization problem at hand (i.e. input variables, constraints, objective function). Finally, in Chapter 4 are presented some indicative results that emerged from the application of the aforementioned algorithmic procedure.

## 2 Theoretical Background

### 2.1 Introduction

The aim of this chapter is to explain as simply and as directly as possible the theoretical background which is necessary for the understanding of the various methods and techniques involved in this thesis. In Chapter 2.2, the fundamental concepts of Finite Element Analysis (FEA) and the characteristics of the Elements used to develop the model of this work, are presented. In Chapter 2.3, the fundamental concepts of structural optimization and optimization in general are discussed while in Chapter 2.4, the method of Genetic Algorithms and the basic concepts related with it are introduced.

### 2.2 Basic Concepts of Finite Element Analysis

#### 2.2.1 The Finite Element Method

The Finite Element Method (FEM), also called Finite Element Analysis (FEA), is a mathematical technique for setting up and solving systems of partial differential (or integral) equations which describe field problems. The application of the finite element method ranges from problems of stress analysis in various types of complex structures to field problems such as heat transfer, magnetic flux as well as other problems of continuum mechanics (fluid and solid). In all these types of field problems, the purpose is to find the spatial distribution of one or more dependent variables. Thus, in a thermal analysis the object of interest might be the thermal distribution along a heated object, while in a structural analysis, as the one concerned in this work, the focus is on calculating the distribution of displacements and stresses in a structural subset. However, it has to be stressed that the FE method aims to provide a numerical solution to a specific problem whose solution cannot be predicted using closed form equations. In other words, a FE analysis does not produce a formula as a solution, nor does it solve a class of problems (Cook, Malkus, & Plesha, 1995, [6]).

In simple terms, the basic idea of the FE method is to divide a complex system whose behavior cannot be predicted using closed form equations into small pieces, or elements whose solution is known or can be approximated. Finite elements are simple geometric shapes, connected to each other through a set of points along their perimeter, called nodes. Each node has a set of degrees of freedom<sup>1</sup> (temperature, displacements, etc.) that can vary based on the input of the system. Depending on the type of the field problem, the proper governing equations are applied over those elements and the degrees of freedom at each node are the unknown values that have to be found in order for the problem to be solved. In terms of structural problems, after the loading and boundary conditions are defined (input of the system), this process leads to a set of simultaneous algebraic equations (equilibrium equations at the nodes) and the continuous problem now becomes discrete. Since it is impossible to divide the system into an infinite number of elements, the finite element method gives an approximation of the behavior of the continuum. Just as a regular polygon approaches a perfect circle as the number of sides approaches infinity, a finite element model approaches a perfect representation of the system as the number of elements becomes infinite. However, one must never forget that increasing the number of elements also increases the computer time required for a solution and therefore increases the cost. Thus, one extra challenge in the application of this method is to use the right amount of mesh density (the particular arrangement of elements is called a mesh) to find a solution quickly, without compromising much with accuracy though. As previously mentioned, the finite element method is very broad and powerful and used in a variety

of problems. In all these types of problems, the solution of the governing equations corresponds to the minimization of a functional. Initially, this process begins by polynomial interpolation of the desirable field quantity (e.g. the displacement), which is interpolated from its initially unknown values at the elements' nodes and subsequently, as the elements are connected together, over the entire region in piecewise fashion. The result of this interpolation is the formulation of the aforementioned algebraic equations. After solving these equations, the resultant values of the field quantity at the nodes are such that they correspond to the minimization of a functional, as previously mentioned. In structural applications, the functional is strain energy. This set of algebraic equations can be written in matrix form as  $\mathbf{Ku} = \mathbf{F}$ , where  $\mathbf{u}$  is a vector of the field quantity at the nodes,  $\mathbf{F}$  is a vector of known loads and  $\mathbf{K}$  is a matrix of known constants. In the context of stress analysis  $\mathbf{K}$  is known as the stiffness matrix of the structure. This formulation of the FE method, reminds the formulation of frame analysis. In fact, the Finite Element method was originally developed for structural problems, arising as an extension of matrix frame analysis to continuum structures such as plates and shells (Hughes & Paik, 2010,9)). Thus, the two methods share similar concepts and terminology. The whole mathematical formulation of the FE method is presented in further detail by several books (such as Cook, Malkus, & Plesha, 1995,6)).

## 2.2.2 Subdivision of the structure

As mentioned above, the basic concepts of the FE method are the same as in matrix frame analysis. More specifically, in both methods the goal is the representation of the structure as an assemblage of individual structural elements interconnected at a discrete number of nodes. This is a distinctive characteristic of frame structures, as they indeed consist of discrete beam members connected at various joints. However, this is not the case in continuum structures which comprise of panels or plates where a natural subdivision does not exist. Therefore, this division of the structure is done artificially, by discretizing it into a number of finite elements, which are, as mentioned in the previous subsection, simple geometric shapes.

The actual shape of these artificial elements varies depending on the problem at hand. Thus, they may be one-dimensional (e.g. beams), two-dimensional (e.g. triangles or quadrilaterals) or even three-dimensional (e.g. cubes). The nodes of each element are usually but not necessarily at the corners and serve to tie them together. An example of this is shown in Figure 2.1, which shows a typical finite element discretization of a beam with a 6x1 mesh of 9 node elements. In this case, the nodes are represented as dots and are located both at the corners of each element but also in the middle of each side and also at its center.

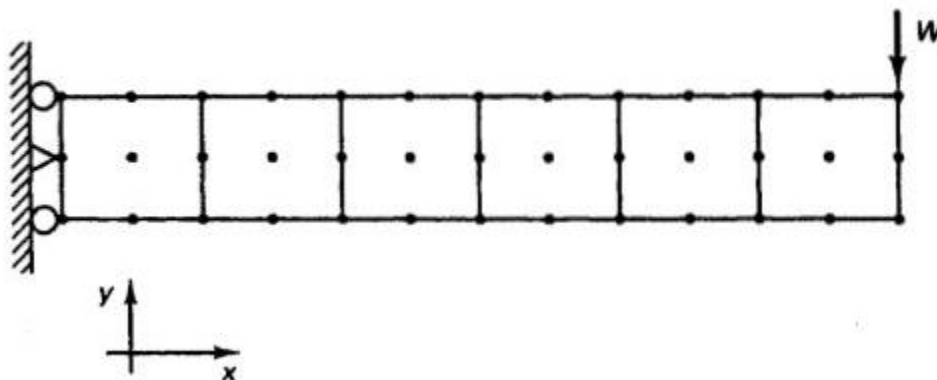


Figure 2.1: Beam modeled by 9-node Rectangular Elements, [2]

Following a more simplistic approach, it would appear that a FE analysis of a structure or a structural subset could be accomplished by simply dissecting it into finite elements, connecting them at their common nodes and finally solving for the unknown displacements. Nevertheless, actual structures such as the ones depicted in Figures 2.1 and 2.2, are continuous. Hence, in the finite element model, it would not be sufficient to connect the elements only at their nodes and to place no conditions on the displacements along the common boundaries. If the latter was done, the model would be much more flexible than the actual structure and as a result in some parts of the structure elements would be overlapping with each other and in other parts gaps would occur between them.

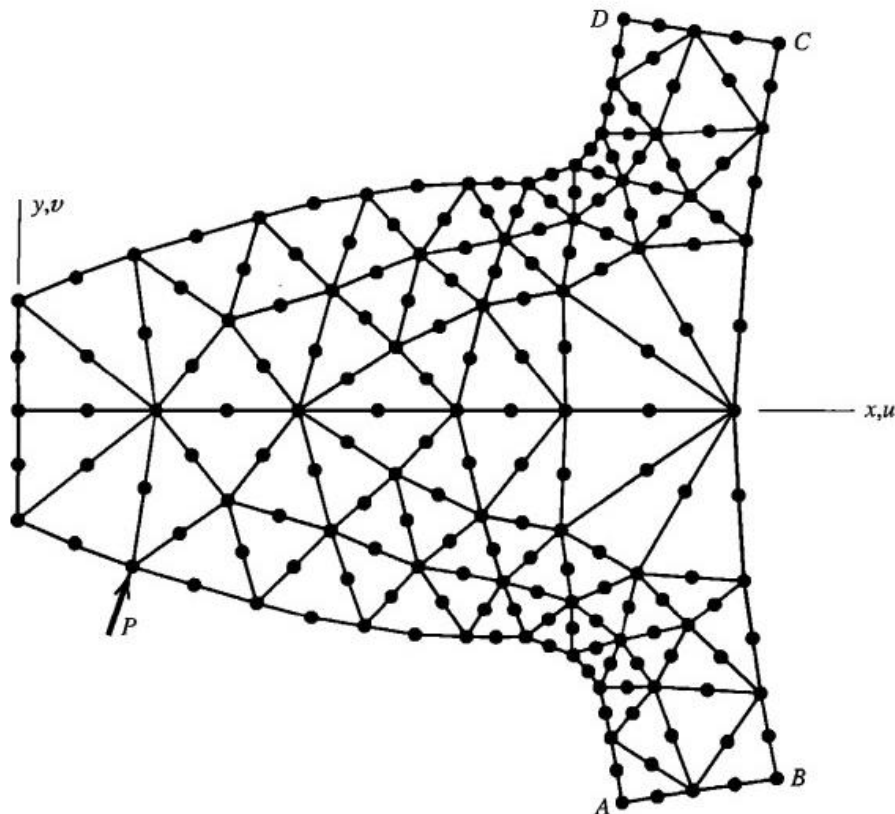


Figure 2.2 Two-dimensional model of a gear tooth comprised of triangular elements, [6]

One way of mitigating these discrepancies between the real structure and the FE model, and thus reinforce the accuracy of the method, is to use smaller and more numerous elements. In this way, the number of points on which displacement of continuity is satisfied increases. However, as already mentioned, of its very nature, a discrete model can never give an exact representation of the continuum regardless of the number of discrete variables it employs. Some error will always be present and the resultant solution will always be an approximate one. Also, at this point it is important to be reminded that increasing the number of discrete variables, increases the number of algebraic equations needed for the problem to be solved and eventually the computational cost of the model.

Therefore, it becomes evident that aside from discretizing the structure in smaller and more numerous elements to minimize the error, a more elegant way of achieving that is required. One such way is by carefully choosing and defining element properties which will essentially dictate each element's deformation pattern. In fact, this is the most fundamental feature of the Finite Element Method, as it ensures that both equilibrium and interelement continuity are satisfied to a sufficient degree although only being explicitly enforced at the nodes. The way this is achieved, is by using a special set of

functions which describe the distribution of a certain field quantity (e.g. displacement or stress) across the element, using only nodal values. These functions are called shape functions and are usually polynomials whose order defines both the element's pattern of deformation, as well as its internal behavior and applicability in general.

In order to highlight the role of shape functions in the FE method, as well as how they ensure interelement compatibility as previously mentioned, an example of a two-dimensional plane stress element will be presented briefly. This element (shown in Figure 2.3) is a flat triangular-shaped element of constant thickness  $t$  and isotropic material properties and is found in the literature as the Constant Strain Triangle (CST) element. This element is chosen to be presented, as due to its shape simplicity complex mathematical formulations can be omitted. In addition, this element is of primary importance and is very commonly used due to its versatility of geometry, as most two-dimensional shapes can be represented as an assemblage of triangles. As this a merely introductory example, only in-plane displacements are considered at the nodes. Thus, each node has two degrees of freedom, as shown in Figure 2.3, giving a total of six degrees of freedom.

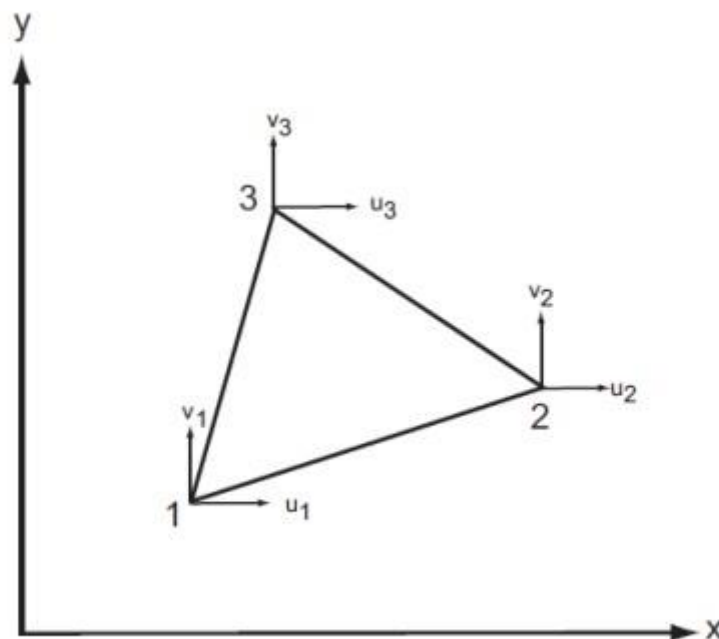


Figure 2.3 Nodal displacements of CST element, [9]

The displacement within the element is defined to be linear which essentially dictates that the relative shape functions will also be linear polynomial functions of  $x$  and  $y$ , with constants dependent solely on the nodal displacement of each element. With this choice of shape functions, the displacement across the element varies linearly in  $x$  and  $y$ . Therefore, it also varies linearly along each boundary of each element and since adjacent elements share a common displacement at each of their two common nodes, then due to the linearity of the shape functions, they must also have equal displacements along their common boundary. Hence, the requirement of interelement compatibility is required. This does not provide perfect equilibrium along the boundaries but rather only at the nodes. However, the mathematical proof for that is beyond the scope of this thesis and besides the only reason for referring to this element was for the sake of shape functions.

### 2.2.3 Finite Elements used in this work

As already mentioned cross-stiffened panels are arguably the most commonly found structural subset, regardless of the scale of the application. This preference to apply thin plates reinforced with beams cross-wise placed is a natural optimization strategy to increase the structure's ratio of strength to weight of material used. More specifically, marine structures are mainly comprised of stiffened panels but also plane plates, beams (small member, secondary member) and girders (big member, primary member) which form the multiple decks, bulkheads and the entire hull structure actually. The plate receives the load such as water pressure, the beam supports the loads from the plate and the girder supports the load from the beam.

As for the elements chosen to model the geometry of a problem, of course, every three-dimensional object can be modeled with three-dimensional solid elements. However, when the geometry of the problem at hand allows it (e.g. thin scantlings), the analyst must be able to deem if a one-dimensional or two-dimensional model would suffice. Lower order models have simpler model geometry and fewer degrees of freedom after meshing, so they generally require a lower computational cost. Thus, in order to decrease the solve time, lower order elements were implemented in this work.

Due to the different nature of the structural components comprising a cross stiffened panel (beams/girders and plates), it is evident that two different types of finite elements are needed in order to model such a structural subset while implementing lower order modeling; one more elongated for the beams/girders and one thinner and plane for the plates. Namely, for the elongated parts of the model (e.g. stiffeners) a beam element would be more suitable and for the plate a shell element. As these two types of elements were used in creating the finite element model in this work, it was deemed to be presented in a brief yet hopefully comprehensive manner.

In the case of beam elements, they are, as their name suggests, bars which must fulfill the condition that the dimension  $d$ , as shown in Figure 2.4, is small in relation in relations to the bar's length  $l$ . These one-dimensional elements have two or three nodes and represent structural beams in either two or three dimensions. They typically have six degrees of freedom at each node. These include translations in the  $x$ ,  $y$  and  $z$  directions and rotations about the  $x$ ,  $y$  and  $z$  directions. A 2-node beam element along with its typical nodal degrees of freedom (in local coordinates) is depicted in Figure 2.5.

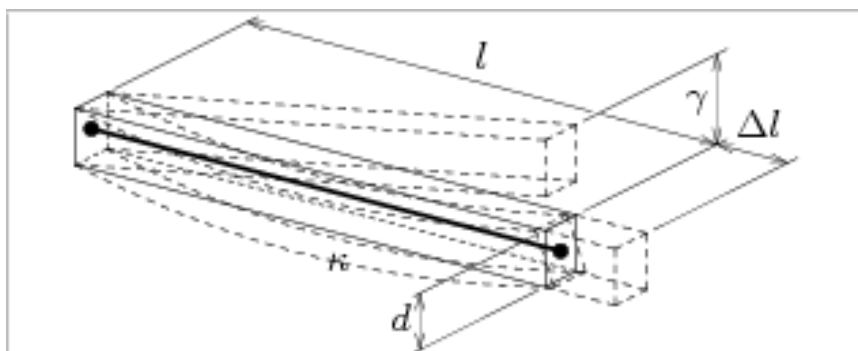


Figure 2.4: Representation of a beam element with given geometrical properties.

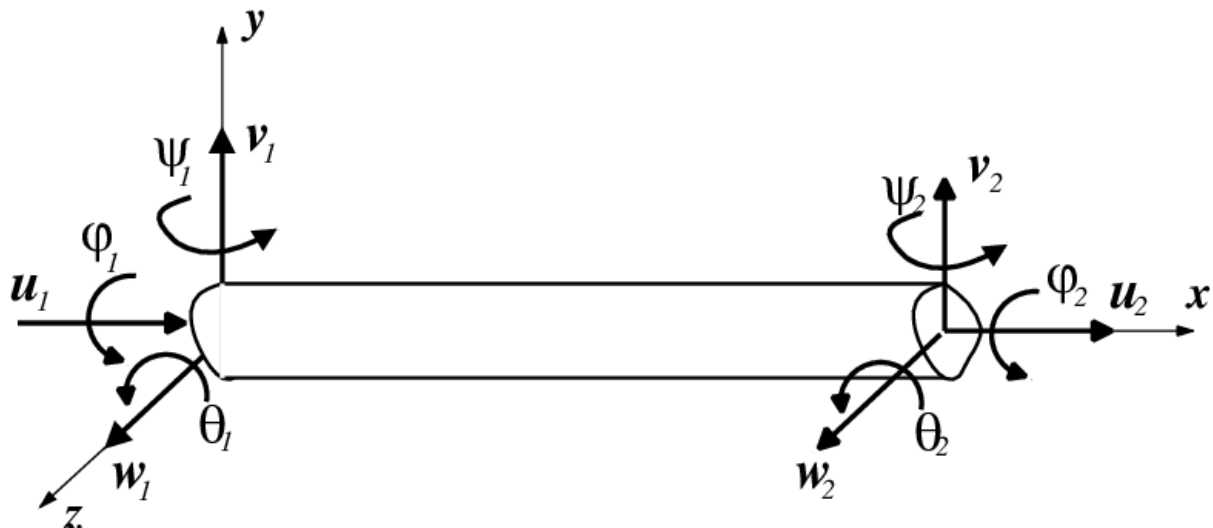


Figure 2.5: 2-node beam element and Typical Nodal Degrees of Freedom., [13]

Beam elements are very widely used in structural engineering and are suitable for analyzing any slender to moderately/thick beam structure. As the elements are by default one-dimensional, the analyst has to give the required data (e.g. section type, dimensions) so that the element acquires a three-dimensional representation. They can support linear, large rotation, and/or large strain nonlinear applications. As for the stiffness properties of a beam element, they are physically the element end forces that correspond to unit element end displacements. These forces can be evaluated by solving the differential equations of equilibrium of the element when it is subjected to the appropriate boundary conditions. This evaluation eventually leads to the calculation of the element's stiffness matrix and the exact element internal displacements.

The other type of finite elements used in cross-stiffened panels in order to mesh the plate is, as mentioned earlier, shell elements. The geometry of a shell element is defined by its thickness and its midsurface. There lies the advantage of shell elements against three-dimensional solid elements, as it is possible for a plate or any axisymmetric structure of constant thickness to be modeled using midsurface modeling, thus eliminating the need for a solid three-dimensional model of the structure to be created. However, this is possible on condition that the structure is thin, as the basic principle in plate bending and shell analyses assumes that the stress through the thickness (i.e. perpendicular to the midsurface) of the plate/shell is zero. In addition, shell elements by virtue of their formulation are able to produce results for both the outermost and innermost fibers of the surface giving the analyst another advantage against solid elements.

The most commonly used shell elements in modern FEA are flat triangular elements or quadrilateral elements. In a thin-walled or plated structure, such as a ship, elements will generally be subjected to both bending and in-plane stresses. Provided that there are not underlying nonlinearities in the FE analysis at hand (e.g. plasticity or large displacements), these stresses impose independent deformations to a flat element. Therefore, the relative stiffness matrix can be obtained by superimposing stiffness matrices of simpler elements already available in the literature.

More specifically, a flat shell element can be directly obtained by combining a plane stress element or membrane element with a plate bending element. Let's take the example of a flat rectangular shell element shown in Figure 2.6 below in local coordinate system  $xyz$ . The total loading of the element can be broken down into two types of stresses; bending (middle) and in-plane (far-right).



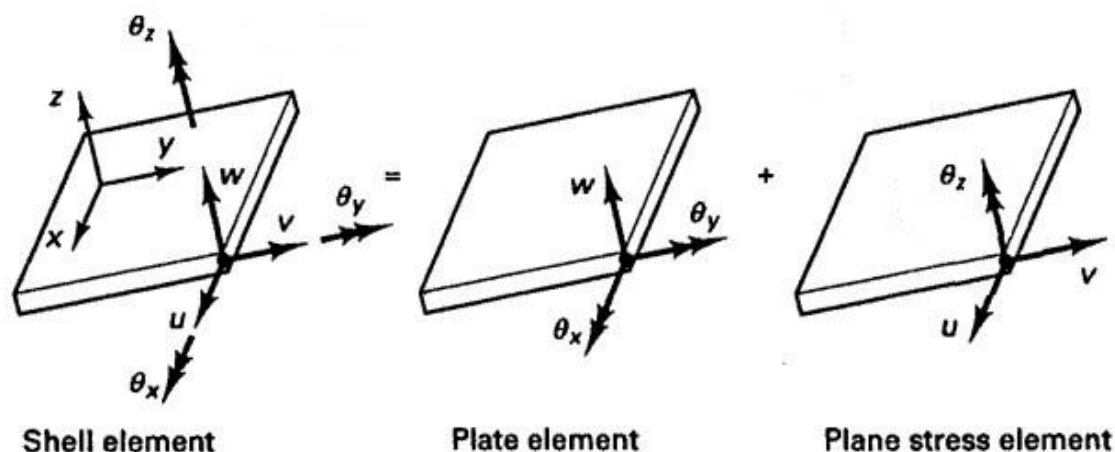


Figure 2.6: Basic shell element with local six degrees of freedom at a node, [2]

It is assumed that the individual stiffness matrices are known for each case in the local coordinate system, and are denoted as  $\tilde{\mathbf{K}}_B$  and  $\tilde{\mathbf{K}}_P$  for the plate bending and plane stress element respectively.

Then the shell element stiffness matrix  $\tilde{\mathbf{K}}_S$  is:

$$\tilde{\mathbf{K}}_S = \begin{bmatrix} \tilde{\mathbf{K}}_B & \\ & \tilde{\mathbf{K}}_P \end{bmatrix} \quad (2.1)$$

$\begin{matrix} 12 \times 12 \\ 12 \times 12 \end{matrix}$

As it is denoted above  $\tilde{\mathbf{K}}_B$  is a 12x12 matrix and  $\tilde{\mathbf{K}}_P$  is an 12x12 matrix (shell normal rotation  $\theta_z$  is included), therefore, adding all the individual DOF's, the resultant matrix  $\tilde{\mathbf{K}}_S$  is 24x24. As these matrices have been derived for a local coordinate system, transformation to the global coordinate system is required to assemble the elements for the entire structure. This is achieved by the use of the transformation matrix  $\mathbf{T}$  and of the following formula:

$$\tilde{\mathbf{K}}_S^* = \mathbf{T}^T \tilde{\mathbf{K}}_S \mathbf{T} \quad (2.2)$$

$\begin{matrix} 24 \times 24 & & 24 \times 24 \end{matrix}$

It should be noted that the flat shell element presented above has 6 degrees of freedom per node; 3 translational ( $u$ ,  $v$ ,  $w$ ) and 3 rotational ( $\theta_x$ ,  $\theta_y$ ,  $\theta_z$ ). This is the most direct way for obtaining the shell element (Cook, 1995). Otherwise, in order to obtain a shell element, one could alternatively make use of isoparametric shell elements which occupy a middle ground between flat elements and curved elements. Such an element is the result of the following process; one starts with a three-dimensional solid element such as the one shown in Figure 2.7-(a), which can accurately model a shell provided that the thickness  $t$  is small in comparison with other dimensions. Subsequently, the element is transformed

by reducing the number of nodes from 20 to 8, by expressing translational DOF's from the 20-node element in terms translational and rotational DOF's on the midsurface of an 8-node element such as the one shown in Figure 2.7-(b). Figure 2.7-(c) shows these DOF's in local coordinates at a typical midsurface node b.

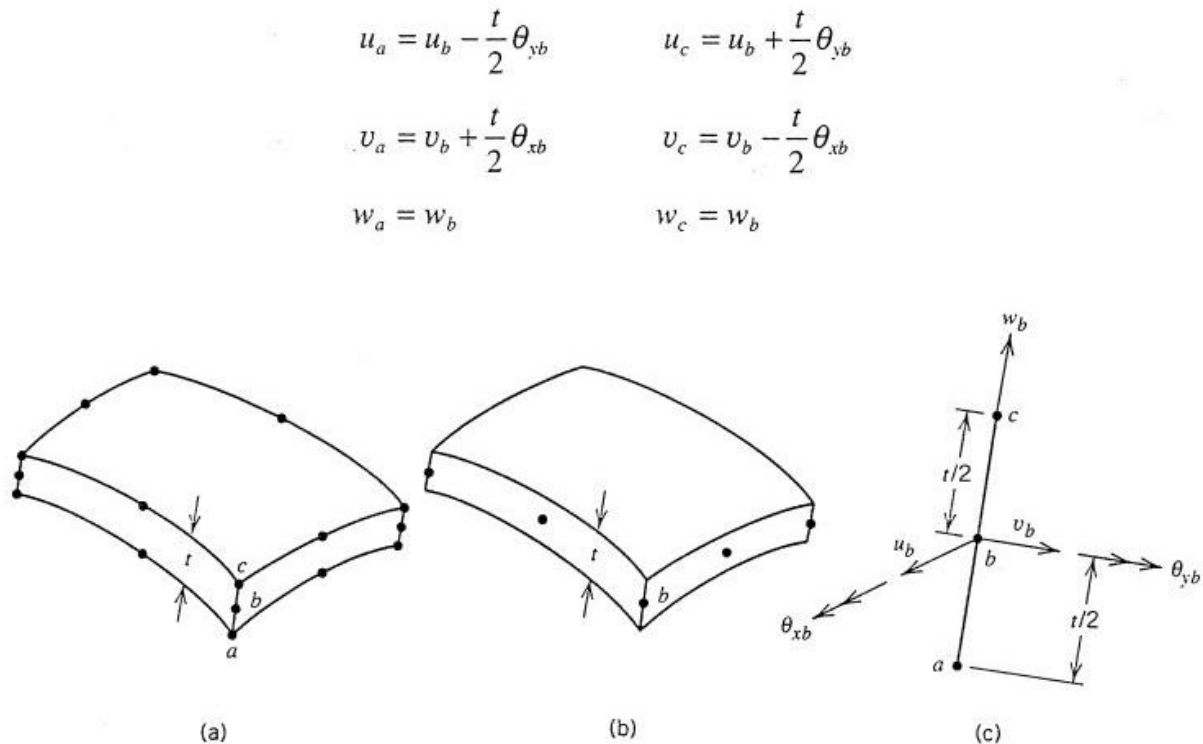


Figure 2.7: (a) A 20-node isoparametric solid element. (b) Reduction to an 8-node shell element. (c) DOF's at node b., [5]

## 2.2.4 Model Verification and Validation

Modeling is the simulation of a physical structure or physical process by means of a substitute analytical or numerical construct and therefore, it is not simply preparing a mesh of nodes and elements. Predominantly, it requires a deep understanding of the physical action of the problem, which in structural terms means understanding the loading and the resultant mode of deformation. As mentioned previously, each element has its own properties and deforms in a specific pattern, thus the ability to understand the way the entire structure deforms is critical in choosing the proper element which meets the demands of the application.

Moreover, being able to envisage the variations and gradient in stress and strain plays a fundamental role in deciding on the density of the mesh used. The mesh density must be such as to avoid too large elements which disclose valuable information regarding variations of stress and strain, or too small elements which essentially surpass the number of elements needed to accurately represent the stress field, resulting to over-refinement and waste of computer resources. In cases where increased accuracy is required in specific regions of the structure, where stress concentrations are anticipated to occur (e.g. in the vicinity of openings and cut-outs or near the point of application of concentrated loads as shown in Figure 2.8), there is a way of achieving the required accuracy without overconsuming computational resources. This is achieved through the implementation of a technique called “mesh grading”. However, due to the enormous variety of structures and of loads, there is no general rule which can be followed as to the number or size of elements to be used in order to provide sufficient accuracy and therefore,

experience of the analyst with similar structures is needed. If the latter is not possible, then a series of appropriate test problems should be solved using different mesh sizes in order to observe the rate of convergence and thereby determine a suitable mesh size for the particular problem.

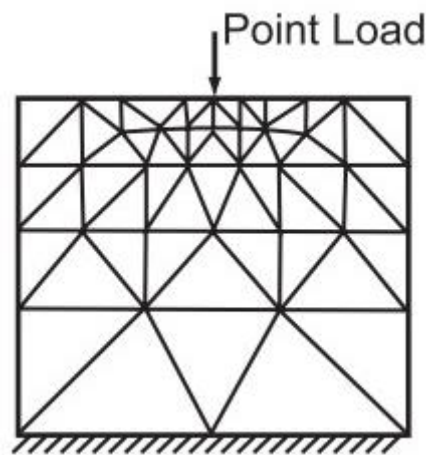


Figure 2.8: Mesh grading near the point of application of a concentrated load., [9]

After the discretization stage, the next step, which is essential to complete the FE analysis of a structural or other problem, is the correct implementation of boundary conditions. This stage includes the modeling of both the support conditions of the structure, as well as of the exerted loads. In FEA, it is a general rule that loads and boundary conditions are applied only at the nodes. Therefore, caution must be taken when applying support conditions and loads to the FE model, as if someone applied them by bearing in mind the notions from classical mechanics, he would not necessarily simulate the actual case. In the case of concentrated loads, this does not require a special treatment, as the analyst would implicitly decide in advance where the load would be placed and subsequently would adjust the mesh accordingly, so that there is a node at the point of application of the load. However, when applying distributed loading the analyst must bear in mind the aforementioned rule. Thus, a distributed load is impossible to be modeled in a continuous way and has to be discretized to equivalent point loads applied at the nodes, in a way similar to that depicted at Figure 2.9.

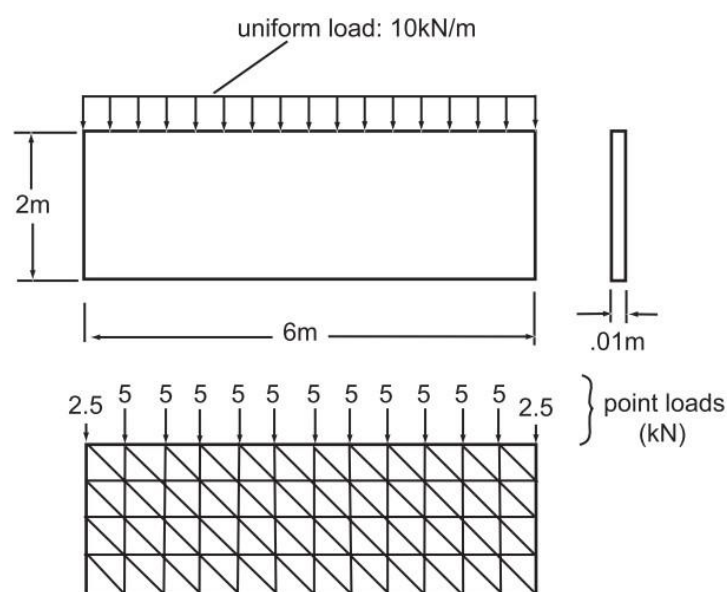


Figure 2.9: Equivalent nodal point loads., [9]

Last but not least, the final step in the process of a FE analysis is to validate the exported results. In the FE method the calculation sequence is as follows; firstly, the displacements are calculated and then the software used uses the displacement information to calculate strains and eventually stresses. The verification process should commence by the resultant displacement field, as this is more convenient for the analyst in order to judge whether the deformed shape is as anticipated or whether the loading and the support conditions have been properly implemented. Subsequently, the analyst can validate the stresses which the software will plot either as contour lines or bands of different colors. A stress contour line connects points that have the same stress. A contour plot that displays significant interelement discontinuities warns that a finer mesh is needed. Hence, in this stage of verification it is crucial to compare the resultant stresses with either analytical or experimental results if the latter are available. However, it is best to gather these results prior to commencing the FE analysis, as there is usually the tendency, perhaps unconsciously, that the analyst tries to obtain analytical results that agree with the numerical results already obtained. So long as the exported FE results are reasonable, and the error discrepancies stemming from the aforementioned comparison are small, then the FE model is acceptable. If not, the entire process should be repeated after proper adjustments have been made, until the model yields satisfactory results or it cannot be further improved.

## 2.3 Structural Optimization: An overview

### 2.3.1 Basic Concepts of Optimization

As it is evident from its title, this chapter deals with Structural Optimization and aims to introduce the basic ideas and terminology related with it. However, it was deemed more rational to present firstly the general context that gathers Structural Optimization, which is Optimization in general, before introducing more specific terms and applications.

According to Rao (2020), [14] an optimization or mathematical programming can be generally defined as follows:

$$\text{Find } \mathbf{X} = \begin{Bmatrix} x_1 \\ x_2 \\ \vdots \\ x_n \end{Bmatrix} \text{ which minimizes } f(\mathbf{X})$$

subject to the constraints

$$\begin{aligned} g_j(\mathbf{X}) &\leq 0, & j &= 1, 2, \dots, m \\ l_j(\mathbf{X}) &= 0, & j &= 1, 2, \dots, p \end{aligned} \tag{2.3}$$

where  $\mathbf{X}$  is an n-dimensional vector called the design vector,  $f(\mathbf{X})$  is termed the objective function, and  $g_j(\mathbf{X})$  and  $l_j(\mathbf{X})$  are known as inequality and equality constraints, respectively.

The number of variables  $n$  and the number of constraints  $m$  and/or  $p$  need not be related in any way. The problem stated in equation (2.3) is called a constrained optimization problem. The above constraints can be removed and then the problem is called unconstrained. It is worth to be noted that the definition of the problem does not imply anything about the continuity of the vector  $\mathbf{X}$  or the function  $f$ . Therefore,  $\mathbf{X}$  is free to be a vector of continuous or discrete variables and  $f$  can be either continuous or discrete. For the better comprehension of the practical meaning of the above terms, a brief description will follow.

During the design process of any engineering system or component there is a set of quantities that define it. Some of them have fixed values at the outset, while others serve as variables during the design process and are called design or decision variables  $x_i$ ,  $i = 1, 2, \dots, n$ . To represent the design variable collectively, a design vector  $\mathbf{X} = \{x_1, x_2, \dots, x_n\}^T$  is formed. If an  $n$ -dimensional Cartesian space with each coordinate axis representing a design variable  $x_i$ ,  $i = 1, 2, \dots, n$  is considered, the space is called design variable space or simply design space. Each point in the  $n$ -dimensional design space is called a design point and represents a possible or an impossible solution to the design problem.

In most practical applications, the design variables cannot be chosen arbitrarily; rather, they have to satisfy certain requirements, functional or other. These restrictions, that must be satisfied in order that an acceptable design is produced, are collectively called design restrictions and are expressed mathematically by the equality and inequality constraints like the ones formulated at relation (2.3). These constraints may be functional or behavioral when they are related with the performance of the system or geometric when aspects such as availability, fabricability or transportability of the system are concerned.

Traditionally, design procedures aim at finding an acceptable or adequate design that merely satisfies the functional and other requirements of the problem. In general, there will be more than one acceptable design. The purpose of optimization is essentially to determine which of the many acceptable designs available is the best one, relative to a specific parameter. Therefore, a proper measure of that acceptability has to be defined to enable the comparison between the different alternative acceptable designs. This measure or criterion, with respect to which the design is optimized, when expressed in mathematical terms is known as the objective function. The choice of the objective function is governed by the nature of the problem and it is of utmost importance in the optimization process.

Although this thesis is related with a single objective problem, there are several problems where more than one criterion may need to be satisfied simultaneously. An optimization problem involving multiple objective functions is known as a multi-objective optimization problem (MOP). Coello Coello, Lamont, & Van Veldhuizen (2007) give a descriptive definition of an MOP, in their book [4], as the process of finding a vector of decision variables which satisfies constraints and optimizes a vector function whose elements represent the objective functions. These functions form a mathematical description of performance criteria which are usually in conflict with each other. Hence, the term “optimize” means finding such a solution which would give the values of all the objective functions that are acceptable to the decision maker.

Regarding the mathematical formulation of an MOP problem, it is very much alike with the one of a single objective optimization problem. The only difference is found in the objective function, which in this case is not a scalar but rather a vector function. The objective functions are designated:  $f_1(\mathbf{X}), f_2(\mathbf{X}), \dots, f_k(\mathbf{X})$  where  $k$  is the number of objective functions in the MOP being solved.

Therefore, the objective functions form the aforementioned vector objective function  $f(\mathbf{X})$  which is defined by:

$$f(\mathbf{X}) = \begin{bmatrix} f_1(\mathbf{X}) \\ f_2(\mathbf{X}) \\ \vdots \\ f_k(\mathbf{X}) \end{bmatrix} \quad (2.4)$$

This means that in addition to the  $n$ -dimensional design space mentioned earlier, a  $k$ -dimensional space of the objective functions, in which each coordinate axis corresponds to a component vector  $f_k(\mathbf{X})$  is also part of the MOP. This additional space is called the objective space. For each solution  $\mathbf{X}$  in the decision variable space, there exists a point in the objective space. In other words, the mapping takes place between an  $n$ -dimensional solution vector and  $k$ -dimensional objective vector. Figure 2.10 illustrates these two spaces and a mapping between them.

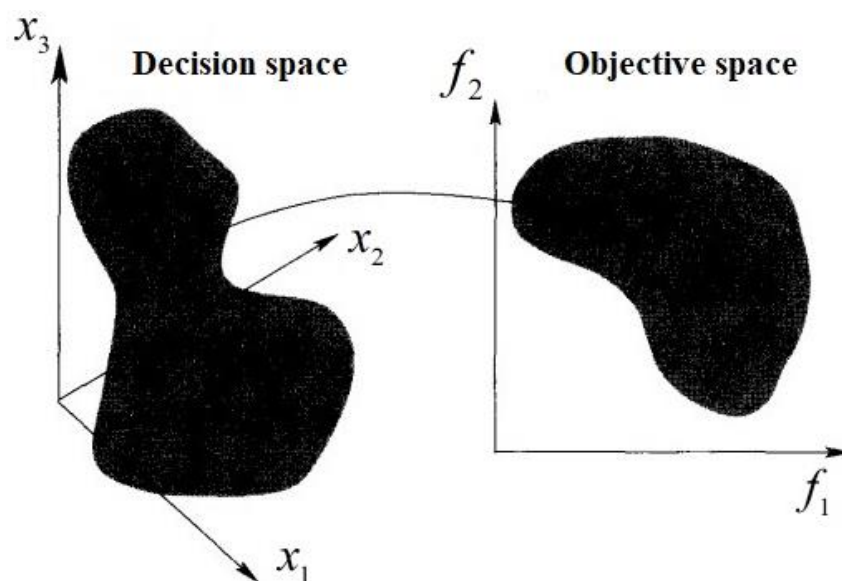


Figure 2.10: Representation of the decision variable space and the corresponding objective space. [7]

The nature of multi-objective problems dictates that there is not a single objective function to optimize, but rather a set of them that must be optimized simultaneously. This may involve the minimization or maximization of all functions or a combination of minimization and maximization of them. The presence of multiple conflicting objectives does not allow one solution to be termed as optimal and thereby the resulting multi-objective optimization problem resorts to a set of solutions obtained through Pareto Optimality Theory. For their selection, a decision maker is required to make a choice of  $x_i$  values. This selection is essentially a compromise (or “trade-off”) between one complete solution  $\mathbf{X}$  and another one in the multi-objective space.

These solutions are known as Pareto optimal solutions and are those whose corresponding objective vector components cannot be all simultaneously improved. The “bottomline” of this discussion is that  $\mathbf{X}^*$  is Pareto optimal if there exists no feasible vector  $\mathbf{X}$  which would decrease some criterion without causing a simultaneous increase in at least one other criterion (assuming minimization). These solutions are also termed non-inferior, admissible, or efficient solutions and their corresponding vector are termed nondominated. The set of those solutions is known as the Pareto optimal set while that of their corresponding objective vectors the Pareto front set. These solutions may have no apparent relationship besides their membership in the Pareto optimal set and together they form the set of all solutions whose associated vectors are nondominated.

### 2.3.2 Fundamental Concepts of Structural Optimization

As already mentioned, structural optimization is about making an assemblage of materials sustain loads the best way. Nevertheless, this could have multiple interpretations as it could be mean to make the structure as light as possible (i.e. to minimize weight) or make the structure as stiff as possible. Another idea of “best” could be to make it as insensitive to buckling or instability as possible.

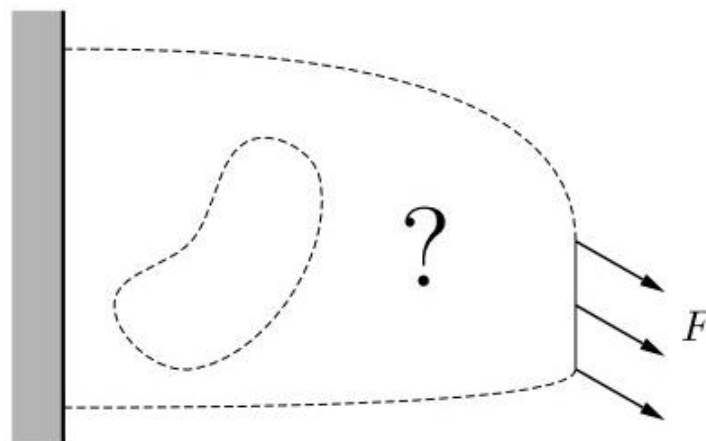


Figure 2.11: Structural Optimization problem. Find the structure which best transmits the load  $F$  to the support., [3]

There shines the importance of the aforementioned constraints, as it is clear that such maximizations or minimizations cannot be performed unrestrictedly. For instance, if there is no limitation on the amount of material that can be used, the structure can be made stiff without limit and this results in an optimization problem without a well-defined solution. Usually, the quantities that are constrained in structural optimization problems are stresses, displacements and/or the geometry. It should be noted that most quantities that one can think of as constraints could also be used as measures of “best”, i.e., as objective functions.

Structural optimization may seem abstract at first as, although the intent may be clear, the way of achieving a best design has not been broken down yet into specific steps. The traditional and still dominant way of optimizing structural components, omitting rigorous mathematical tools, can be described as follows:

- a) A specific design is suggested.

b) Requirements based on the function are investigated.

c) If they are not satisfied, say the stress are too large, a new design must be suggested, and even if such requirements are satisfied the design may not be optimal so still a new design can be suggested.

d) The suggested new design is brought back to step b)

As it is obvious, an iterative process is formed here, where on mainly intuitive grounds, a series of designs are created which hopefully converges to an acceptable final design. For mechanical structures, step b) of this iterative-intuitive procedure is today almost exclusively performed by means of computer-based methods, like the FE Method. The FE method ensures that every design iteration can be analyzed with greater confidence and undoubtedly, makes every step of the above procedure more effective.

The mathematical design optimization method is conceptually different from the iterative-intuitive one. In this method a mathematical optimization problem is formulated, where requirements due to the function act as constraints and the concept “as good as possible” is given mathematical form. Therefore, the entire optimization process is much more automated and precise in the mathematical design approach than in the iterative-intuitive one. In addition, this optimization approach was employed in this work.

In the context of structural optimization, the aforementioned design vector  $X$  almost always represents some sort of geometric feature of the structure. Depending on the geometric feature, structural optimization problems are divided into 3 classes:

- *Sizing optimization*: This is when  $X$  is some type of structural thickness, i.e. cross-sectional areas of truss members, or the thickness distribution of a sheet. A sizing optimization problem for a truss structure is shown in Figure 2.10.

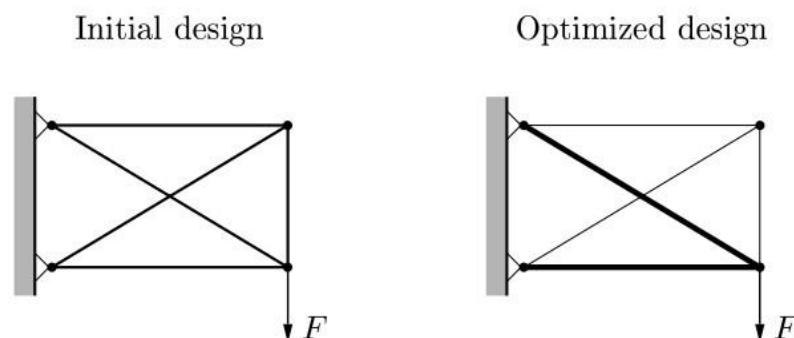


Figure 2.12: A sizing structural optimization problem. Change in the size of the cross-sectional area of truss members can be observed., [3]

- *Shape optimization*: In this case  $X$  represents the form or contour of some part of the boundary of the structural domain. Suppose a solid body, the state of which is described by a set of partial differential equations. The optimization consists in choosing the integration domain for the differential equations in an optimal way. It should be noted that the connectivity of the structure is not changed during shape optimization. In other words, new boundaries are not formed. A two-dimensional shape optimization problem is depicted in Figure 2.11.



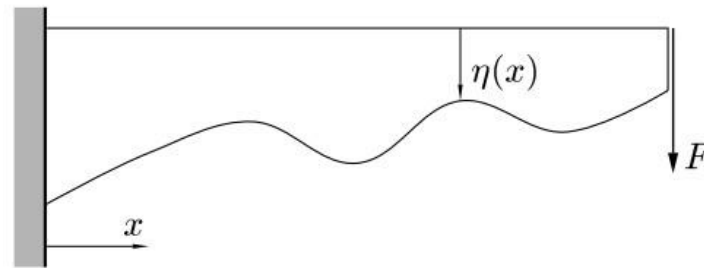


Figure 2.13: A shape optimization problem. Find the function  $\eta(x)$ , describing the shape of the beam-like structure., [3]

- Topology optimization:* In a discrete case, such as for a truss, it is achieved by taking cross-sectional areas of truss members as design variables, and then allowing these variables to take the value zero, i.e. bars are removed from the truss. In this way the connectivity of nodes is variable so it may be considered that the topology of the truss changes, as shown in Figure 2.12. If instead of a discrete structure, a continuum type of structure such as a two-dimensional sheet is considered, then topology changes can be achieved by letting the thickness of the sheet take the value zero. If pure topological features are optimized, the optimal thickness should only take two values: 0 and a fixed maximum sheet thickness. In a three-dimensional case the same effect can be achieved by letting  $\bar{X}$  be a density like variable that can only take the values 0 and 1. Figure 2.13 shows another example of topology optimization.

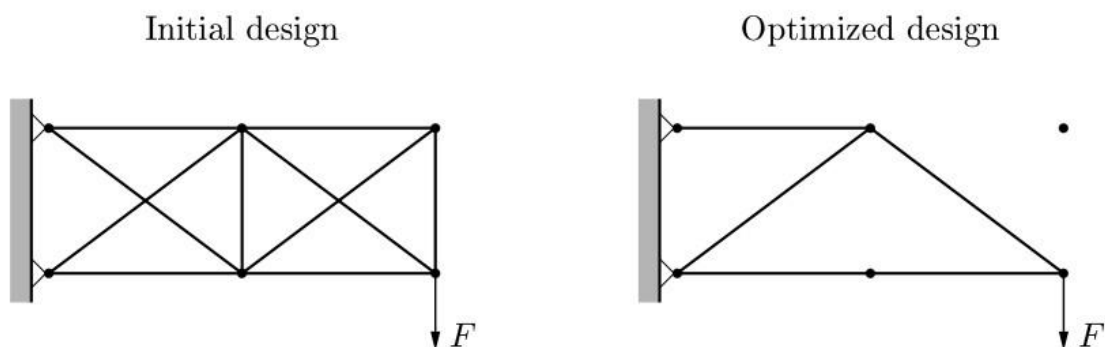


Figure 2.14: Topology optimization of a truss. Bars are removed by letting cross-sectional areas take the value zero., [3]

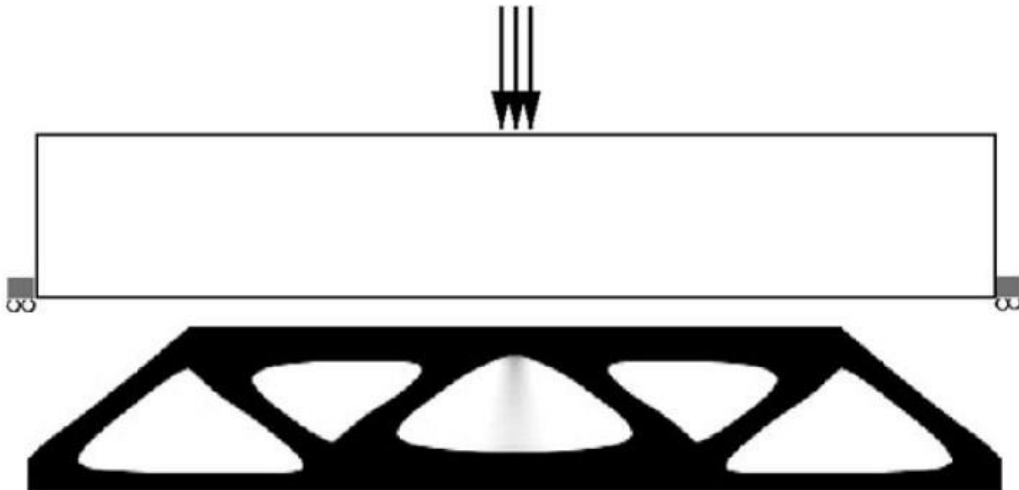


Figure 2.15: Two-dimensional topology optimization. The box in the above picture is to be filled 50% by material and the question is what is the proper material distribution for optimal performance under loads and boundary conditions. The result is shown in the 2nd., [3]

## 2.4 Genetic Algorithms: An overview

### *Introduction*

In recent years, some optimization methods that are conceptually different from the traditional mathematical programming techniques have been developed. These methods are labeled as modern or nontraditional methods of optimization. Nature has always been a great source of inspiration to all mankind and these methods are no exception. Most of these methods are based on certain characteristics and behavior of biological, molecular, swarm of insects and neurobiological systems. In this thesis, only one of these methods is used and its basic concepts are introduced in this section. The method which will be discussed herein is referred to in the literature as Genetic Algorithms (GA).

In modern engineering applications, many practical design problems which request the optimal solution are characterized by increased complexity due to mixed continuous-discrete design variables and discontinuous and non-convex design spaces. If standard nonlinear programming techniques are used for this type of problem, they will be inefficient, computationally expensive, and, in most cases, find a relative optimum that is closest to the starting point. Genetic algorithms are well suited for solving such problems, and in most cases, they can find the global optimum solution with a high probability. Historically, GAs were developed by John Holland and his students and colleagues at the University of Michigan, most notably David E. Goldberg and have since been tried on various optimization problems. Philosophically, GAs are based on Darwin's theory of survival of the fittest.

Genetic Algorithms is a search-based optimization technique based on the principles of Genetics and natural selection. The basic elements of natural genetics -reproduction, crossover and mutation- are used in the genetic search procedure. Following is an overview of the basic terminology required to understand GAs, the representation of the basic elements involved in them and also the description of the process for the solution of an optimization problem.

### Basic Terminology

- **Population:** It is a subset of all the possible solutions to the given problem. The population for a GA is analogous to the population for human beings except that instead of human beings, there are Candidate Solutions representing human beings.
- **Chromosomes:** A chromosome is one such solution to the given problem.
- **Gene:** A gene is one element position of a chromosome.
- **Allele:** It is the value a gene takes for a particular chromosome.
- **Fitness Function:** A fitness function simply defined is a function which takes the solution as input and produces the suitability of the solution as the output how “fit” or how “good” the solution is with respect to the problem in consideration. As it will be discussed later, in some cases, the fitness function and the objective function may be the same, while in others it might be different based on the problem.
- **Genetic Operators:** These produce new population of points or alter the genetic composition of the offspring. These include reproduction, crossover and mutation.

The basic structure of a GA is as follows; there is an initial population and parents are selected from this population for mating. After reproduction, crossover and mutation operators are applied on the parents, new off-springs occur. Finally, these off-springs replace the existing individuals in the population and the process repeats. In this way, GAs actually try to mimic the human evolution to some extent. Each of the aforementioned steps are covered in further detail in the following paragraphs.

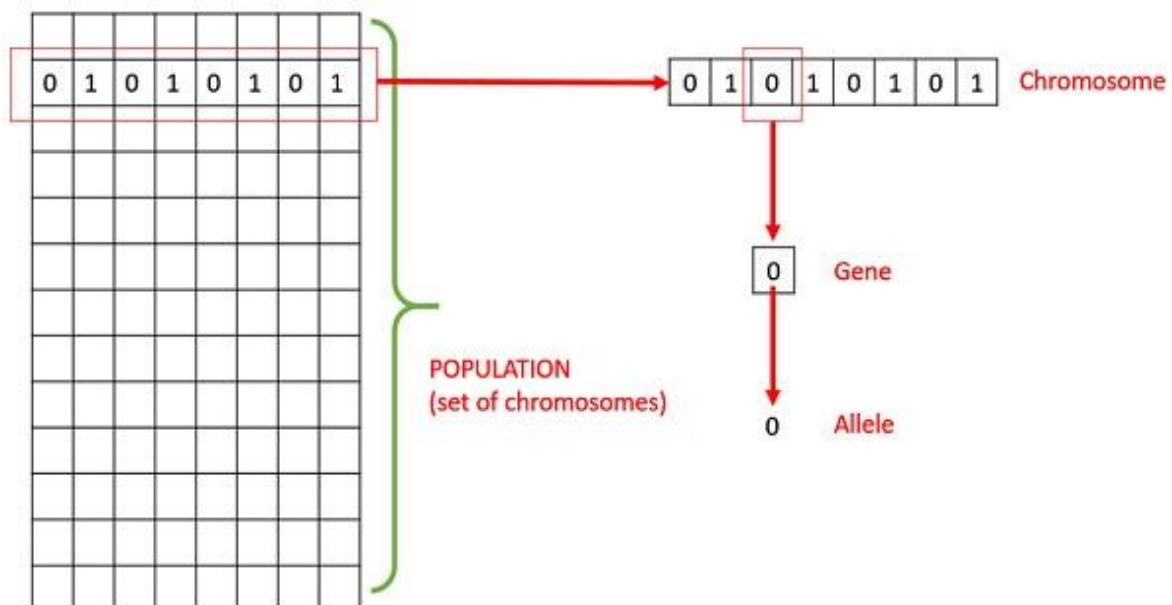


Figure 2.16: Basic terminology of GAs., [16]

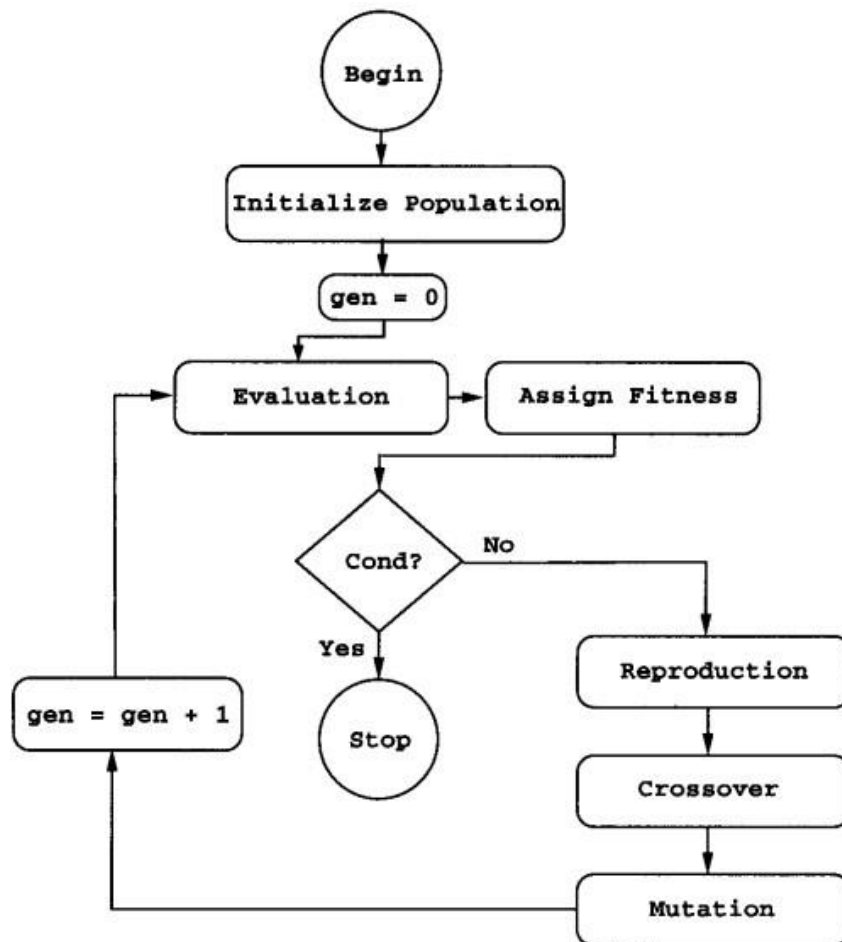


Figure 2.17: A flowchart of the working principle of a GA., [7]

### Representation of the basic elements

As indicated in Figure 2.14, in GAs the design variables are often represented as strings of binary numbers, 0 and 1, that correspond to chromosomes in natural genetics. This makes the method naturally applicable for the representation of Boolean design variables. For other problems, specifically for those dealing with integer numbers, it is possible to represent the numbers with their binary representation. For problems where it is desirable to define the genes using continuous rather than discrete variables, the real valued representation is the most natural. The precision of these real valued floating point numbers is however limited to the computer.

Because genetic algorithms are based on the survival of the fittest principle of nature, they try to maximize a function called the fitness function. The fitness function,  $F(\mathbf{X})$ , can be taken to be same as the objective function  $f(\mathbf{X})$  of a maximization problem so that  $F(\mathbf{X}) = f(\mathbf{X})$ . A minimization can be transformed into a maximization problem before applying the GA. Usually the fitness function is chosen to be nonnegative. The commonly used transformation to convert an unconstrained minimization problem to a fitness function is given by the following formula:

$$F(\mathbf{X}) = \frac{1}{1 + f(\mathbf{X})} \quad (2.5)$$

This transformation does not alter the location of the minimum of  $f(\mathbf{X})$  but converts the minimization problem into an equivalent maximization problem. (Rao, 2020 [14])

### Population

The solution of an optimization problem using a GA initiates with an initial sample of random design vectors, previously defined as population. These vectors, also known as individuals, are represented as by a string of genes forming a chromosome, in keeping with the theme of natural selection. The population size in GAs ( $n$ ) is usually fixed. The size of a GA's population should be large enough for the diversity to be maintained and not lead to premature convergence, but not excessively large as this can cause a GA to slow down. Therefore, an optimal population size needs to be decided upon trial and error.

As for the population initialization, there are two primary methods to achieve that; randomly or using a known heuristic. It has been observed that the entire population should not be initialized using a heuristic, as it can result in the population having similar solutions and very little diversity. Also, it has been experimentally observed that the random solutions are the ones to drive the population to optimality. Therefore, heuristic initialization is implemented partially, just to seed the population with a couple of good solutions, and the remaining positions are filled up with random solutions.

Regarding population models, there are two types widely in use; steady state and generational. In a steady state GA (also known as Incremental GA), in each generation one or two off-springs are generated and they replace one or two individuals from the population. In a generational model, " $n$ " off-springs are generated, where  $n$  is the population size, and the entire population is replaced by the new one at the end of the iteration.

### Operators

#### 1) Reproduction

Reproduction is the first operation applied to the population to select fit individuals to form a mating pool. The reproduction operator is also called the 'selection operator' because it selects good strings (parents) of the population. Reproduction is very crucial to the convergence rate of the GA as good parents drive individuals to better and fitter solutions.

However, care should be taken to prevent one extremely fit solution from taking over the entire population in a few generations, as this leads to the solutions being close to one another in the solution space thereby leading to a loss of diversity. Maintaining good diversity in the population is extremely crucial for the success of a GA. This taking up of the entire population by one extremely fit solution is known as premature convergence and is an undesirable condition in a GA. Therefore, to select parents wisely, one of the following methods is used.

#### *a) Fitness Proportionate selection*

Fitness Proportionate Selection is one of the most popular ways of reproduction. In this every individual can become a parent with a probability,  $p_r$ , which is proportional to its fitness. Therefore, fitter individuals have a higher chance of mating and propagating their features to the next generation.

Therefore, such a selection strategy applies a selection pressure to the more fit individuals in the population, evolving better individuals over time.

Let's consider a circular wheel. The wheel is divided into  $n$  pies, where  $n$  is the number of individuals in the population. Each individual gets a portion of the circle which is proportional to its fitness value.

Two implementations of fitness proportionate selection are possible:

*a1) Roulette Wheel Selection*

In a roulette wheel selection, the circular wheel is divided as described before. A fixed point is chosen on the wheel circumference as shown and the wheel is rotated. The region of the wheel which comes in front of the fixed point is chosen as the parent. For the second parent, the same process is repeated.

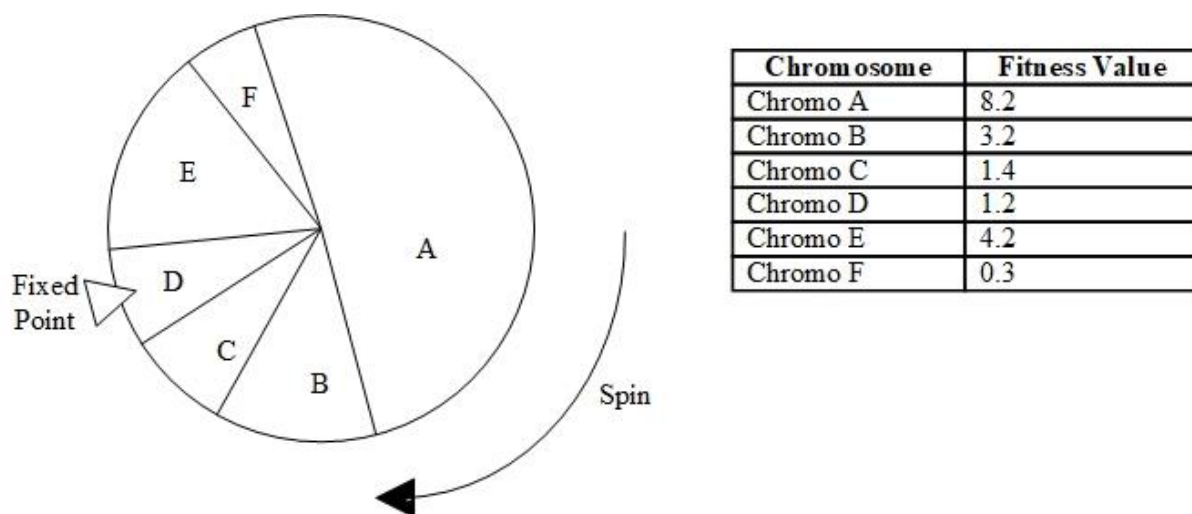


Figure 2.18: Roulette Wheel Selection for reproduction in GAs.

It is clear that a fitter individual has a greater pie on the wheel and therefore a greater chance of landing in front of the fixed point when the wheel is rotated. Therefore, the probability of choosing an individual depends directly on its fitness.

*a2) Stochastic Universal Sampling (SUS)*

Stochastic Universal Sampling is quite similar to Roulette wheel selection, however instead of having just one fixed point, there are multiple fixed points as shown in the following image. Therefore, all the parents are chosen in just one spin of the wheel. Also, such a setup encourages the highly fit individuals to be chosen at least once.

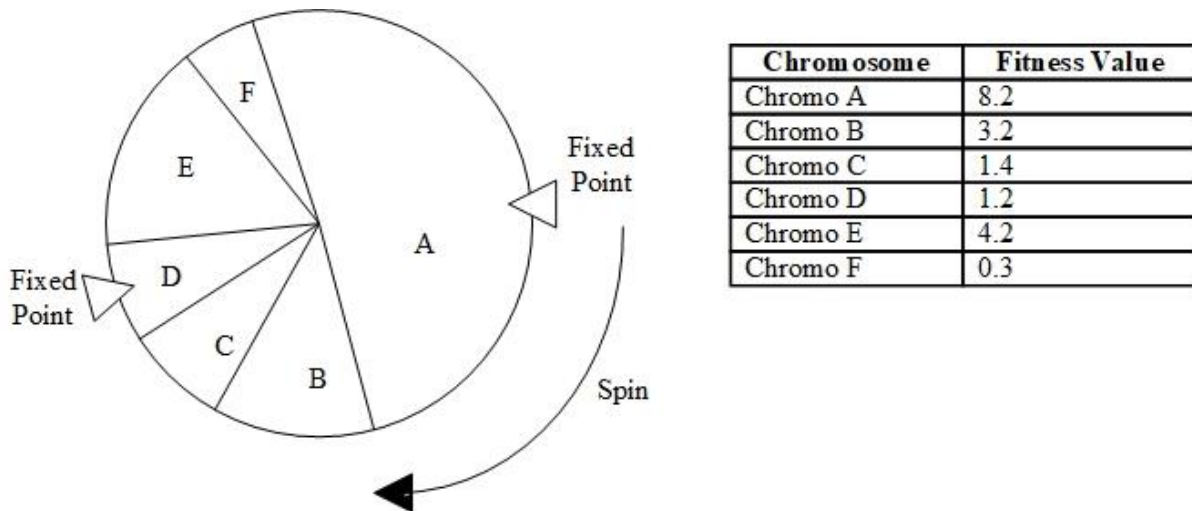


Figure 2.19: Stochastic Universal Sampling Method for reproduction in GAs.

It is to be noted that fitness proportionate selection methods don't work for cases where the fitness can take a negative value.

*b) Tournament Selection*

In K-Way tournament selection, K individuals are selected from the population at random the best out of these is chosen to become a parent. The same process is repeated for selecting the next parent. Tournament Selection is also extremely popular in literature as it can even work with negative fitness values, while the proportionate selection operator cannot since in this operator fitness values are converted to probability measures directly.

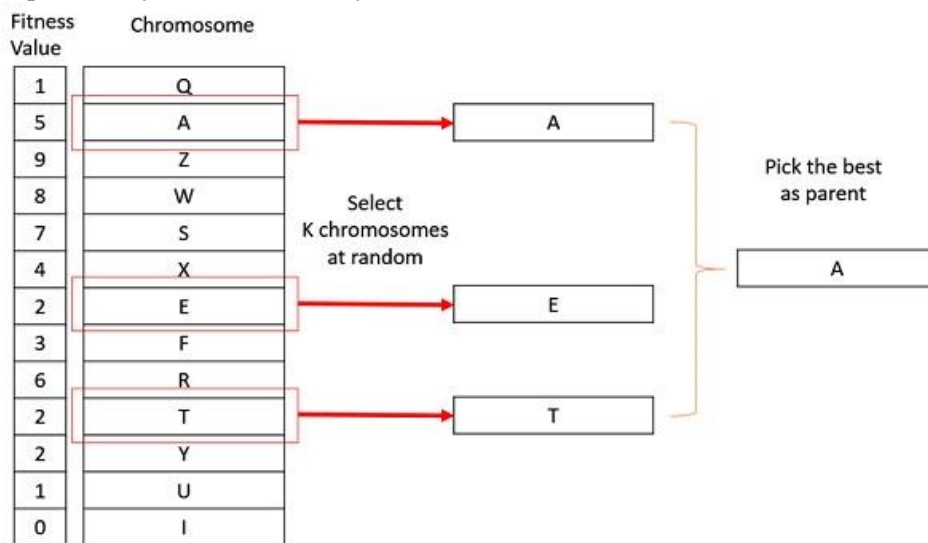


Figure 2.20: Tournament Selection method for reproduction in GAs [16]

*c) Rank Selection*

Rank Selection also works with negative fitness values and is mostly used when the individuals in the population have very close fitness values (this happens usually at the end of the run). This leads to each individual having an almost equal share of the pie (like in case of fitness proportionate selection) as shown in Figure 2.19 and hence each individual no matter how fit relative to each other has an approximately same probability of getting selected as a parent. This in turn leads to a loss in the selection pressure towards fitter individuals, making the GA to make poor parent selections in such situations.

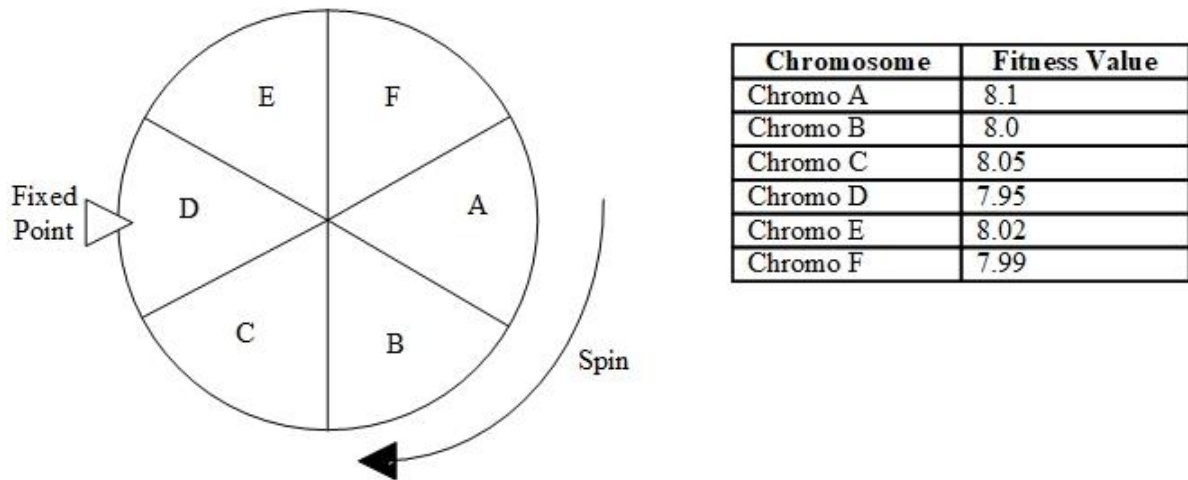


Figure 2.21: Very close fitness values of individuals in a GA.

In order to circumvent the aforementioned scenario, the concept of a fitness value while selecting a parent is partially adjusted. Instead of assigning a probability proportional to the fitness of each individual, every individual in the population is ranked according to their fitness. Therefore, the selection of the parents depends on the rank of each individual and not the fitness. As it is obvious, the higher ranked individuals are preferred more than the lower ranked ones.

Table 2.1: Example of a Rank Selection in GAs

Chromosome	Fitness Value	Rank
A	8.1	1
B	8.0	4
C	8.05	2
D	7.95	6
E	8.02	3
F	7.99	5

#### d) Random Selection

In this strategy, parents are randomly selected from the existing population. There is no selection pressure towards fitter individuals and therefore this strategy is usually avoided.

## 2) Crossover

After reproduction has been completed and the mating pool has been formed, the crossover operator is implemented. The purpose of crossover is to create new strings by exchanging information among individuals existing in the mating pool. Many crossover operators have been used in the literature of GAs. Below are presented some of the most popularly used crossover operators.

#### a) One-point crossover

In this one-point crossover, a random crossover point is selected and the tails of its two parents are swapped to get new off-springs.



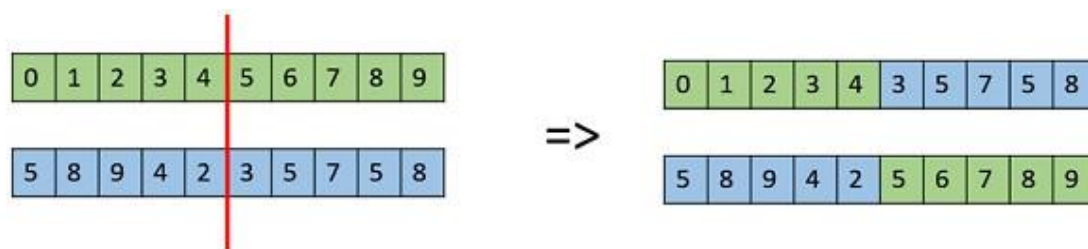


Figure 2.22: Example of One-point crossover

### b) Multi-point crossover

Multi point crossover is a generalization of the one-point crossover wherein alternating segments are swapped to get new off-springs.

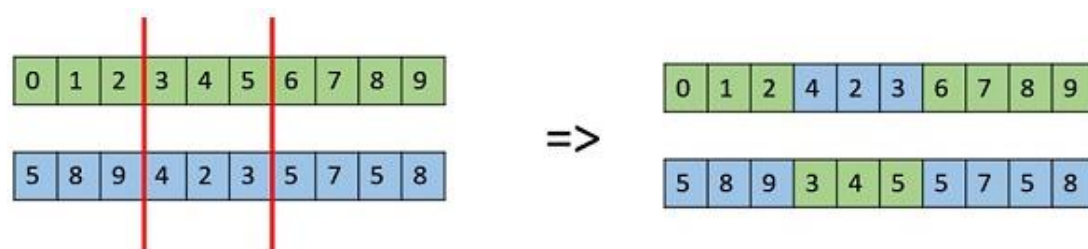


Figure 2.23: Example of Multi-point crossover

### c) Uniform Crossover

In a uniform crossover, the chromosome is not divided into segments, but rather each gene is treated separately. In this, whether a chromosome will be included in the off-spring or not, is decided upon a coin flip like experiment. There is also the possibility to bias the coin towards one parent, so as to have more genetic material in the child from that parent.



Figure 2.24: Example of Uniform crossover

Since the crossover operator combines substrings from parents with good fitness values, it is expected that their offspring will be better in that regard, provided that a suitable crossover site is selected. However, this is not known in advance and thereby is selected randomly. Hence, as one might reasonably think, it is possible that the offspring may have worse fitness than the parents. As it will be explained in the survivor selection stage, this does not ultimately affect the success of the GA. On the other hand, this ambiguity in the result of the crossover operation, indicates that not all individuals from the mating pool should be used; rather, the better ones should be preserved as part of the population in the next generation. In practice, this is achieved by using a crossover probability,  $p_c$ , to select the parent strings from the mating pool.

### 3) Mutation

The final genetic operator is mutation. As it was mentioned before, crossover is the main operator responsible for producing new strings, known as offsprings, which constitute a new generation of the

population. In simple terms, the mutation operator makes a small random tweak in the chromosome, in order that a new solution is acquired. It is used to maintain and introduce diversity in the genetic population and is usually applied with a low probability –  $p_m$ . Mutation also serves as a local search around the current solution, as it generates an individual, that is a string or design point, in the neighborhood of a current individual. If the probability is very high, the GA gets reduced to a random search.

Several methods can be used for implementing the mutation operator and below are presented some of the most commonly used ones. Like the crossover operators, this is not an exhaustive list and several different methods for mutation can be found in the literature.

#### a) Bit Flip Mutation

In this bit flip mutation, one or more random bits are selected and then flipped. This is used for binary encoded GAs.

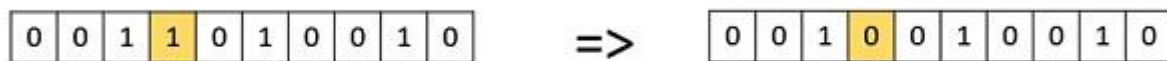


Figure 2.25: Example of a Bit Flip Mutation

#### b) Random Resetting

Random Resetting is an extension of the bit flip for the integer representation. In this, a random value from the set of permissible values is assigned to a randomly chosen gene.

#### c) Swap Mutation

In swap mutation, two positions on the chromosome are selected at random, and their values are interchanged.

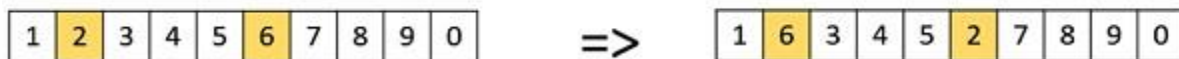


Figure 2.26: Example of a Swap Mutation

#### d) Scramble Mutation

In scramble mutation, from the entire chromosome, a subset of genes is chosen and their values are scrambled or shuffled randomly.

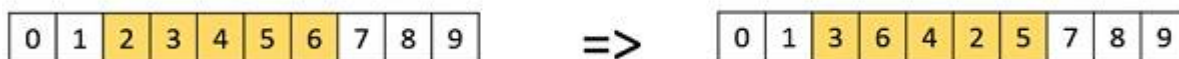


Figure 2.27: Example of a Scramble Mutation

#### e) Inversion Mutation

In inversion mutation, a subset of genes is selected, like in scramble mutation, but instead of shuffling the subset, the entire string is merely inverted in the subset.

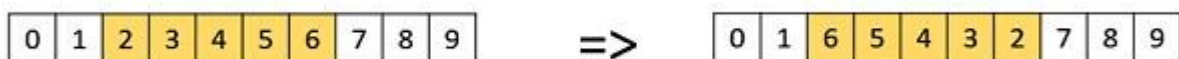


Figure 2.28: Example of an Inversion Mutation

## Survivor Selection

The Survivor Selection Policy determines which individuals are to be kicked out and which are to be kept in the next generation. It is crucial as it should ensure that the fitter individuals are not kicked out of the population, while at the same time diversity should be maintained in the population.

Some GAs employ Elitism. In simple terms, it means the current fittest member of the population is always propagated to the next generation. Therefore, under no circumstance can the fittest member of the current population be replaced.

The easiest policy is to kick random members out of the population, but such an approach frequently has convergence issues, therefore the following strategies are widely used.

### 1) Fitness Based Selection

In this fitness-based selection, the children tend to replace the least fit individuals in the population. The selection of the least fit individuals may be done using a variation of any of the selection policies described before – tournament selection, fitness proportionate selection, etc.

For example, in the following image, the children replace the least fit individuals P1 and P10 of the population. It is to be noted that since P1 and P9 have the same fitness value, the decision to remove which individual from the population is arbitrary.

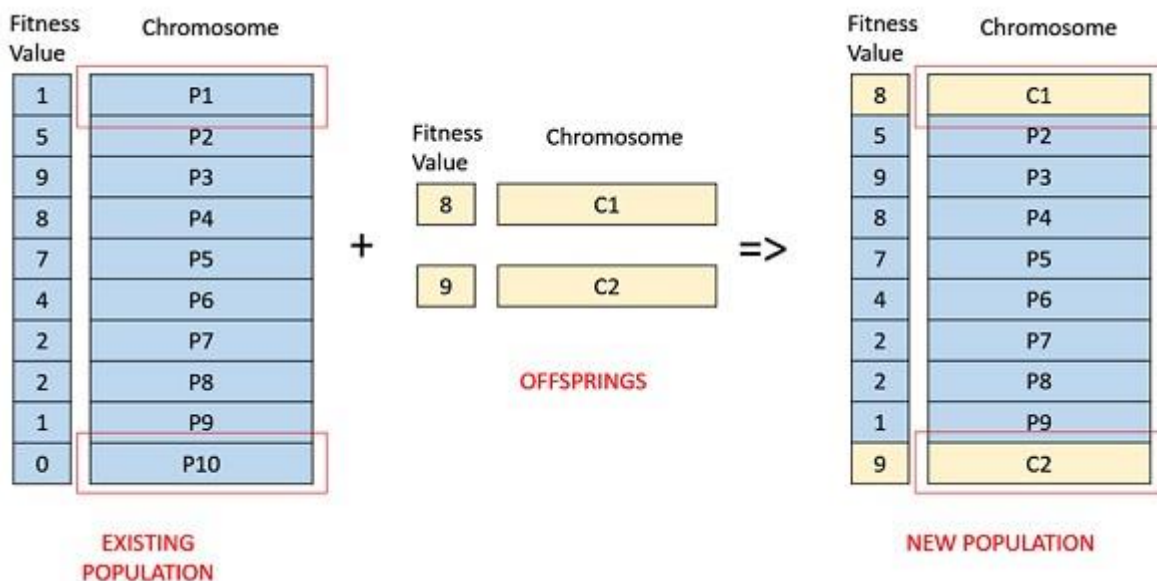


Figure 2.29: Example of a Fitness Based Survival Selection [16]

### 2) Age Based Selection

In Age-Based Selection, the notion of fitness is disregarded. This method of selection is based on the premise that each individual is allowed in the population for a finite generation where it is allowed to reproduce, after that, it is kicked out of the population no matter how good its fitness is.

For instance, in the following example, the age is the number of generations for which the individual has been in the population. The oldest members of the population i.e. P4 and P7 are kicked out of the population and the ages of the rest of the members are incremented by one.

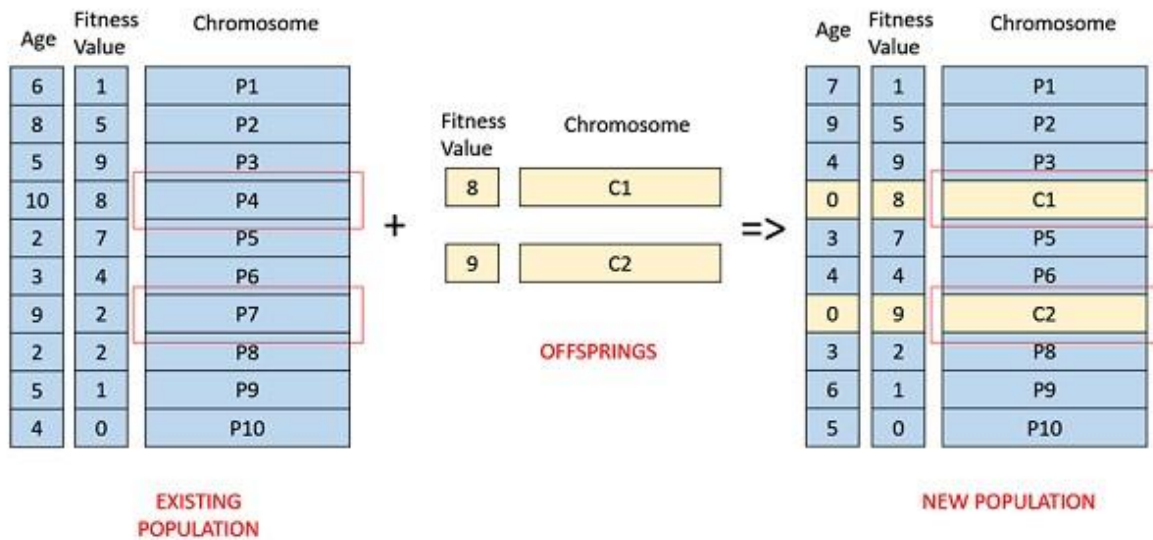


Figure 2.30: Example of an Age Based Survival Selection [16]

### Termination Condition

Every Genetic Algorithm needs a termination condition as this essentially determines when a GA run will end. Everyone running a GA will observe that initially the process progresses very quickly, with better solutions coming in every few iterations. However, this tends to saturate in later generations where the improvements are not that significant. The terminal condition has to be such that the final solution is close to optimal, at the end of the run. Usually, one of the following termination conditions are implemented:

- When there has been no improvement in the population for X iterations.
- When a certain number of generations is reached.
- When a certain pre-defined value of the objective function has been reached.

## 3 Development of the FE model

### 3.1 Introduction

The focus of this chapter is to describe the process that was followed for the development of the FE-based model of a cross-stiffened panel, often found in naval structures, subjected to loads relative to its usual applications; that is vertical pressure and tensile stress. Although, the process is the same, two different in size cross-stiffened panels were considered for reasons that will be later explained. These models were then subjected into various optimization procedures with the purpose to find the optimal design for every loading case which was considered. The chapter is organized as follows.

In Chapter 3.2, the two cross-stiffened panels which were studied are presented along with the loading scenarios for each one. After having introduced the cases under study, Chapter 3.3 is devoted to the description of the development process of the basic FE model. The process of constructing the model, the selection of elements, its discretization and meshing and finally the application of boundary conditions and loading are thoroughly explained. Finally, Chapter 3.4 focuses on the presentation of the algorithmic process developed in this work, which included creating a script code written in APDL, introducing it to the ANSYS optimizer, and finally visualizing the results.

### 3.2 Panels modeled and loading scenarios

As already mentioned ships are complex structures, comprised of various structural subsets but mostly panels. Depending on the location on the vessel, the panels can be either plane or curved and could be part of the deck or the bulkheads. In addition, the panels are stiffened accordingly (in one or two directions) in order to sustain both the global and local loads and also prevent excessive bending which in most cases is unwanted. Of course, in order to accommodate all these issues, there are different types of stiffened panels. In this work, two types of them were studied and afterwards put into optimization processes in order to compare the traditional designing methods with the more precise approach of structural optimization.

#### Cases modeled

The first type was a smaller panel which is traditionally stiffened only in one direction and is a subset of the inner bottom of almost every kind of cargo ship. That panel is found between two neighboring girders and floors as it is shown in Figure 3.1. For the purpose of this work, the dimensions of the panel's sides were derived from the midship section of an actual bulk carrier. As for the acting loads considered, a realistic approach was followed with a lean on the safer side, which means that the load considered was possibly a bit larger than the actual load.

As for the reasons behind choosing to model this type of a stiffened panel, there are several reasons for this. First of all, this is arguably the most commonly stiffened panel found in almost every kind of cargo ship, as stated above. This type of panels is ubiquitous in bulk carriers and oil tankers, although they are employed in different shapes and sizes at each case. The second reason for this choice was the interest to see how an optimizer would choose to distribute the number of stiffeners along the 2 possible directions (transverse and longitudinal) and the quantity of material in general, in a panel which is

located between two neighboring girders and floors and is traditionally stiffened only in the longitudinal direction.

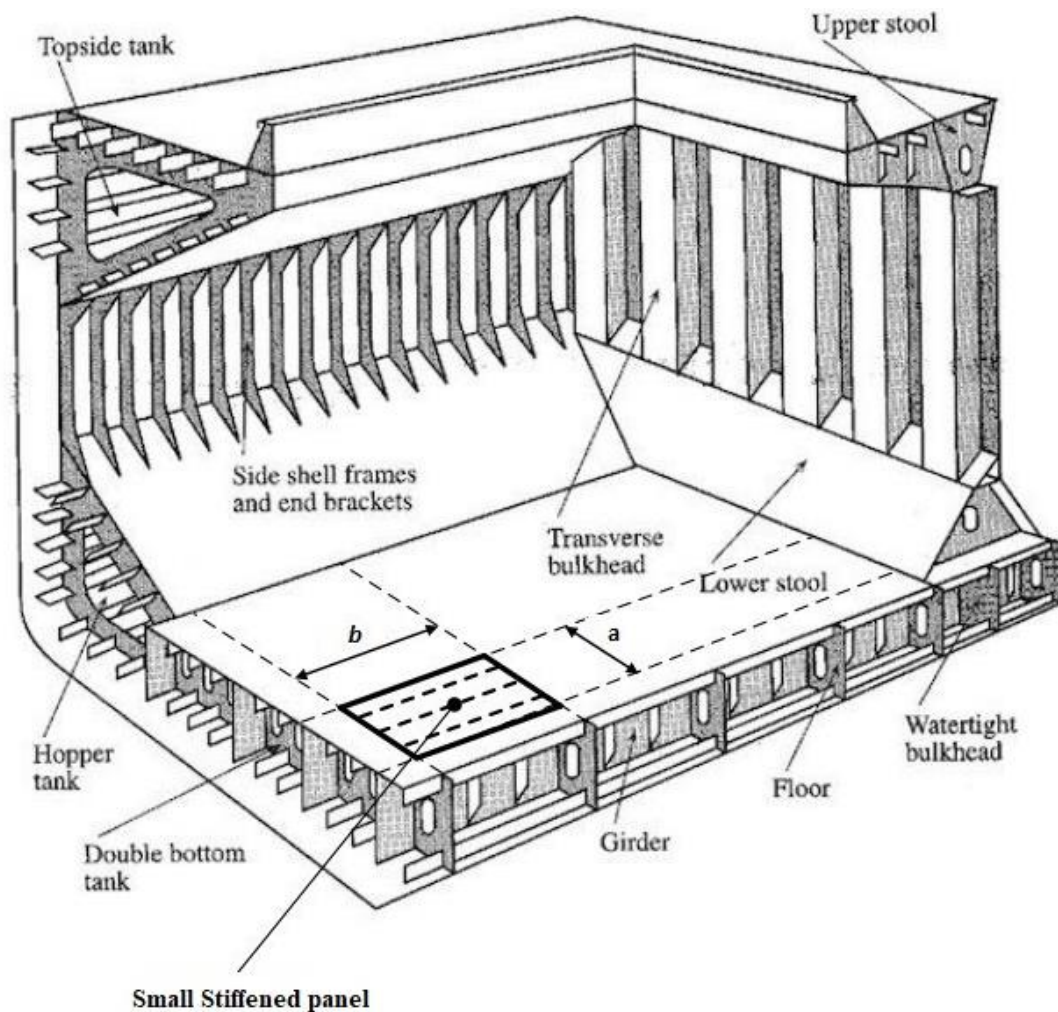


Figure 3.1: Stiffened panel between 2 neighboring girders and floors at a bulk carrier's hold., [11]

The second type of panel modeled in this work was a bigger panel which is traditionally cross stiffened and that is the car deck or tween deck of most passenger ships. These panels are usually fixed at their ends at the side shells of the vessel and are supported by vertical pillars at specific points along their length. The reference model for this second panel was derived from a Ferry RO-RO studied in [17)18)] and is depicted in Figure 3.2. From this work, the length of the two sides and the number of vehicles loading the plate were kept as guides. As for why this case of a cross-stiffened panel was chosen to be modeled, one reason was to see how a panel with longer sides would affect the configuration of the stiffeners after the optimization process would have taken place. In this second case, the panel is not supported with proximate boundaries (e.g. girders and floors) and so the unsupported length of the plate is greater than in the first case. The second reason for choosing to model a panel with more elongated sides was to see how the optimizer would choose to reinforce such a panel, which is traditionally cross-stiffened as mentioned earlier, in terms of stiffener type and scantlings.



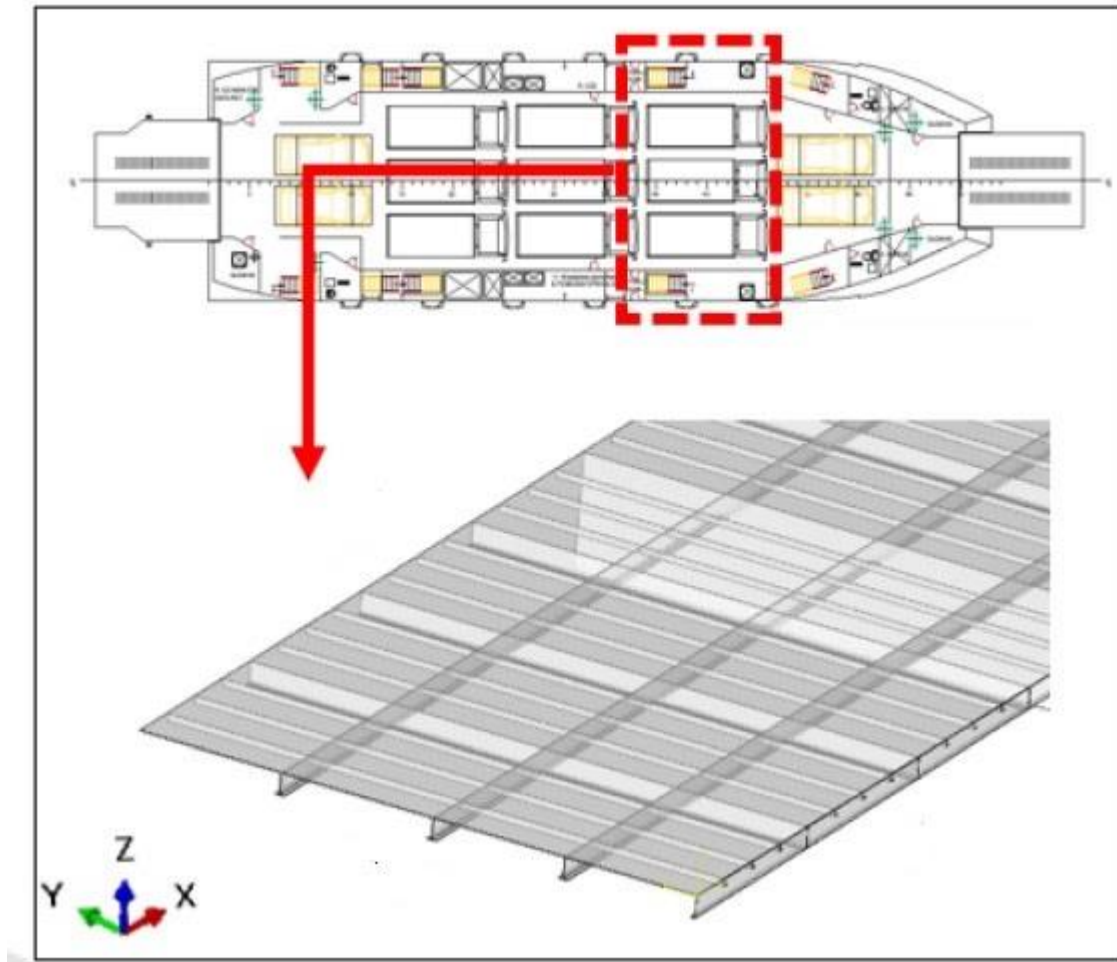


Figure 3.2: CS panel from the car deck of a passenger ship [17]18]

The dimensions of sides of each panel are given in Table 3.1. To avoid misconceptions, from now on the side named as “a” is parallel to the x axis, and the side named as “b” is parallel to the y axis.

Table 3.1: Dimensions of the sides of the two panels modeled

	a (mm)	b (mm)
<b>Small stiffened panel (case 1)</b>	2580	2850
<b>Car Deck (case 2)</b>	14000	11000

### Loads

As the inspiration for this work were structural subsets often found in naval structures and specifically ships, the loads ought to resemble to the loads that are exerted in such structural parts.

Traditionally, the study of ship strength is divided in various stages, during which the entire structure or certain of its components are considered as if subjected individually to some form of structural loading. In the first stage, which comprises a coarser approach, the ship is supposed to be afloat in still water and only static loads act on it, as a result of the combination of gravity forces, i.e. weight and buoyancy forces. Buoyancy forces occur as the integration of the hydrostatic pressure on the immersed

external area of the ship's hull. On the other hand, weight forces occur from the structure's own weight along with the loading due to cargo. The load effect caused by the unequal distributions of weight and buoyancy along the length of the ship, accentuated by waves, is what is essentially considered at this first stage. A typical case of this type of loading, as well as the resultant shear force ( $Q$ ) and bending moment ( $M$ ) distributions are shown in Figure 3.3.

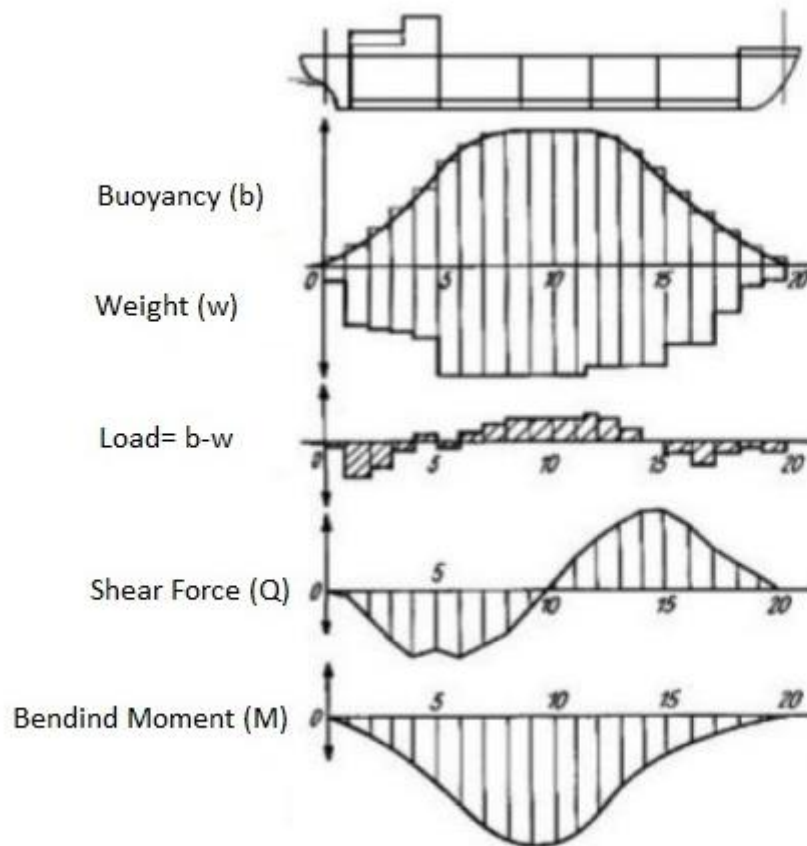


Figure 3.3: Ship static loads, Shear Force and Bending Moment Distributions, [1]

That bending moment results in a linear distribution of normal stress, also called the bending stress distribution, along the vertical axis of every section of the ship. The longitudinal bending stress is greatest at the extreme upper or lower edge of the section (deck and keel) and has a zero value at the neutral axis, as it is shown in Figure 3.4 from Hughes and Paik (2010), [9].

As the values of the normal stress pass from positive to negative, the corresponding structural members, which receive those stresses, pass from tension to compression. The studying of the local loading of each structural member comprises the second stage of study of a ship's strength. Finally, the third stage of the study of a ship's strength, copes with the strength calculation of the plates which are between the stiffeners, under the action of hydrostatic pressure.



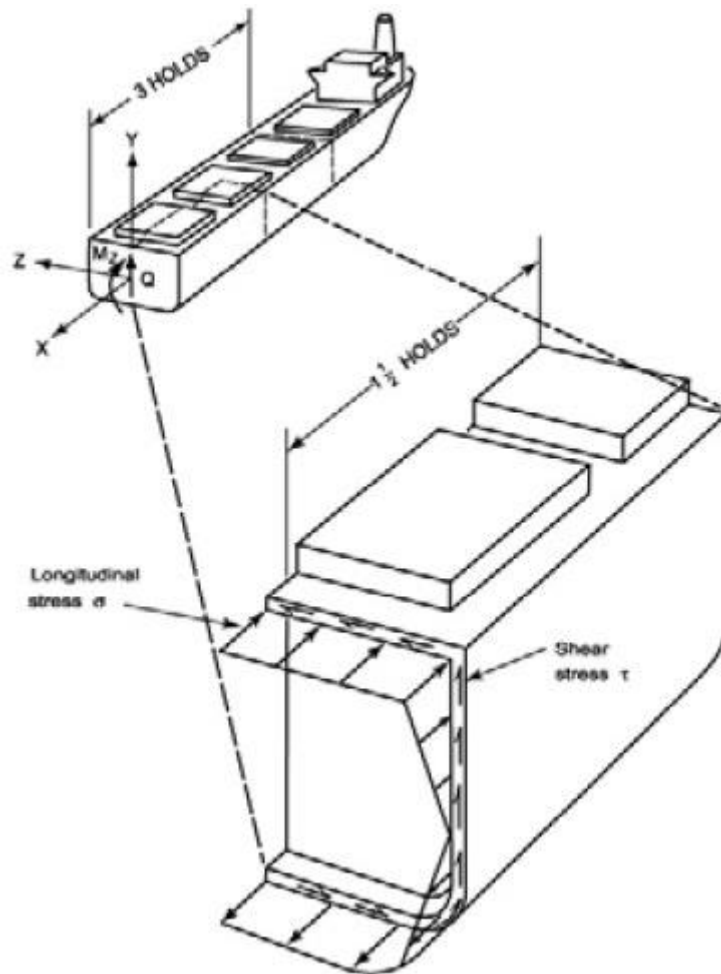


Figure 3.4: Bending stress distribution of a midship section., [1]]

In this work, the necessary theoretical background for the induced phenomena was provided by the 2<sup>nd</sup> and 3<sup>rd</sup> aforementioned stages. More specifically, the loading conditions to which the cross stiffened panels were subjected are divided into two categories: a) uniform vertical pressure on the unstiffened side of the cross stiffened panel and b) uniform vertical pressure on the unstiffened side of the cross stiffened panel and uniform axial stress along side “b”. To give an illustration of the loading conditions, a figure of the compound loading on an unstiffened panel is given below.

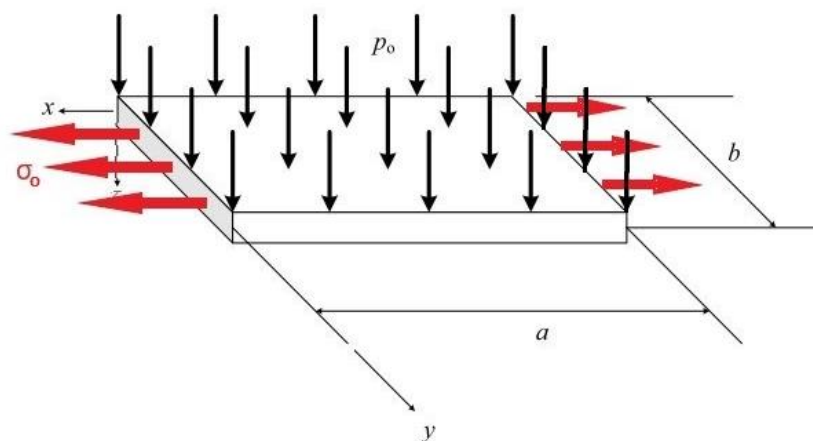


Figure 3.5: Compound loading on an unstiffened panel., [1]]

In order to have a better insight of the way the loading affects the design of a cross-stiffened panel, three levels of intensity were considered for each loading case: low, medium and high. The levels of loading for the two panels examined are presented below.

Table 3.2: The 3 Levels of intensity for the loading of the panels

Intensity	Pressure only	Pressure and stress
LOW	$\frac{p}{4}$	$\frac{p}{4} + \frac{\sigma}{4}$
MEDIUM	$\frac{p}{2}$	$\frac{p}{2} + \frac{\sigma}{2}$
HIGH	$p$	$p + \sigma$

Obviously, the table above contains parameters and not exact numerical values. However, the numerical values that those parameters got were carefully chosen so that they respond to a real case loading scenario in which each panel would be subjected to.

### Pressure p

#### A) Small stiffened panel

As it was mentioned earlier, the initial inspiration for the small cross stiffened panel was the inner bottom of a cargo hold of a bulk carrier. The heaviest loading condition for such kind of a hold (located near the midship section) is when they are used as heavy ballast tanks (i.e. when they are filled with water for strength or stability reasons). Thus, the pressure  $p_0$  is representing the hydrostatic pressure exerted from the ballast into the hold. In fact, the procedure prescribed by the CSR[10] for the calculation of internal loads was followed in order to secure the rationality of the loads and also that they are relatable to the scale of the structural subset to be modeled. More specifically, the pressure  $p$  was calculated by the following formula:

$$p = \rho_L g (Z_{top} - Z) \approx 200 \text{ kN} / \text{m}^2$$

where:

- $\rho_L = 1,025 \text{ t/m}^3$ , density of liquid in the tank
- $g = 9,81 \text{ m/s}^2$ , acceleration of gravity
- $Z_{top} = 20,5 \text{ m}$ , Z coordinate of the highest point of tank
- $Z = Z_{INNER \text{ BOTTOM}} = 1,95 \text{ m}$

#### B) Car Deck

The dimensions for the big cross stiffened panel were chosen so that it fits 3 trucks, as it is shown in Figure 3.2. The weight of each truck was estimated at 25t. The total weight was hypothesized to be distributed evenly upon the surface of the panel. Thus, the pressure for the 2<sup>nd</sup> case, was a result of the following calculations.

$$A = a \cdot b = 14m \cdot 11m = 154m^2$$

$$p = \frac{W_{total}}{A} = \frac{3 \cdot 25t}{154m^2} = 0,487 \frac{t}{m^2} = 4,777kPa \approx 5kPa$$

### Axial Stress $\sigma$

In order not overcomplicate things and as the purpose of this thesis is in essence demonstrational and not design, the value for the axial stress chosen was  $\sigma=120$  MPa for both cases. In this way, there was adequate of room for stressing the plate more (with vertical pressure) until it reaches its yield stress limit.

### Boundary Conditions

As already mentioned, cross stiffened panels are often smaller structural members in bigger structural entities. The boundaries, i.e. the four sides of a plate, are considered as fixed, simply supported, or elastically supported, in accordance with the kind of loads. The type of boundary supporting conditions is very important because the calculated deformation and stress depend on these conditions.

Regarding the boundary conditions in this work, all the simulations were concerning only clamped panels. The mathematical formulation of the boundary conditions for a clamped plate are presented below. The vertical deflection is signed as “w”.

The vertical translation of all sides is restricted. This is translated in mathematical terms as:

$$w = 0 \Big|_{x=0, x=a, y=0, y=b}$$

In addition, each side is restricted from freely rotating around the global cartesian axis parallel to it. This means that the slope is equal to zero at all sides and in mathematical terms:

a) For sides  $x=0$  and  $x=a$ :

$$\frac{\partial w}{\partial x} = 0 \Big|_{x=0, x=a}$$

b) For sides  $y=0$  and  $y=b$

$$\frac{\partial w}{\partial y} = 0 \Big|_{y=0, y=b}$$

### 3.3 The FE model

For the two types of stiffened panels presented in the previous chapter, one unified model was developed using the commercial software ANSYS 19.2, and more specifically using its built-in programming language APDL. The reason why APDL scripting was chosen as the way to develop the model, was that it allows for it to be parametrically built, which was essential for the optimization process that followed afterwards. In addition, APDL scripting allowed for certain post-processing functions to be included in the code, which were also necessary for the definition of the constraints required for the optimization problem. At this point, a detailed description of how the FE model was developed is made.

As in every FE commercial software, the first step towards a structural analysis is to develop the geometric model of the structural subset. However, during the shaping of the geometry of the model, the analyst must bear in mind the fashion that this model will be meshed and that is what happened also in this work. As it will be explained later in this chapter, the goal was to model the mid-surface of the plate as all the finite elements that would be used at the meshing stage were two-dimensional elements. Thus, the creation of the geometry began by creating small rectangles next to each other as it is shown in Figure 3.6, almost replicating the way a floor would be filled with tiles. More specifically, the imaginary floor of area " $a \times b$ " was filled in the following fashion; beginning from the origin of a cartesian coordinate system, a rectangle was copied  $i$  times to the x-direction therefore forming a row of rectangles. For each rectangle of this row, a relative column was formed by copying a similar rectangle  $j$  times to the y-direction. The values the parameters  $i$  and  $j$  got, were dictated by the desirable number of stiffeners the user would define. The end result of this process is given in Figure 3.7, which shows a model developed with ANSYS. The formed lines that distinguish each rectangle from the other will enable the meshing of the plate with two different finite elements, without though requiring a three-dimensional geometry.

As for the material properties of the panel, these were chosen based on what is mostly applied on naval structures and that is some type of steel. For the specific models developed for this thesis, it was chosen Grade "A" mild steel with  $E=207$  GPa and  $\nu=0,3$ .

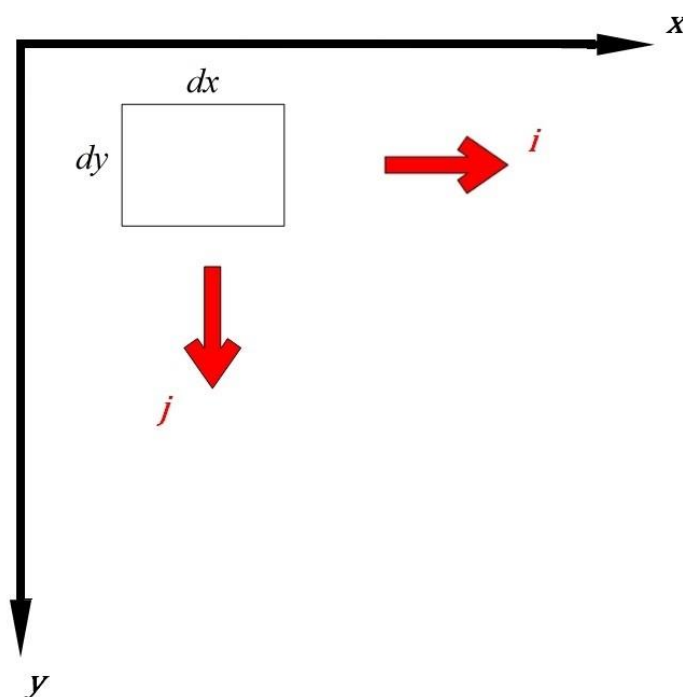


Figure 3.6: Creation of the cross-stiffened panel in "tile-wise" fashion

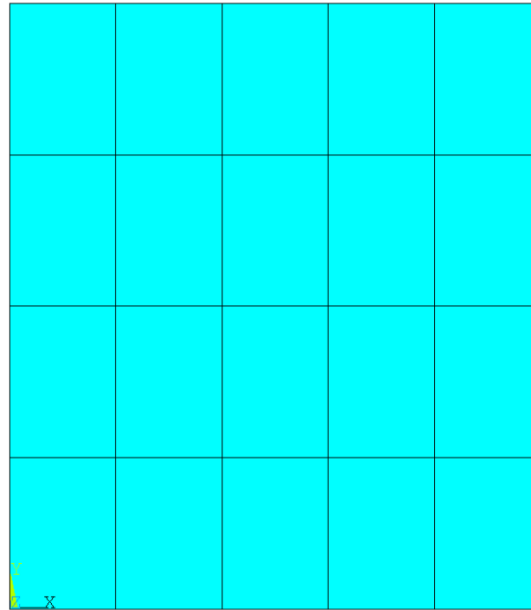


Figure 3.7: 2D model of a cross stiffened panel created in “tile-wise” fashion

After having established the geometry along with its physical and material properties, the next step in the development of the FE model was to select the types of elements to be used. As the model would be subsequently put in an optimization process which requires this model to be solved numerous times, a complex three-dimensional model with multiple DOF's and thus unknown variables would be undesirable as it would increase computational cost. Instead, a simplified version of a cross-stiffened panel requiring only the midplane to be created for its representation was chosen to be developed. This was possible because the models that were solved were adequately thin so that they could be considered as a two-dimensional problem. Thus, two-dimensional elements were the qualified choice, contributing to the creation of a versatile and computationally advantageous model.

As mentioned also in the Chapter 2.2.4, for the meshing of the solid model two elements were needed; one beam element for the stiffeners and one shell element for the plate. The beam element that was used as featured in ANSYS was BEAM189, a quadratic three-node beam element with six DOFs occurring at each node; these include translations in the x, y and z directions and rotations about the x, y and z directions. The shell element supported by ANSYS that was used was SHELL281, an eight-node shell element (i.e. shell element with a mid-side node) with the same six DOFs as the beam element at each node.

With the element types selected, the next step in the process is the discretization of the model. Having created the solid model of the cross-stiffened panel in “tile-wise” fashion, the available way of meshing it was to divide the sides of each small rectangular created (i.e. sides dx and dy in Figure 3.6). The initial idea was to make a structured mesh with elements having length equal to  $a/20$  and width of  $b/20$ . However, due to the aforementioned dependency of the mesh to the stiffeners' configuration, the best way found by the writer to emulate the initial idea was to divide the sides of the each small rectangular in such number of elements so that the total elements per sides a and b would be close to 20. To achieve that, the following command was written in the APDL script:

$$\text{number of deviations per side } dx = \text{NINT} \left( \frac{\text{number of deviations per side } a \text{ (i.e. 20)}}{n_y + 1} \right) \quad (3.1)$$

where  $n_y$  is the number of transverses and  $NINT(X)$  is an APDL command which gives the nearest integer to  $X$ . Similarly, for the transverses the relative command was:

$$\text{number of deviations per side } dy = NINT\left(\frac{\text{number of deviations per side } b \text{ (i.e. 20)}}{n_x + 1}\right) \quad (3.2)$$

where  $n_x$  is the number of longitudinas.

During the meshing stage they were also some properties assigned to the aforementioned element types. More specifically, for the beam elements there were three possible options for the user to choose between section types and these were: a) flat bar, b) T-type and c) L-type. To fully define each of these sections, there are four parameters that have to be given numerical values and these are  $tw$  (i.e. web thickness),  $hw$  (i.e. height of web),  $bf$  (i.e. breadth of flange) and  $tf$  (i.e. flange thickness). Obviously, in case the flat bar is chosen as section type, the last two parameters will be ignored. As for the shell elements, only the plate thickness ( $tpl$ ) is needed to be given. Those five parameters are depicted in Figure 3.8 for the case of a T section.

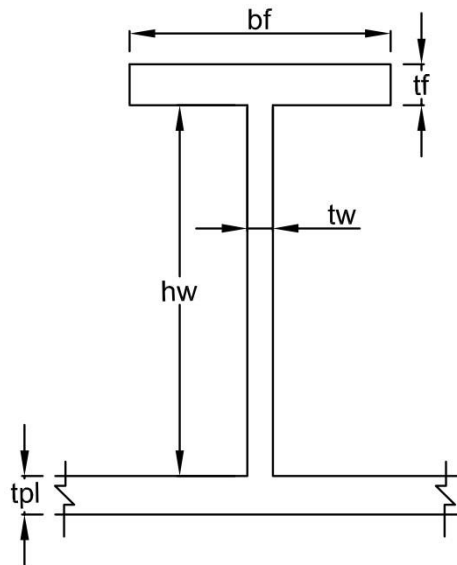


Figure 3.8: T section along with its 5 parameters

Finally, the last step before obtaining post-processing results is the correct implementation of the boundary conditions and loads described in Chapter 3.2. However, the numerical implementation of the boundary conditions was not the same for the two types of loading scenarios described in the previous chapter. As already mentioned in Chapter 3.2, the model was clamped at all four edges. Therefore, for all the loading scenarios where only uniform vertical pressure was applied, the three translational DOFs ( $u_x, u_y, u_z$ ) of all the nodes located on the four edges were set to zero. In addition to this, for the sides parallel to the  $x$ -axis the rotational DOF  $\theta_x$  was restricted, while for the sides parallel to the  $y$ -axis the rotational DOF  $\theta_y$  was restricted. As for the loading scenarios including the application of the tensile stress  $\sigma_x$  the rotational and translational constraints stayed the same, with the exception that the sides located at  $x=L$ ,  $y=0$  and  $y=b$  were left to move freely along the  $x$ -axis (i.e.  $u_x \neq 0$ ) in order that the model would not become over-constrained.

As for the application of loads, the only particularity was found at the application of the tensile stress. Since only the midplane of the cross-stiffened panel was designed, it was not possible to apply uniform pressure on the side  $x=L$  as there was no cross section there in the sense of a transverse plane. To bypass this problem, a statically equivalent force with value  $F = \sigma_x \cdot A$  (given that the value of  $\sigma_x$  is known) where  $A$  is the cross-sectional area of the side  $x=L$  (including the area of both the plate's lateral area and the stiffeners' area). Obviously, to avoid uneven pulling of the side (as shown in Figure 3.9), the displacement  $u_x$  was coupled for all the nodes lying at the side  $x=L$ . In Figure 3.10, an example of the solid modeling is shown, along with the all the boundary conditions and loads applied.

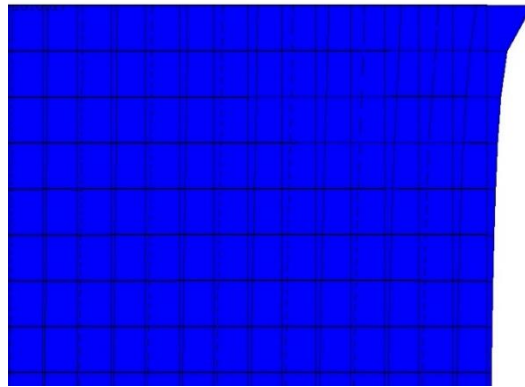


Figure 3.9: Uneven pulling of the plate in case DOFs of side are not coupled

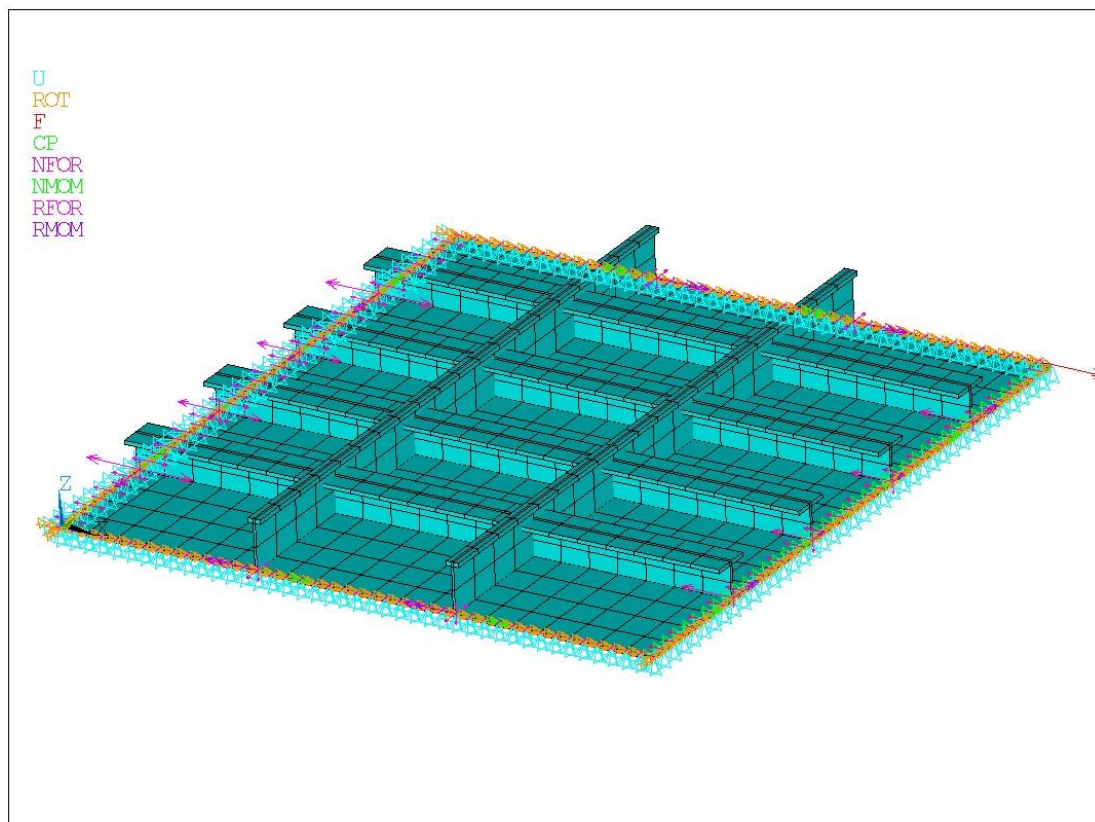


Figure 3.10: Solid element model with all the loads and boundary conditions applied

The results that occurred from the post-processing stage of the best candidate solutions from the optimization process will be presented in the next Chapter.

### 3.4 Algorithmic Process

As it was mentioned in the Abstract, the goal of this thesis is to provide a tool towards optimization-based design. Thus, since the beginning, the main objective of this work was to develop an algorithmic process, comprised of discrete steps, which if followed, will hopefully provide the designer with a better, more optimized design than what the rule-based approach would. To fully understand the optimization problem with which this thesis deals, its fundamental elements have to be presented first. Hence, in this chapter, the basic features related to problem will be introduced and these are the input variables, the constraints, the objective function and some optimization settings that ANSYS Workbench requires.

First of all, it should be noted that before commencing this optimization process 4 parameters should be given by the designer as initial data and remain constant and these are the length of the two sides of the plate (i.e.  $a$ ,  $b$ ) and also the loading of the plate (i.e. the magnitude of pressure  $p$  and that of tensile stress  $\sigma_x$ ). Furthermore, as the title of this thesis suggests, this is a weight optimization of a cross-stiffened panel, thus the objective function should be the mass. However, for the sake of ease and also to simplify the objective function, it was chosen to calculate the volume of the cross-stiffened panel instead of the mass, as the density of the material (here the steel) remains constant throughout the whole structure (isotropy). Therefore, the objective was eventually the minimization of the volume of the cross-stiffened panel.

As it is known from the theory of optimization, the objective function can approach its optimum value, if the values of the design variables are altered appropriately. The optimization problem in here was comprised of thirteen variables in total. The name of each variable is presented below along with the upper and lower limit of each one, as they were set for the optimization process. The increment for each variable was 1 unit. For the car deck the upper bound for the number of stiffeners ( $n_x$ ,  $n_y$ ) was set to 20 (i.e.  $**$  sign) instead of 10 as the covering area was larger. It should be noted that the ranges for the sections' parameters were chosen according to the scantlings of stiffened panels found in naval structures.

Table 3.3: Design variables and their ranges of value

<b>Input Variables</b>	<b>Lower Bound</b>	<b>Upper Bound</b>
<b>nx</b>	0	10(20**)
<b>ny</b>	0	10(20**)
<b>t_pl</b>	5	30
<b>Stif_type_long</b>	1	3
<b>Stif_type_trans</b>	1	3
<b>tw_x</b>	5	30
<b>hw_x</b>	100	500
<b>bf_x</b>	50	250
<b>tf_x</b>	5	30
<b>tw_y</b>	5	30
<b>hw_y</b>	100	500
<b>bf_y</b>	50	250
<b>tf_y</b>	5	30



where:

- nx=number of stiffeners which extend along the x-axis (i.e. longitudinals)
- ny=number of stiffeners which extend along the y-axis (i.e. transverses)
- t\_pl=thickness of plate
- Stif\_type\_long= Stiffener type of longitudinals (1=flat bar, 2=T, 3=L)
- Stif\_type\_trans= Stiffener type of transverses (1=flat bar, 2=T, 3=L)
- tw\_x=thickness of web of longitudinals
- hw\_x=height of web of longitudinals
- bf\_x=beam of flange of longitudinals
- tf\_x=thickness of flange of longitudinals
- tw\_y=thickness of web of transverses
- hw\_y=height of web of transverses
- bf\_y=beam of flange of transverses
- tf\_y=thickness of flange of transverses

As every well-defined optimization problem, this one as well is subjected to some constraints. In this problem, the measures that act as constraints are related to the mechanical strength of the material used as well as some geometric constraints, taken from the CSR [10]), which ensure that buckling of the stiffeners will be avoided. As it has already been mentioned, the chosen material for these simulations was mild steel whose yield tensile strength is 235 MPa. All the constraints implemented and their meaning are presented in the table below.

Table 3.4: Constraints and their ranges of value

Constraints	Lower Bound	Upper Bound
<b>rf_x</b>	1	-
<b>rf_y</b>	1	-
<b>rw_x</b>	1	-
<b>rw_y</b>	1	-
<b>Maxshellstress</b>	-	235
<b>t_x</b>	-	135,6
<b>sb_max_x</b>	-	235
<b>t_y</b>	-	135,6
<b>sb_max_y</b>	-	235

where:

- $r_f = \frac{t_f C_f}{b_{f-out}}$ , where pointers x and y correspond to longitudinals and transverses

respectively (the ratio will be explained further right below)

- $r_w = \frac{t_w C_w}{h_w}$ , where pointers x and y correspond to longitudinals and transverses

respectively (the ratio will be explained further right below)

- Maxshellstress=maximum Von Mises stress at shell elements
- t\_x, t\_y=Maximum shear stress at longitudinals and transverses respectively
- sb\_max\_x, sb\_max\_y=maximum bending stress at longitudinals and transverses respectively

The ratios  $\Gamma_f$  and  $\Gamma_w$  were initially taken from the CSR but were appropriately modified afterwards so that they suit the needs of the problem. More specifically, in order that the buckling of the stiffeners is avoided, it is advised by the CSR [10] that the inequalities shown in Figure 3.11 apply. The modification in the below inequalities was that the terms  $h_w$ ,  $C_w$  and  $b_{f-out}$ ,  $C_f$  were taken to the left hand-side of the inequality, so that the right-hand side includes only known quantities (i.e. here it is equal to 1).

a) Stiffener web plate:

$$t_w \geq \frac{h_w}{C_w} \sqrt{\frac{R_{eH}}{235}}$$

b) Flange:

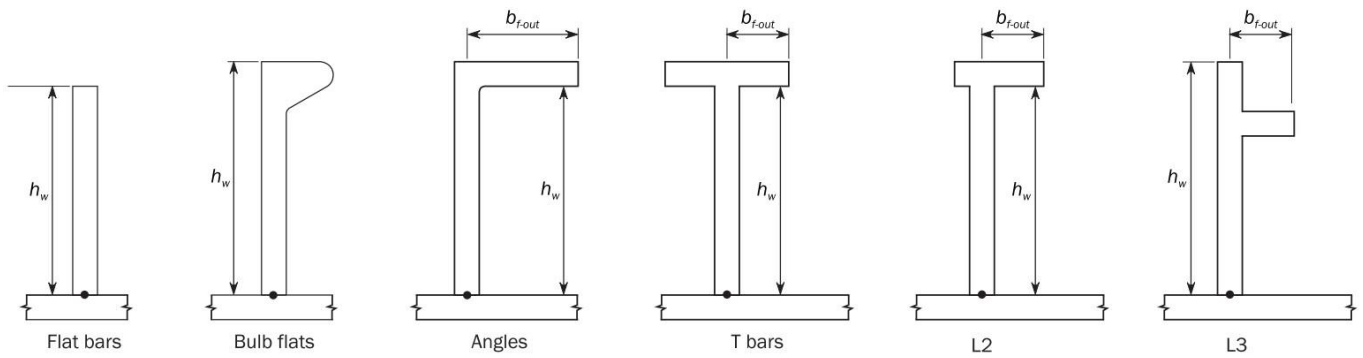
$$t_f \geq \frac{b_{f-out}}{C_f} \sqrt{\frac{R_{eH}}{235}}$$

Figure 3.11: Criteria for net thickness of stiffeners., [10]

where  $R_{eH}$  is the yield stress limit. For mild steel  $R_{eH}=235$  MPa so the fraction under the square root equals to 1 (which explains the value of the lower bound of  $\Gamma_f$ ,  $\Gamma_w$  at Table 3.12)

$C_f$  and  $C_w$  are slenderness coefficients whose value differentiates depending on the type of the stiffener. The value for each type and the meaning of the parameter  $b_{f-out}$  are given in Figure 3.12 which was taken from the CSR [10].

As for the optimization settings required by ANSYS Workbench environment, the optimization method used was MOGA (i.e. Multi-objective Genetic Algorithm) which, as its name suggests, can solve optimizations problems comprised of one or even more criteria. In addition, the number of initial samples was set to 100 and within each iteration 50 more samples were produced. As an alternative termination criterion to the convergence of the objective function, the maximum number of iterations was set to 30 and the maximum number of Candidate points produced per case was 3. Lastly, the sequence of actions that comprise the algorithmic process followed in this work are presented in a flowchart in Figure 3.13.

**Table 1 : Slenderness coefficients**

Type of Stiffener	$C_w$	$C_f$
Angle, L2 and L3 bars	75	12
T-bars	75	12
Bulb bars	45	-
Flat bars	22	-

Figure 3.12: Values of Slenderness coefficients for each case., [10]

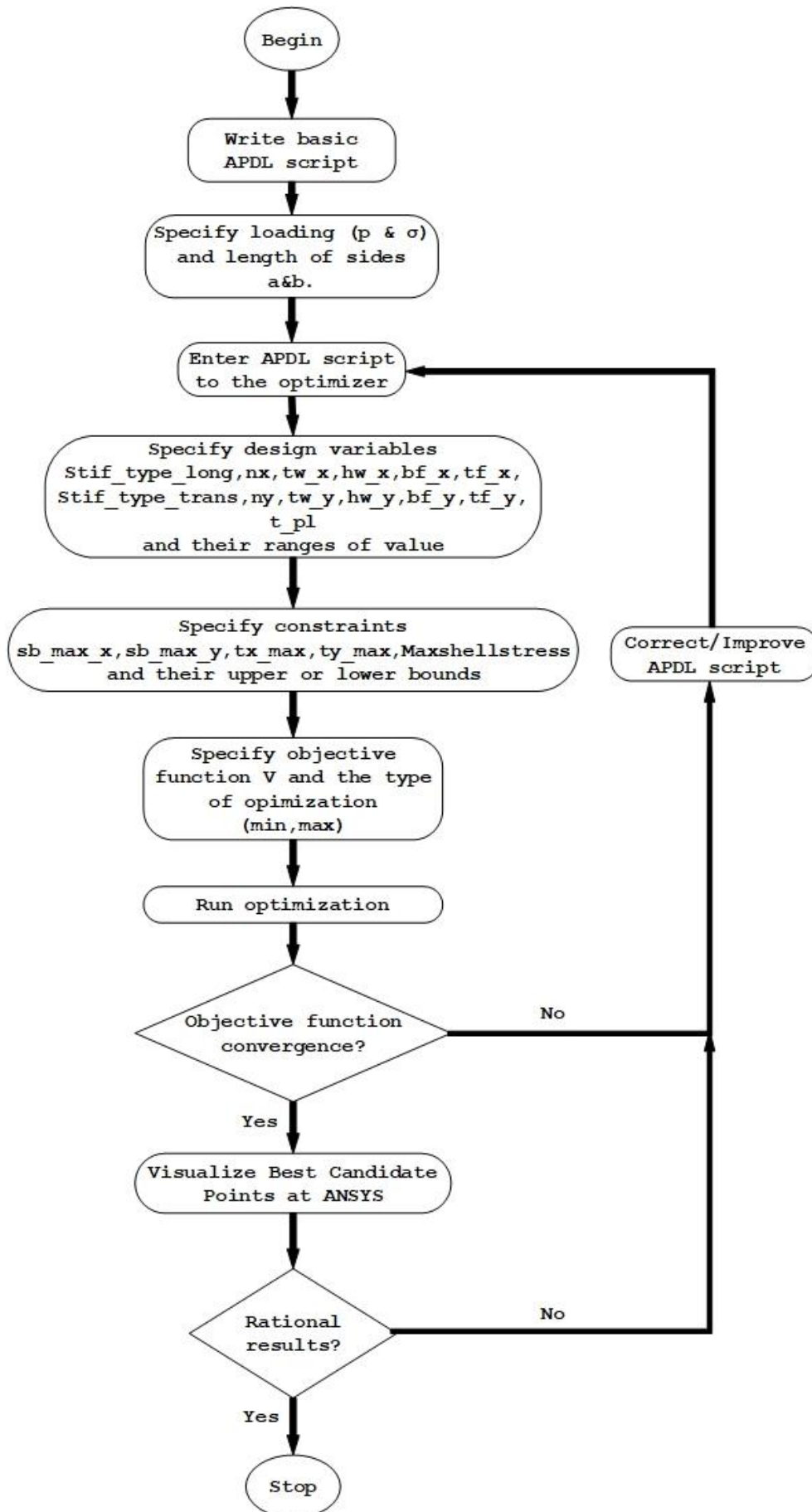


Figure 3.13: Flowchart of algorithmic process

## 4 Indicative results

### 4.1 Introduction

In this chapter some indicative results from the optimization processes performed will be introduced. More specifically, for every loading scenario described in Chapter 3.2 the results will be presented in the following fashion; For every case, the values of the 13 input variables of the 3 Candidate Points that the Algorithm gave will be listed. As previously stated, the optimization method was set to give at maximum 3 Candidate Points as solutions of the optimization problem. In order to give an illustration of the solution, there will be four contour plots of one Candidate point for each case. The first contour plot will be showing the Von Mises Stress for the shell elements, the second and the third one (transverses and longitudinals) will be showing the bending stress for the beam elements and the fourth one will be showing the vertical translation ( $U_z$ ) of the whole cross-stiffened panel. If all the values of the input parameters of 2 or more Candidate points coincide, only one of them will be presented in the solution table.

### 4.2 Results presentation

#### A) *Small stiffened panel*

The dimensions for the Small stiffened panel were a=2580mm and b=2850mm.

##### 1.1 Pressure only: LOW

For this case the loading is: p=50kPa

Table 4.1: Candidate points for Small stiffened panel. Loading case: Pressure only // LOW

Input Variables	Candidate point 1	Candidate point 2
<b>nx</b>	0	0
<b>ny</b>	7	5
<b>t_pl</b>	5	5
<b>Stif_type_long</b>	-	-
<b>Stif_type_trans</b>	1	2
<b>tw_x</b>	-	-
<b>hw_x</b>	-	-
<b>bf_x</b>	-	-
<b>tf_x</b>	-	-
<b>tw_y</b>	8	8
<b>hw_y</b>	143	141
<b>bf_y</b>	70	68
<b>tf_y</b>	7	7

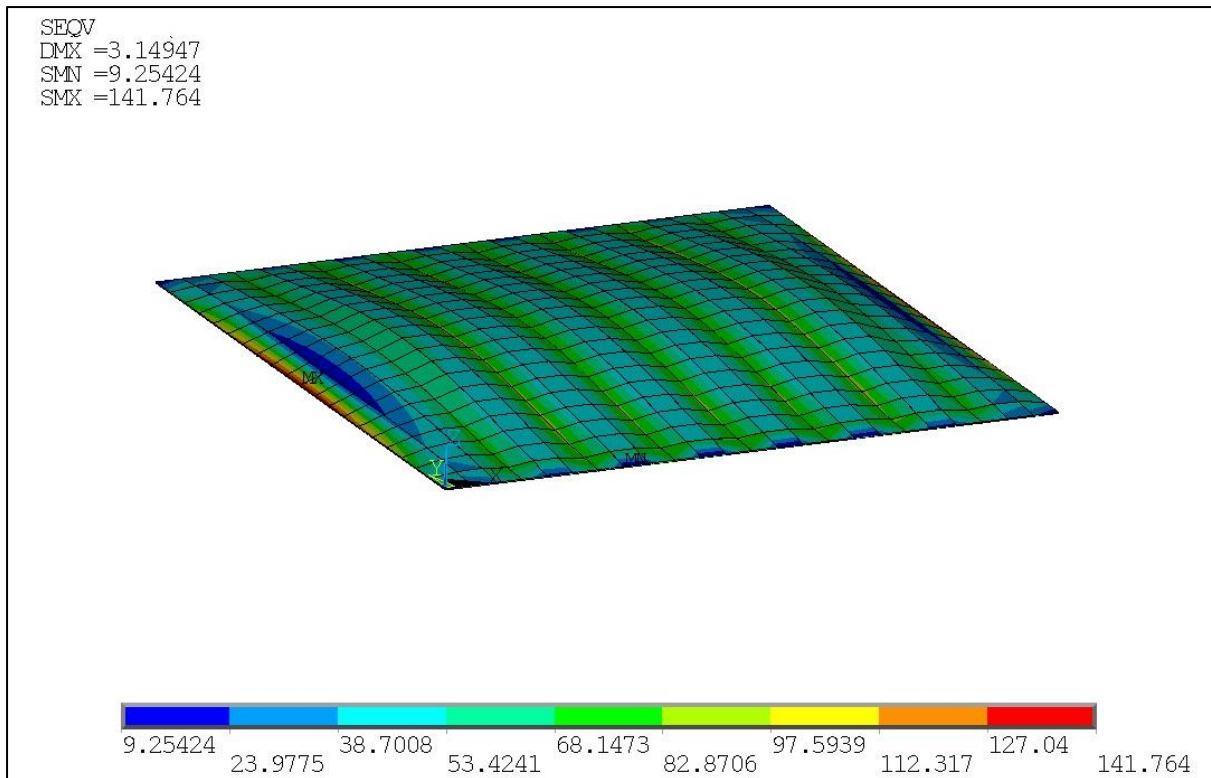


Figure 4.1: Contour plot of Von Mises Stress at Shell Elements. Small stiffened panel. Loading case: Pressure Only // LOW

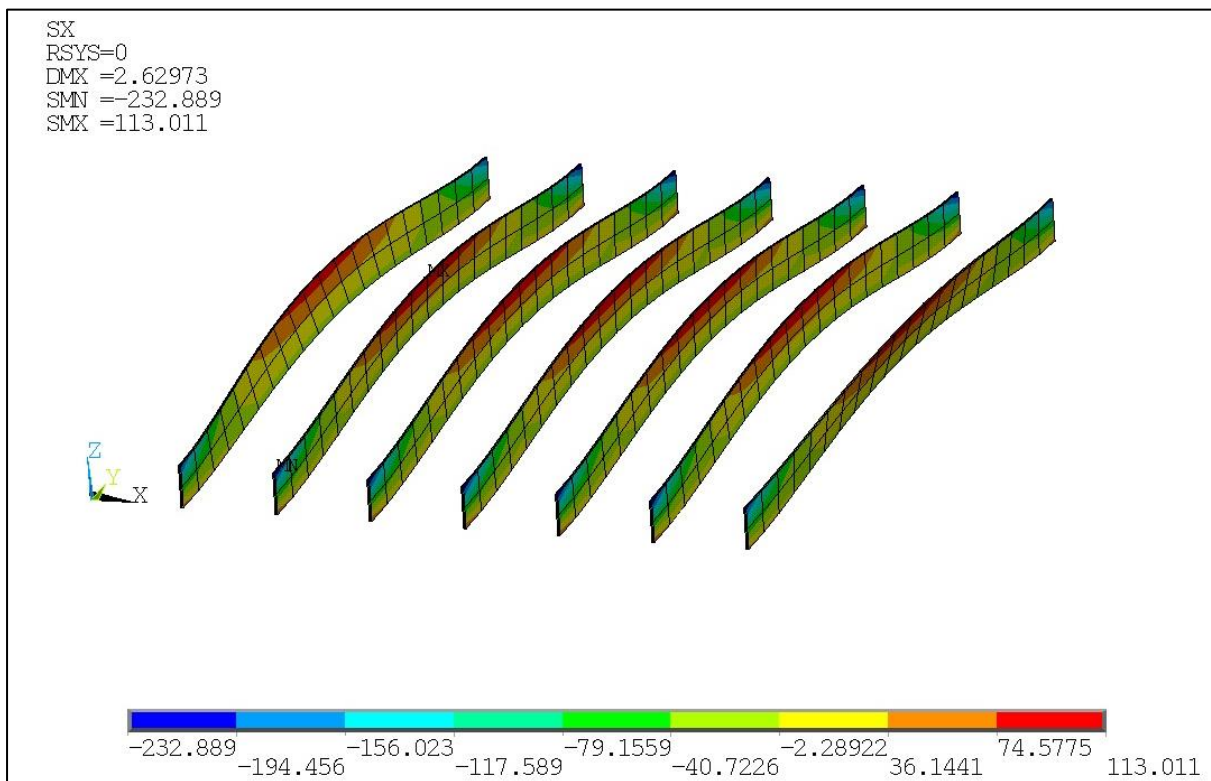


Figure 4.2: Contour plot of Sx Stress at Beam Elements (Transverses). Small stiffened panel. Loading case: Pressure Only // LOW

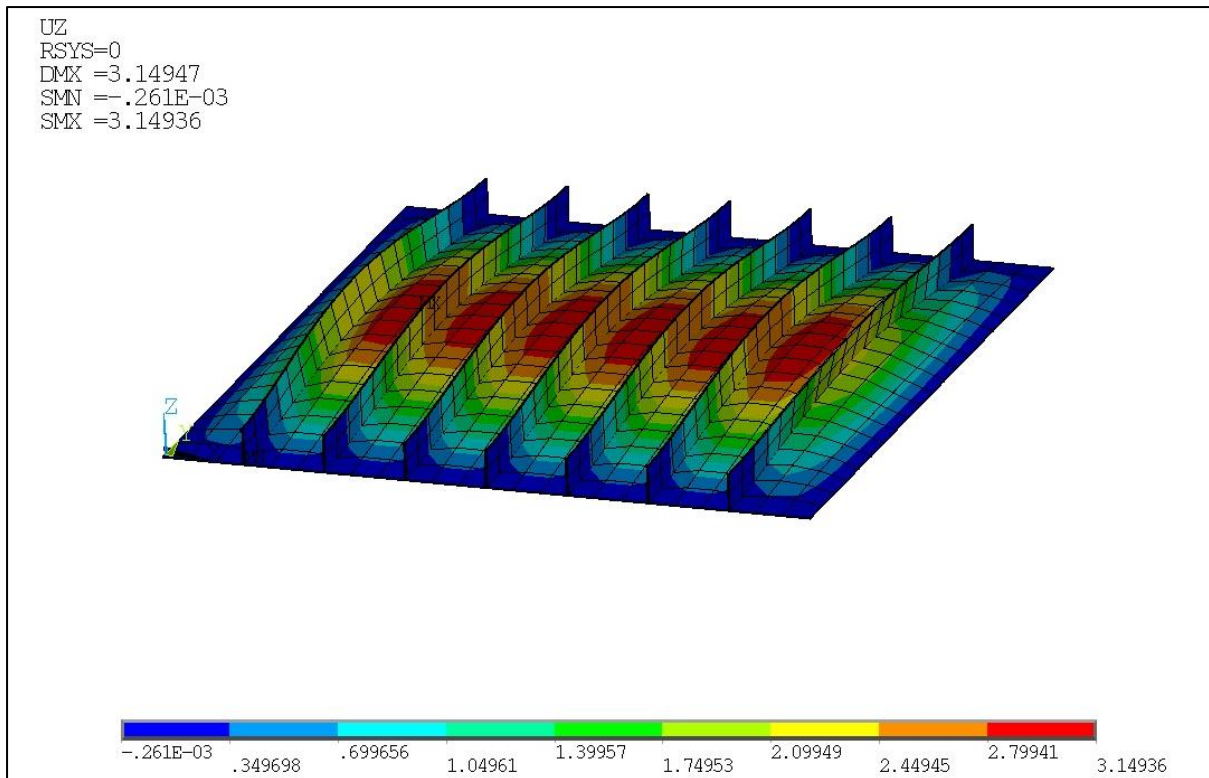


Figure 4.3: Contour plot of vertical displacement  $U_z$ . Small stiffened panel. Loading case: Pressure Only // LOW

### 1.2 Pressure only: MEDIUM

For this case the loading is:  $p=100\text{kPa}$

Table 4.2: Candidate points for Small stiffened panel. Loading case: Pressure only // MEDIUM

Input Variables	Candidate point 1
<b>nx</b>	0
<b>ny</b>	7
<b>t_pl</b>	5
<b>Stif_type_long</b>	-
<b>Stif_type_trans</b>	1
<b>tw_x</b>	-
<b>hw_x</b>	-
<b>bf_x</b>	-
<b>tf_x</b>	-
<b>tw_y</b>	9
<b>hw_y</b>	196
<b>bf_y</b>	55
<b>tf_y</b>	10

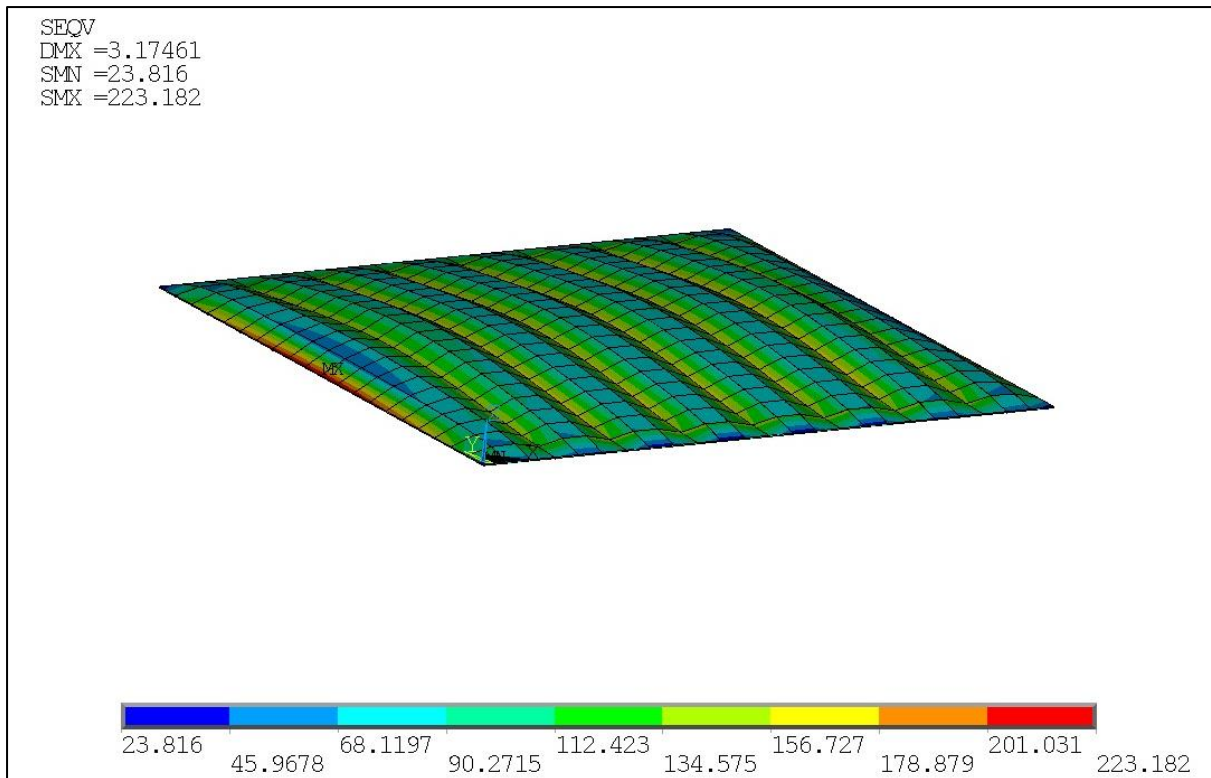


Figure 4.4: Contour plot of Von Mises Stress at Shell Elements. Small stiffened panel. Loading case: Pressure Only // MEDIUM

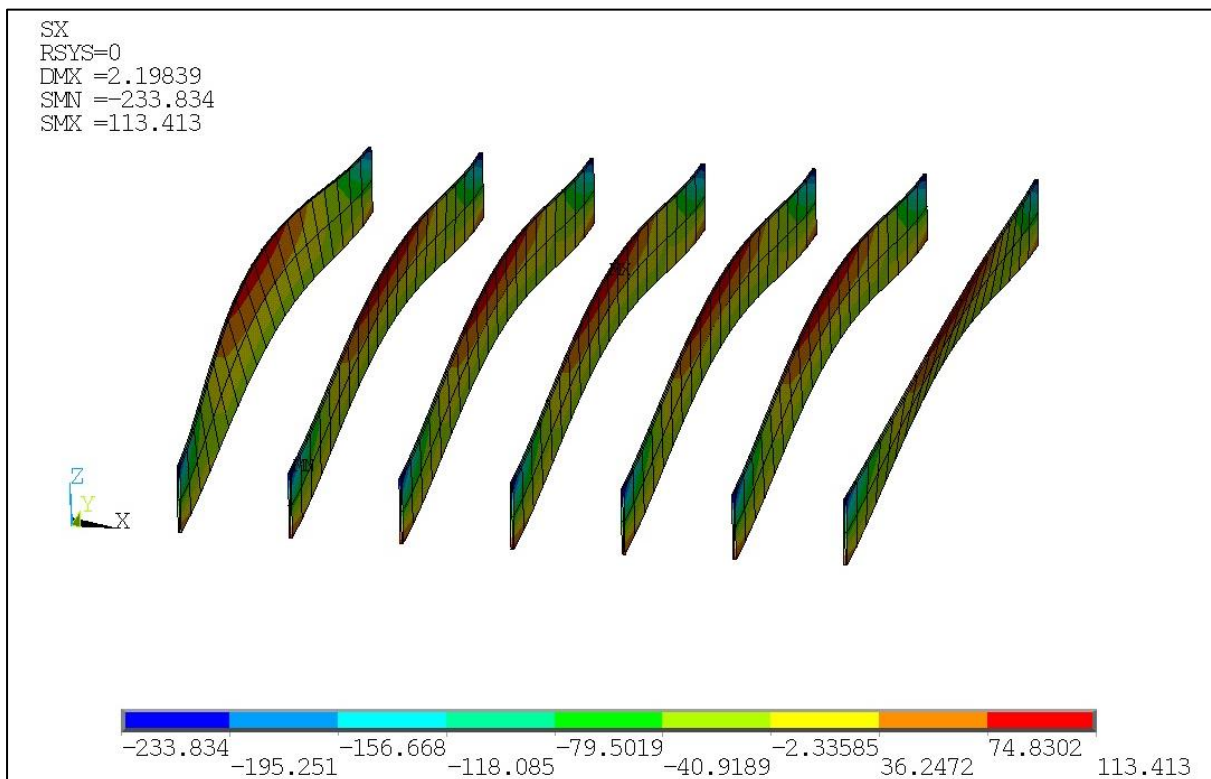


Figure 4.5: Contour plot of Sx Stress at Beam Elements (Transverses). Small stiffened panel. Loading case: Pressure Only // MEDIUM



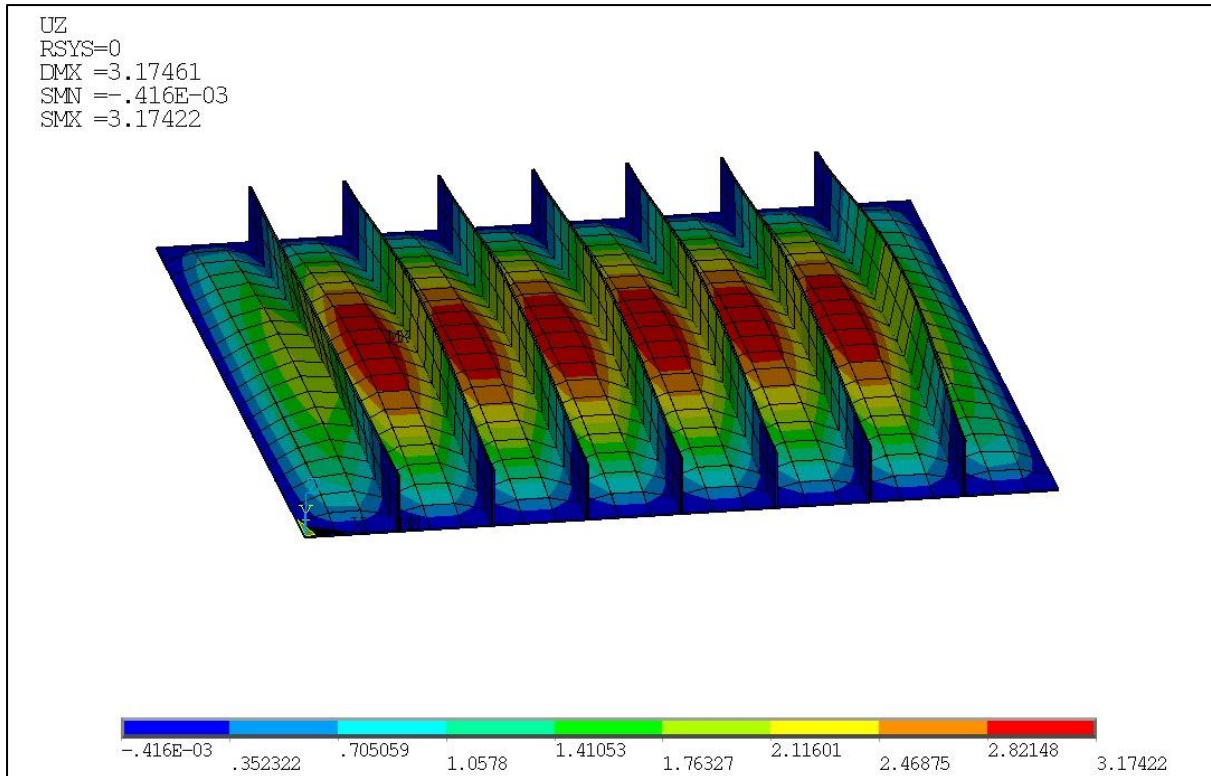


Figure 4.6: Contour plot of vertical Displacement ( $U_z$ ). Small stiffened panel. Loading case: Pressure Only // MEDIUM

### 1.3 Pressure only: HIGH

For this case the loading is:  $p=200\text{kPa}$

Table 4.3: Candidate points for Small stiffened panel. Loading case: Pressure only // HIGH

Input Variables	Candidate point 1	Candidate point 2	Candidate point 3
<b>nx</b>	3	3	3
<b>ny</b>	9	9	9
<b>t_pl</b>	5	5	5
<b>Stif_type_long</b>	1	1	1
<b>Stif_type_trans</b>	2	2	2
<b>tw_x</b>	15	15	15
<b>hw_x</b>	122	122	122
<b>bf_x</b>	95	95	95
<b>tf_x</b>	6	6	6
<b>tw_y</b>	8	8	8
<b>hw_y</b>	253	256	258
<b>bf_y</b>	86	87	87
<b>tf_y</b>	18	18	18

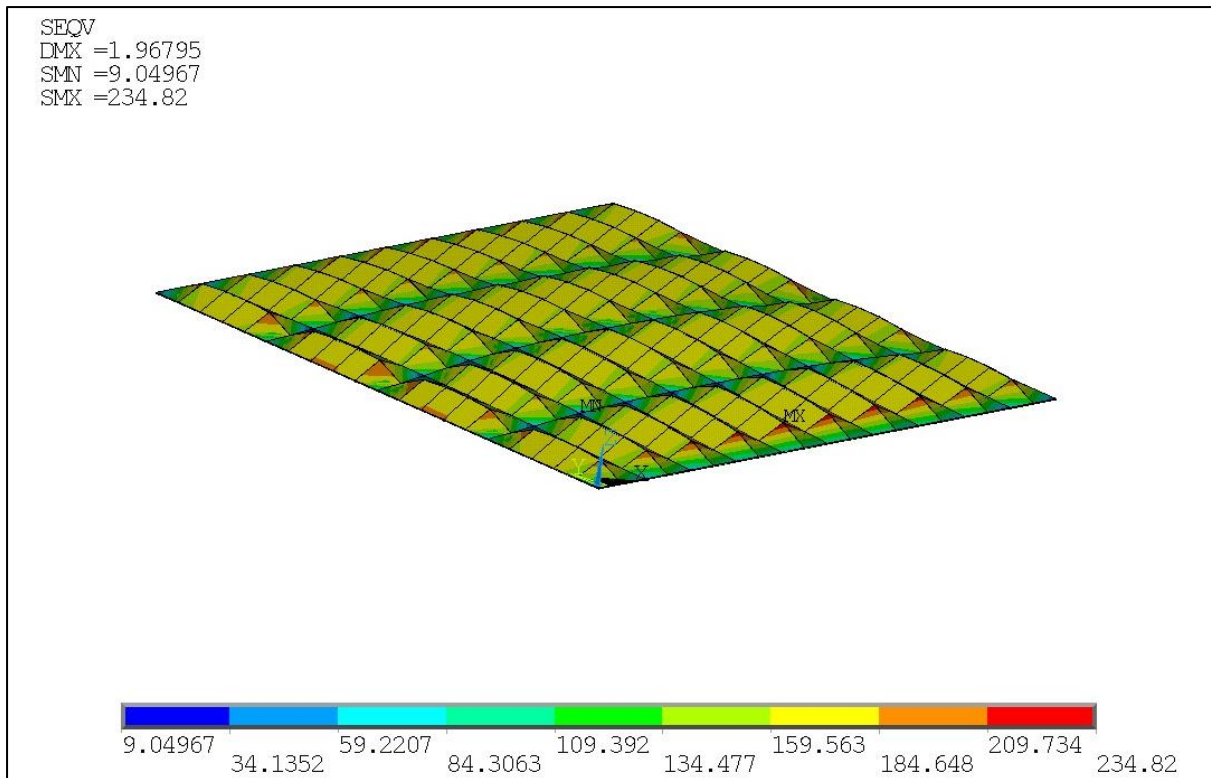


Figure 4.7: Contour plot of Von Mises Stress at Shell Elements. Small stiffened panel. Loading case: Pressure Only // HIGH

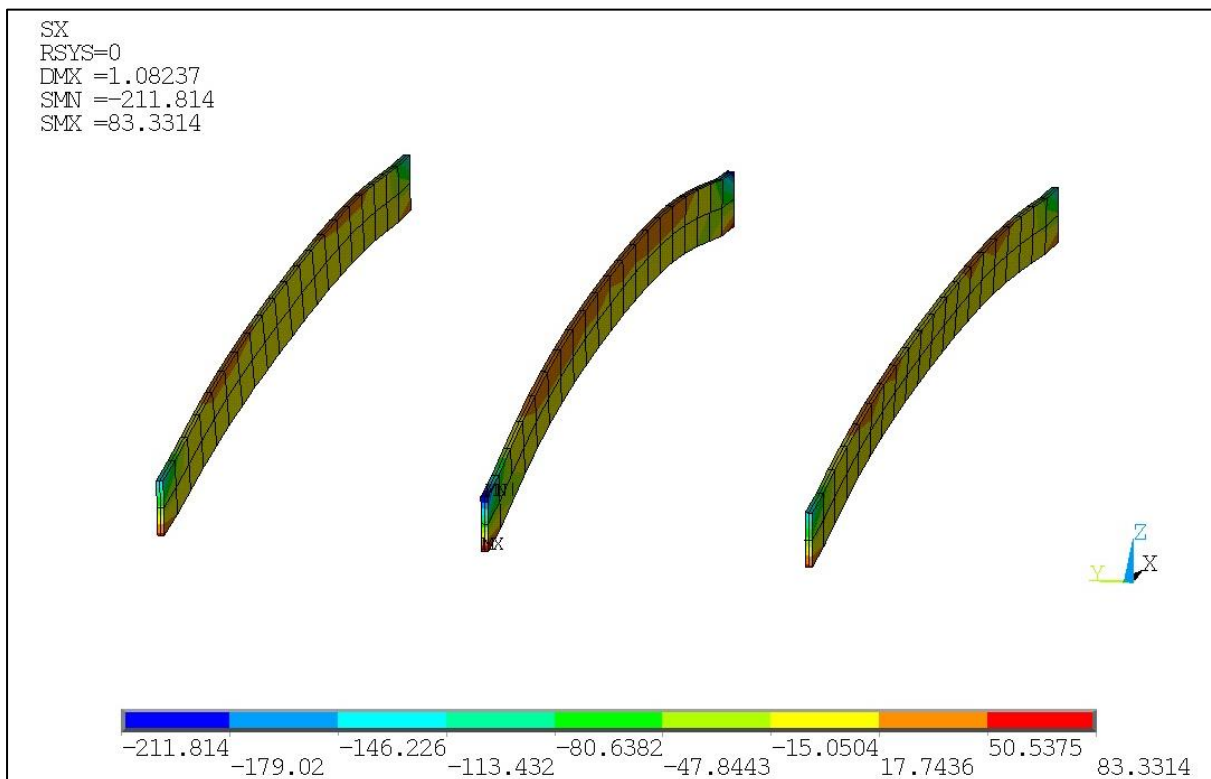


Figure 4.8: Contour plot of Sx Stress at Beam Elements (Longitudinals). Small stiffened panel. Loading case: Pressure Only // HIGH

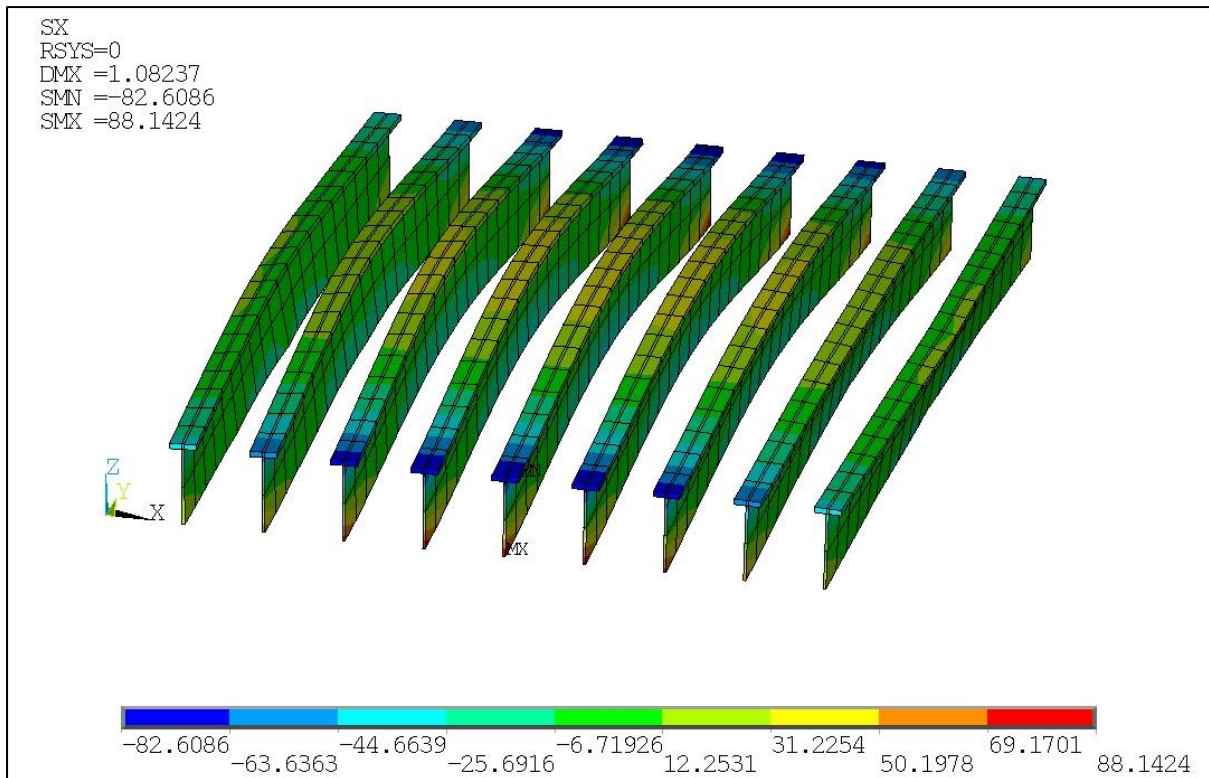


Figure 4.9: Contour plot of Sx Stress at Beam Elements (Transverses). Small stiffened panel. Loading case: Pressure Only // HIGH

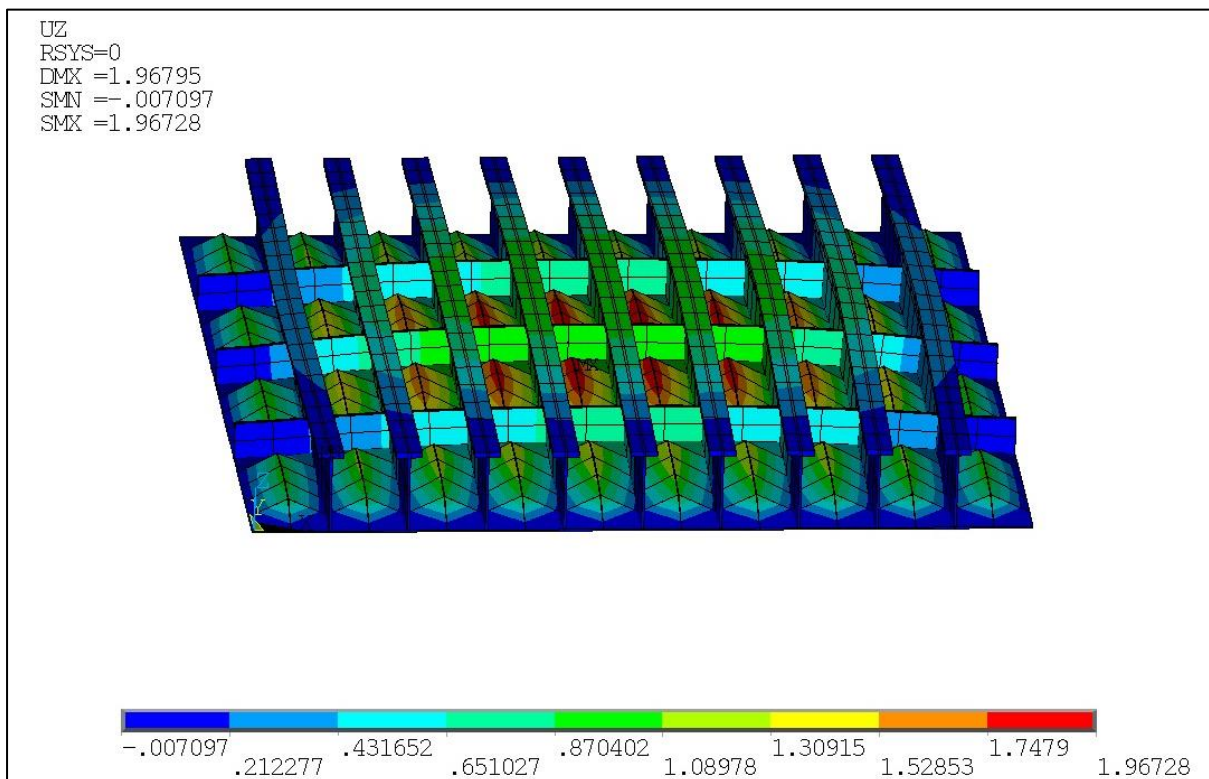


Figure 4.10: Contour plot of vertical Displacement (Uz). Small stiffened panel. Loading case: Pressure Only // HIGH

### 2.1 Pressure and stress: LOW

For this case the loading is:  $p=50$  kPa and  $\sigma=30$  MPa

Table 4.4: Candidate points for Small stiffened panel. Loading case: Pressure and Stress // LOW

Input Variables	Candidate point 1	Candidate point 2
<b>nx</b>	5	5
<b>ny</b>	0	0
<b>t_pl</b>	5	5
<b>Stif_type_long</b>	2	2
<b>Stif_type_trans</b>	-	-
<b>tw_x</b>	5	5
<b>hw_x</b>	132	132
<b>bf_x</b>	75	78
<b>tf_x</b>	9	9
<b>tw_y</b>	-	-
<b>hw_y</b>	-	-
<b>bf_y</b>	-	-
<b>tf_y</b>	-	-

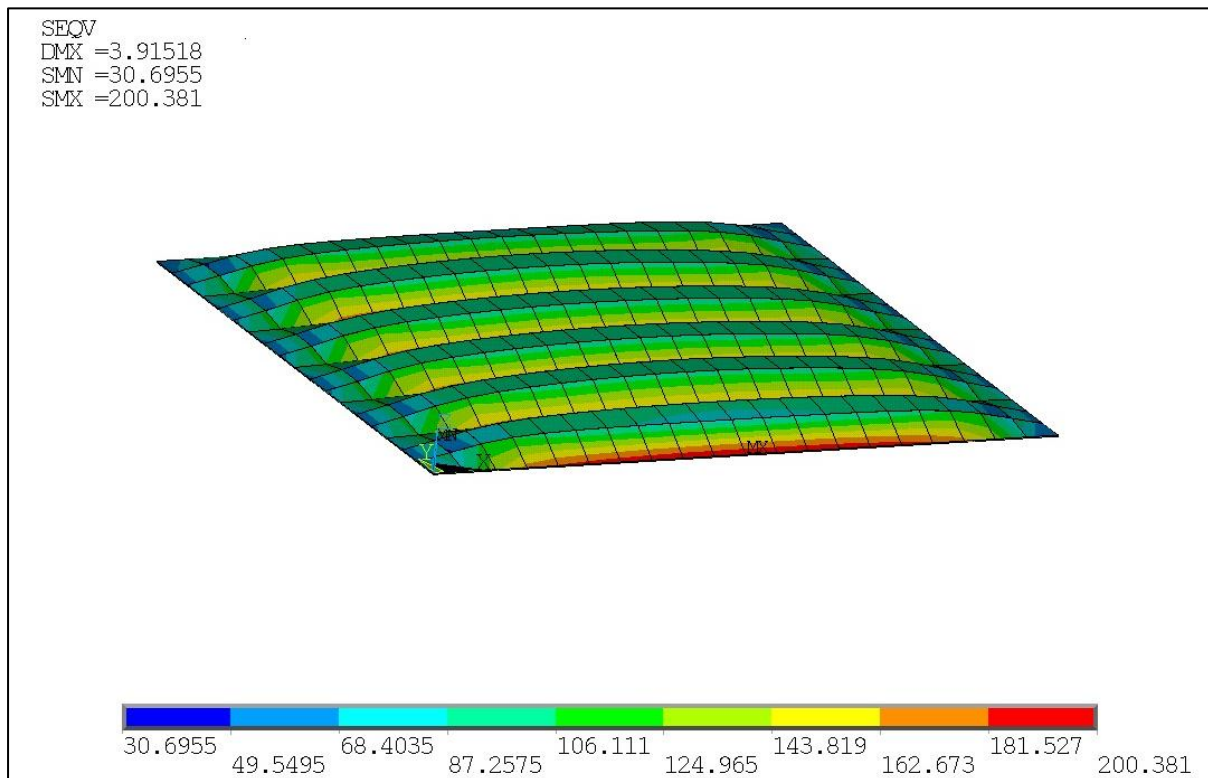


Figure 4.11: Contour plot of Von Mises Stress at Shell Elements. Small stiffened panel. Loading case: Pressure // LOW



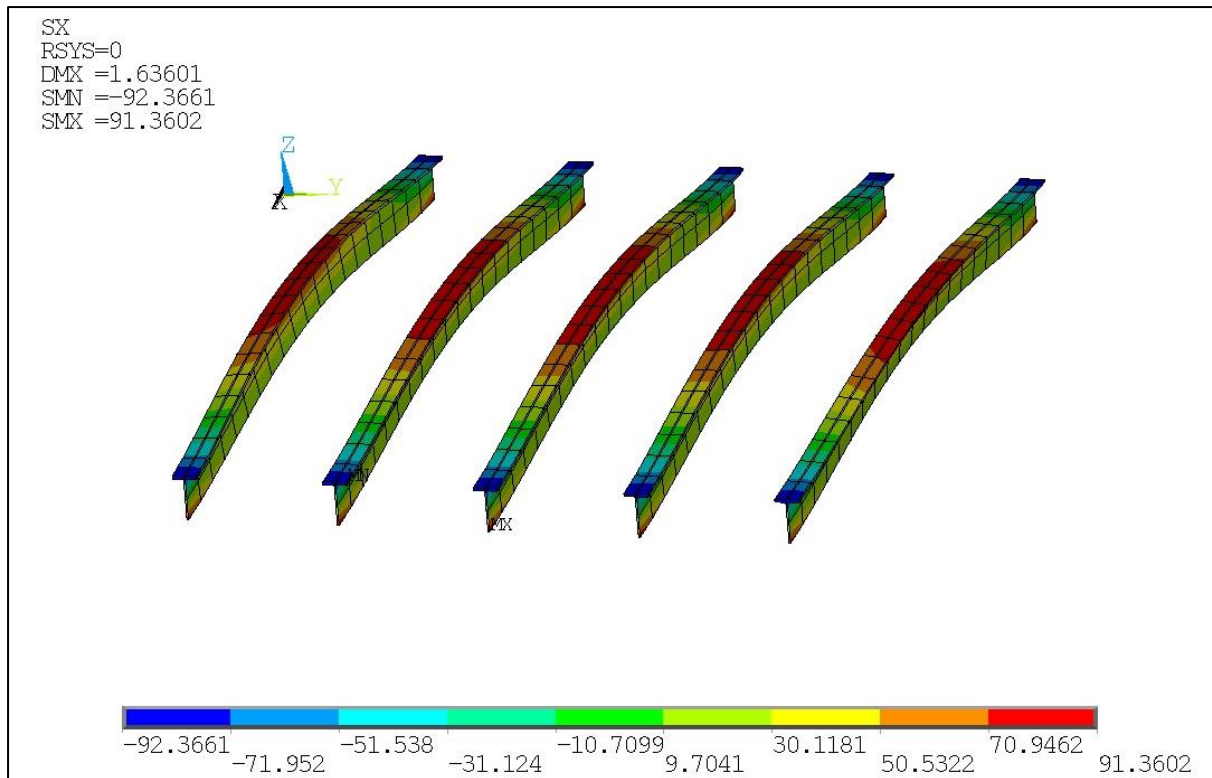


Figure 4.12: Contour plot of Sx Stress at Beam Elements (Longitudinals). Small stiffened panel.  
Loading case: Pressure and Stress // LOW

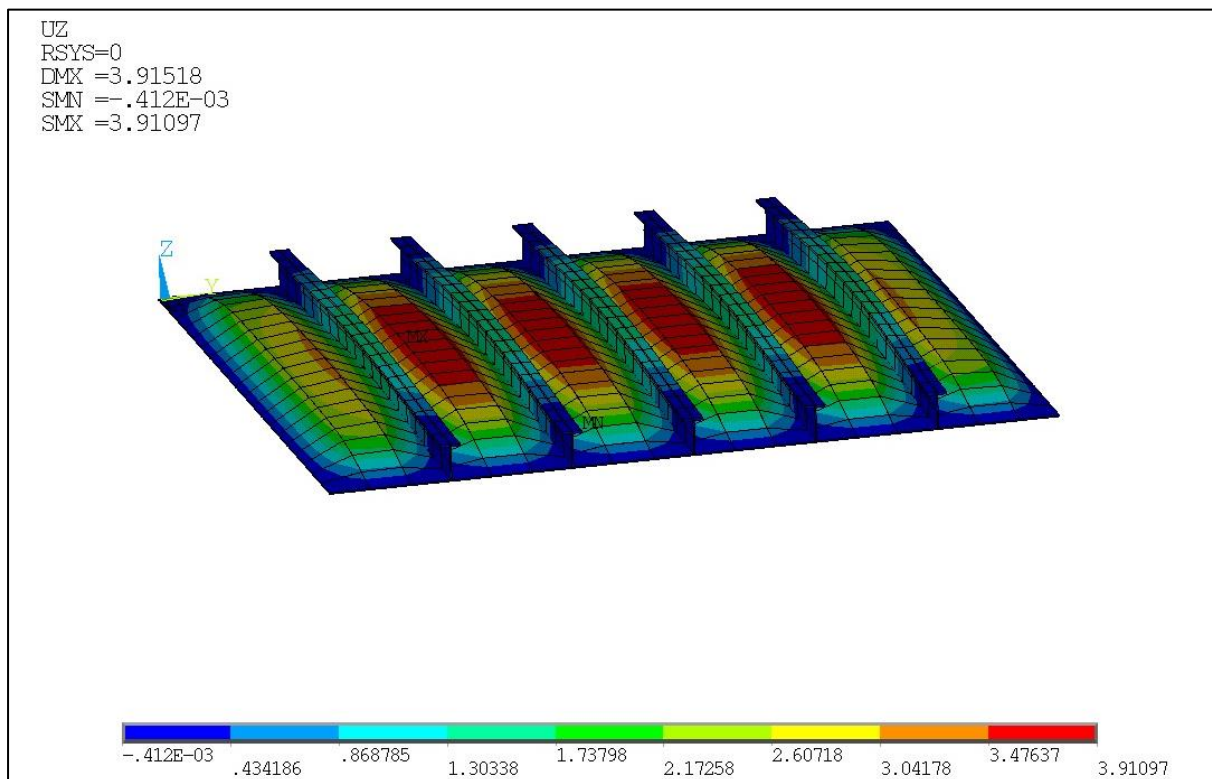


Figure 4.13: Contour plot of vertical Displacement (Uz). Small stiffened panel. Loading case:  
Pressure and Stress // LOW

## 2.2 Pressure and stress: MEDIUM

For this case the loading is:  $p=100$  kPa and  $\sigma=60$  MPa

Table 4.5: Candidate points for Small stiffened panel. Loading case: Pressure and Stress // MEDIUM

Input Variables	Candidate point 1	Candidate point 2
<b>nx</b>	8	8
<b>ny</b>	0	0
<b>t_pl</b>	5	5
<b>Stif_type_long</b>	1	1
<b>Stif_type_trans</b>	-	-
<b>tw_x</b>	13	13
<b>hw_x</b>	135	138
<b>bf_x</b>	-	-
<b>tf_x</b>	-	-
<b>tw_y</b>	-	-
<b>hw_y</b>	-	-
<b>bf_y</b>	-	-
<b>tf_y</b>	-	-

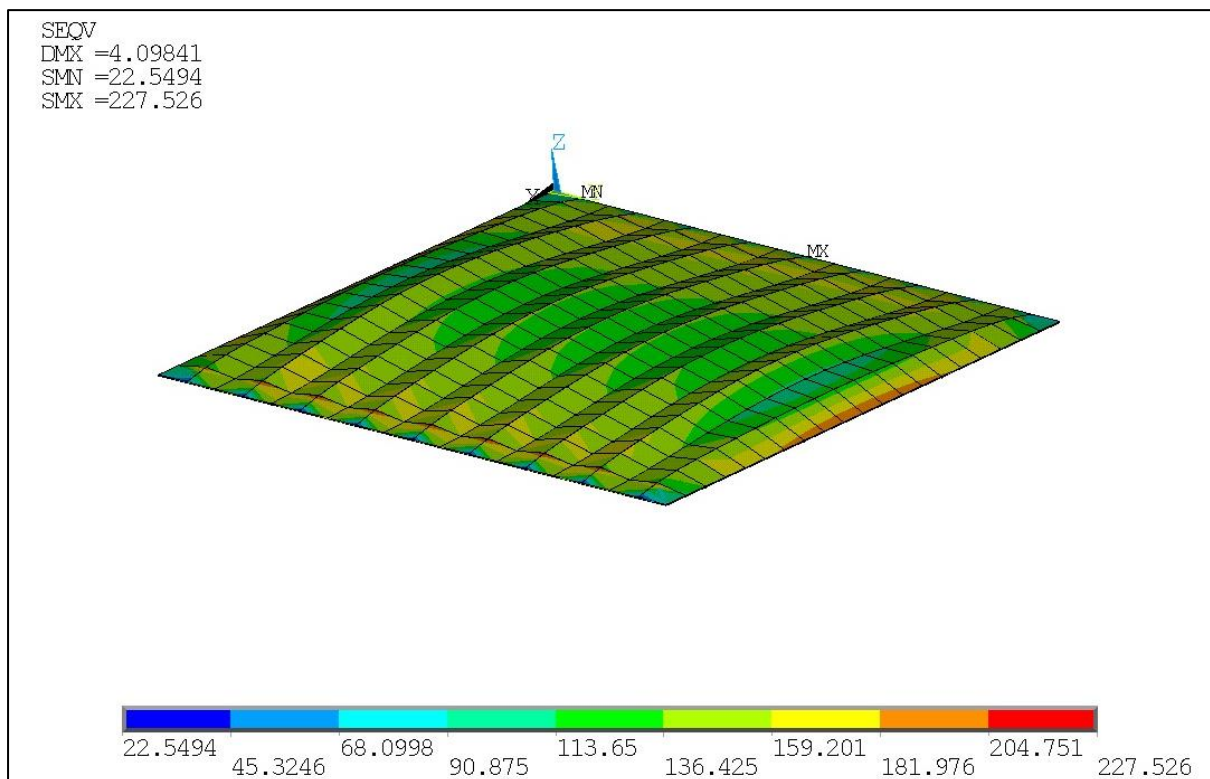


Figure 4.14: Contour plot of Von Mises Stress at Shell Elements. Small stiffened panel. Loading case: "Pressure and Stress // MEDIUM"

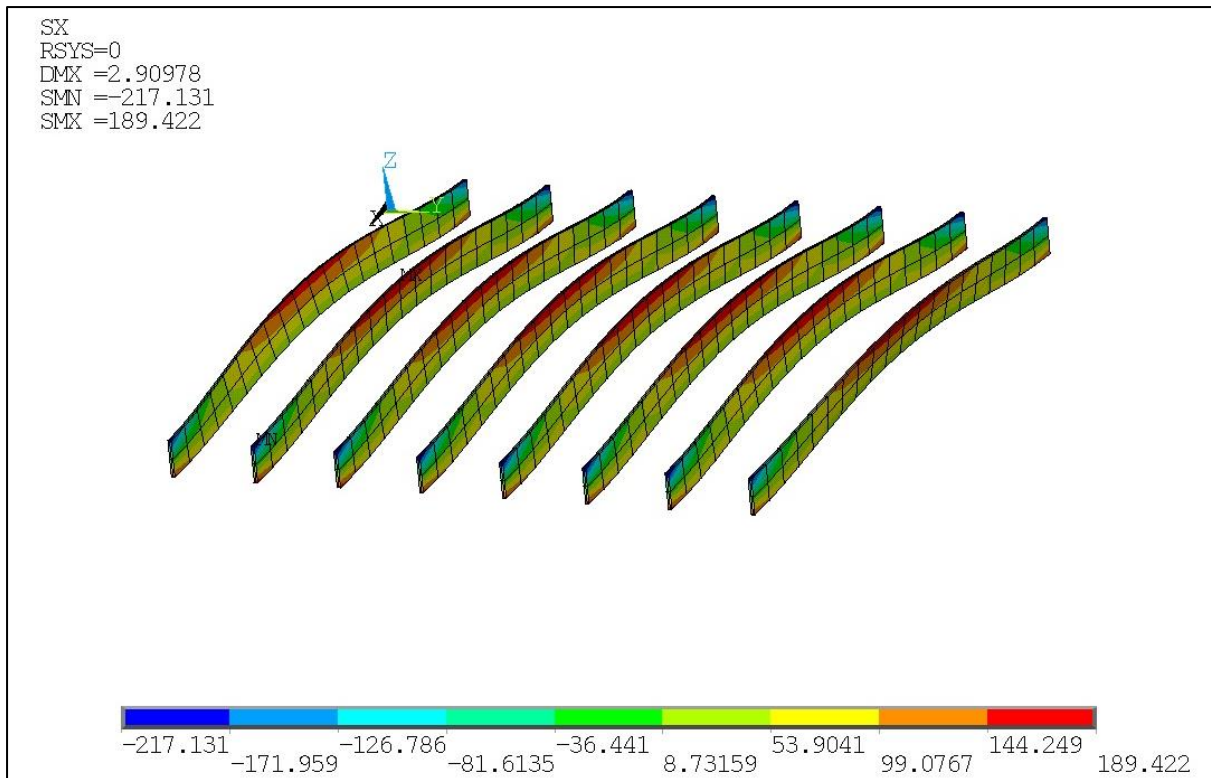


Figure 4.15: Contour plot of Sx Stress at Beam Elements (Longitudinals). Small stiffened panel.  
Loading case: Pressure and Stress // MEDIUM

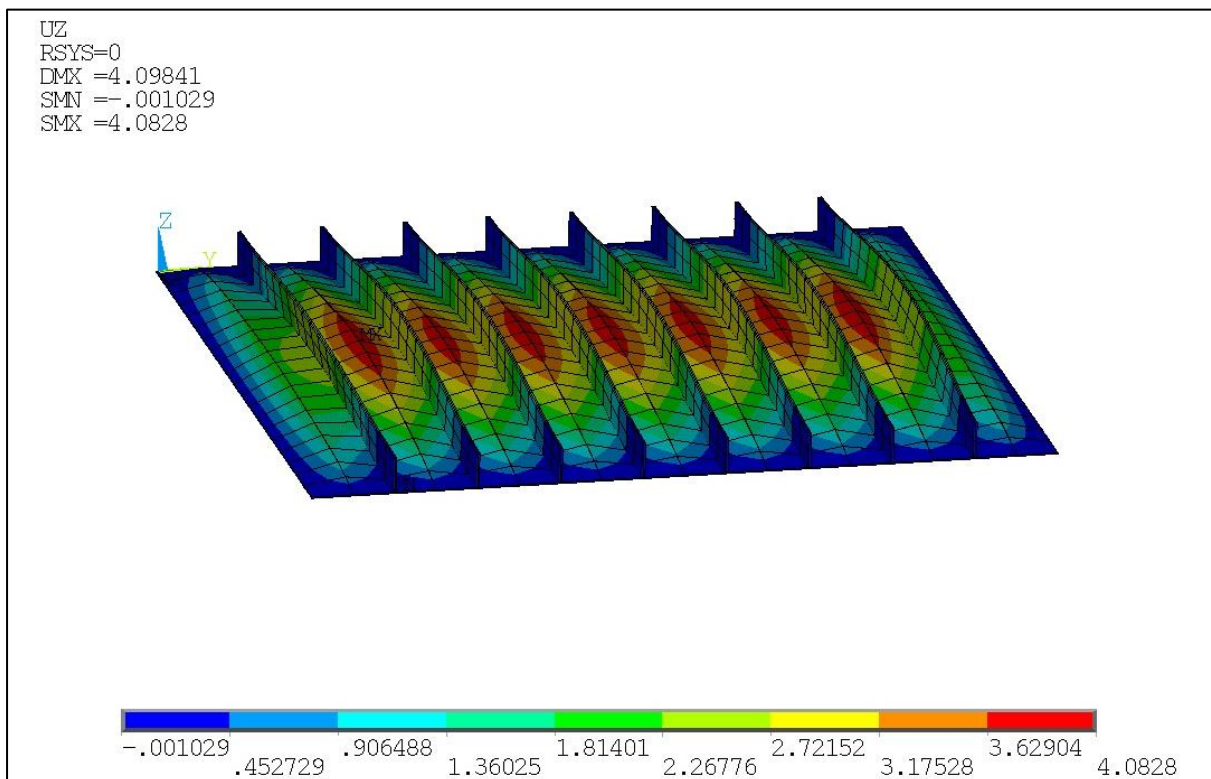


Figure 4.16: Contour plot of vertical Displacement (Uz). Small stiffened panel. Loading case:  
Pressure and Stress // MEDIUM

### 2.3 Pressure and stress: HIGH

For this case the loading is:  $p=200$  kPa and  $\sigma=120$  MPa

Table 4.6: Candidate points for Small stiffened panel. Loading case: Pressure and Stress // HIGH

Input Variables	Candidate point 1	Candidate point 2	Candidate point 3
<b>nx</b>	2	2	2
<b>ny</b>	8	8	8
<b>t_pl</b>	9	9	9
<b>Stif_type_long</b>	2	2	2
<b>Stif_type_trans</b>	2	2	2
<b>tw_x</b>	5	5	5
<b>hw_x</b>	125	123	124
<b>bf_x</b>	95	98	98
<b>tf_x</b>	5	5	5
<b>tw_y</b>	5	5	5
<b>hw_y</b>	178	178	178
<b>bf_y</b>	51	51	51
<b>tf_y</b>	18	18	18

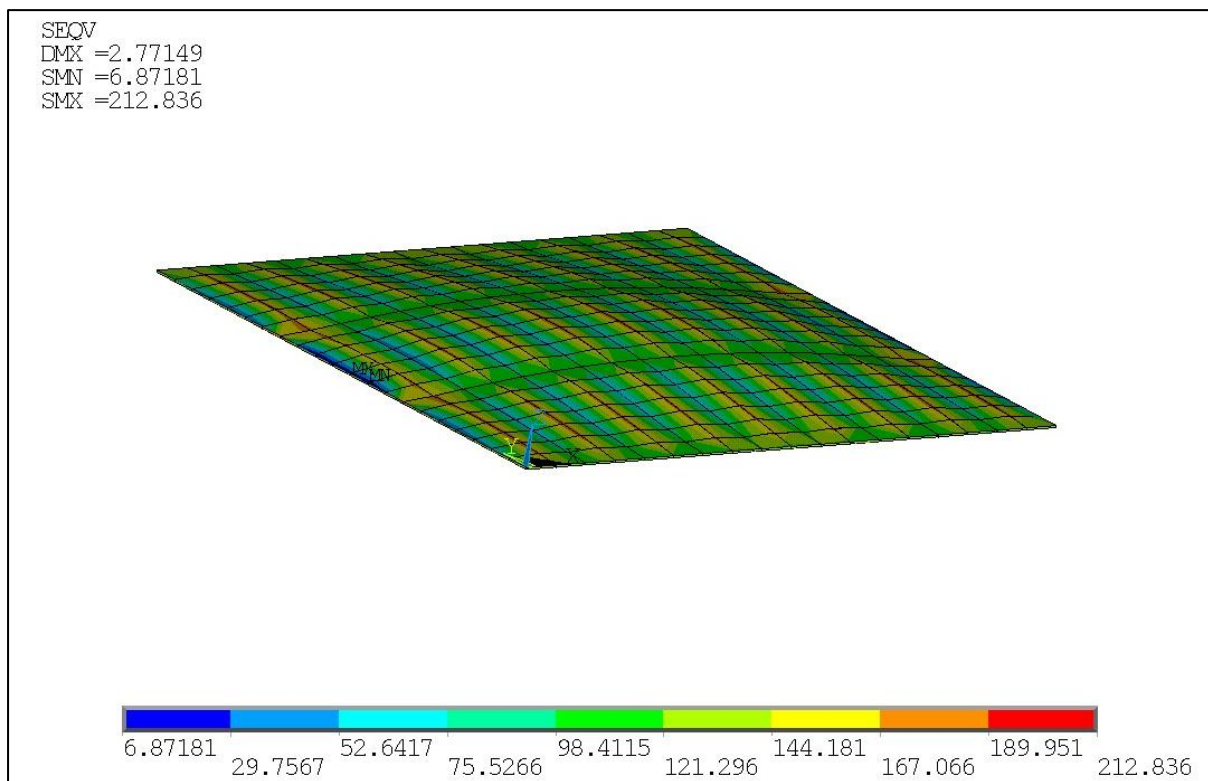


Figure 4.17: Contour plot of Von Mises Stress at Shell Elements. Small stiffened panel. Loading case: Pressure and Stress // HIGH



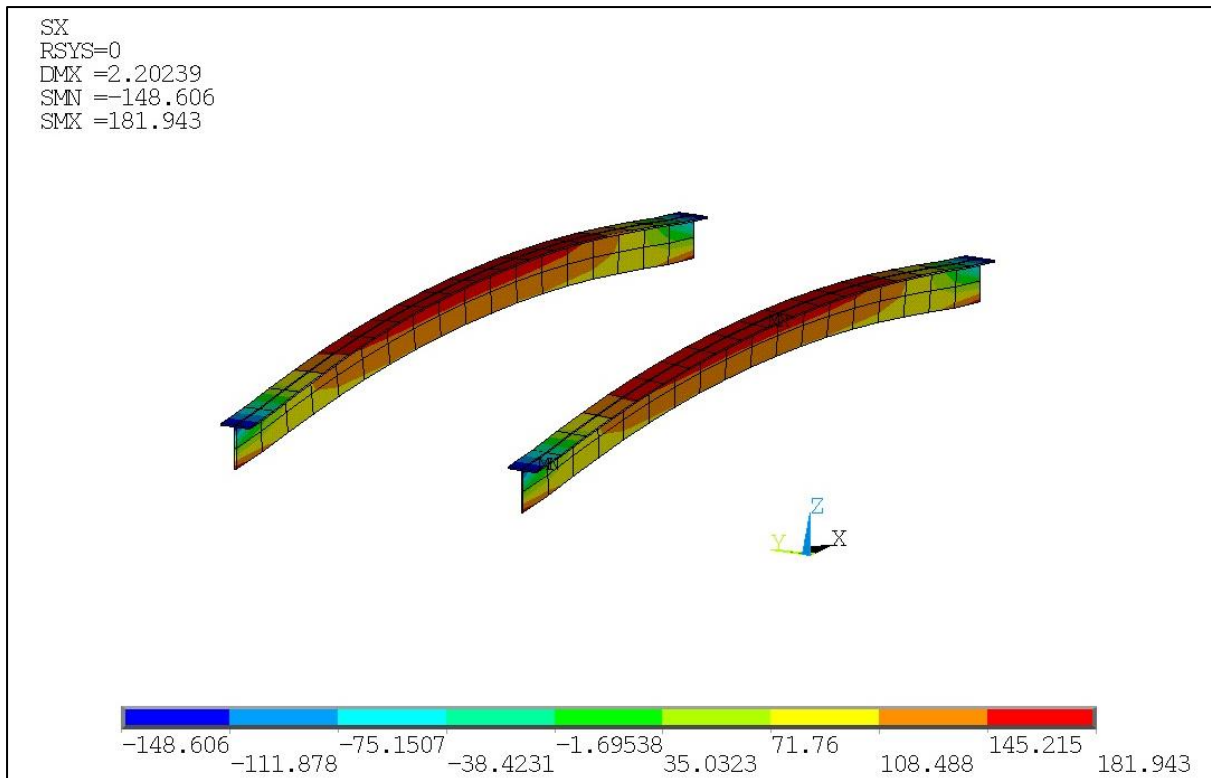


Figure 4.18: Contour plot of Sx Stress at Beam Elements (Longitudinals). Small stiffened panel.  
Loading case: Pressure and Stress // HIGH

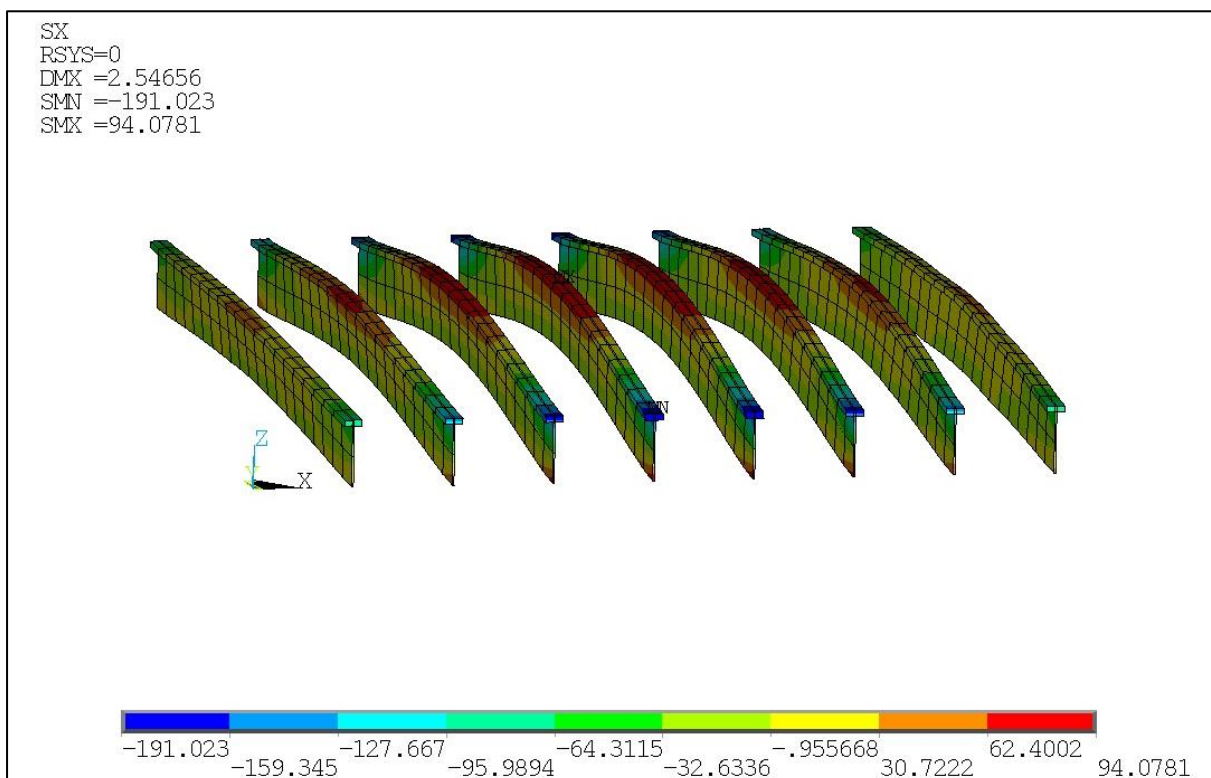


Figure 4.19: Contour plot of Sx Stress at Beam Elements (Transverses). Small stiffened panel.  
Loading case: Pressure and Stress // HIGH

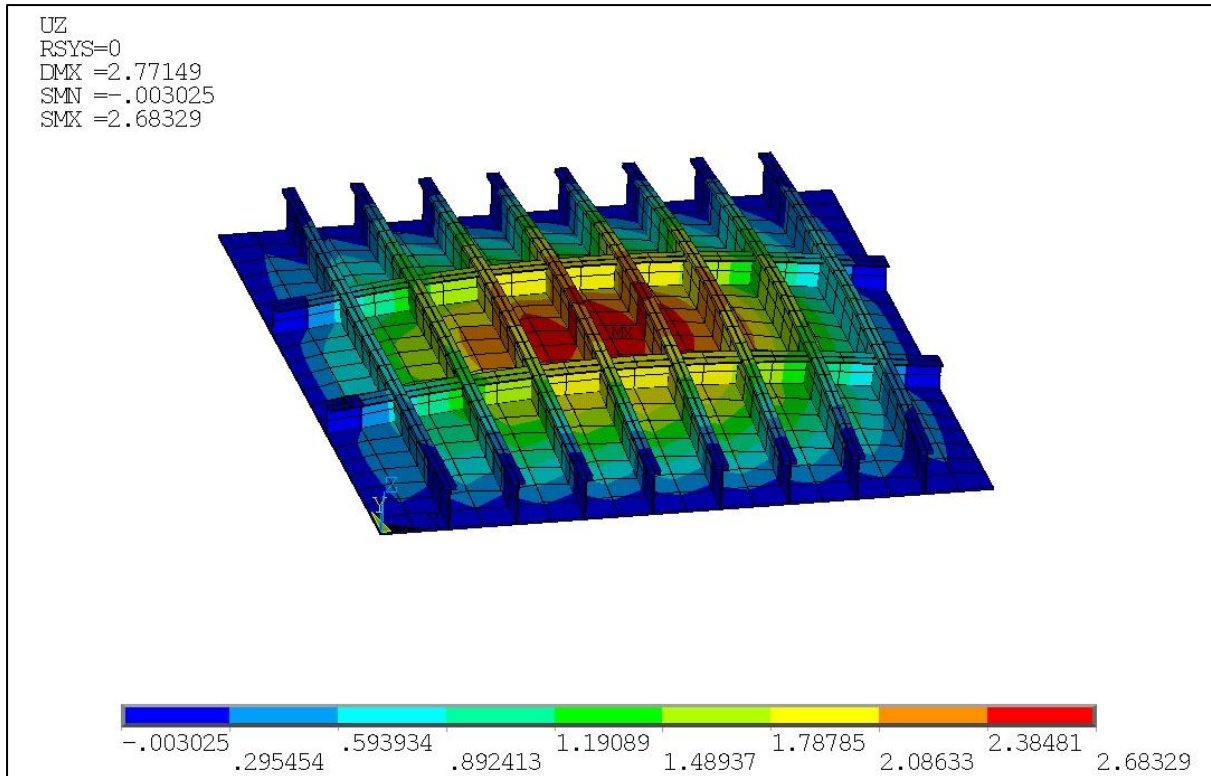


Figure 4.20: Contour plot of vertical Displacement (Uz). Small stiffened panel. Loading case: Pressure and Stress // HIGH

## B) *Car Deck*

The dimensions of the Car Deck were  $a=14000$  mm and  $b=11000$ mm

### 1.1 Pressure only: LOW

For this case the loading is  $p=1,25$  kPa

Table 4.7: Candidate points for Car Deck. Loading case: Pressure only// LOW

Input Variables	Candidate point 1	Candidate point 2
<b>nx</b>	0	0
<b>ny</b>	4	4
<b>t_pl</b>	5	5
<b>Stif_type_long</b>	-	-
<b>Stif_type_trans</b>	2	2
<b>tw_x</b>	-	-
<b>hw_x</b>	-	-
<b>bf_x</b>	-	-
<b>tf_x</b>	-	-
<b>tw_y</b>	8	8
<b>hw_y</b>	173	174
<b>bf_y</b>	62	61
<b>tf_y</b>	7	7

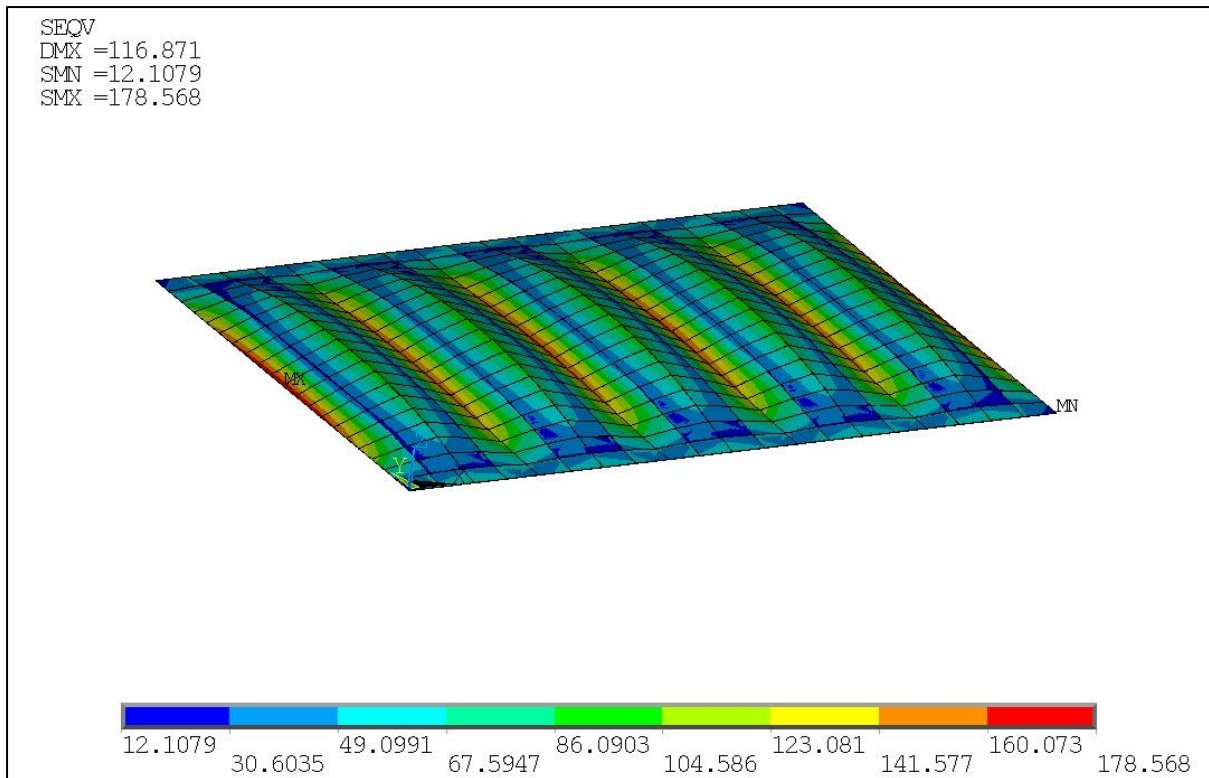


Figure 4.21: Contour plot of Von Mises Stress at Shell Elements. Car Deck. Loading case: Pressure only // LOW

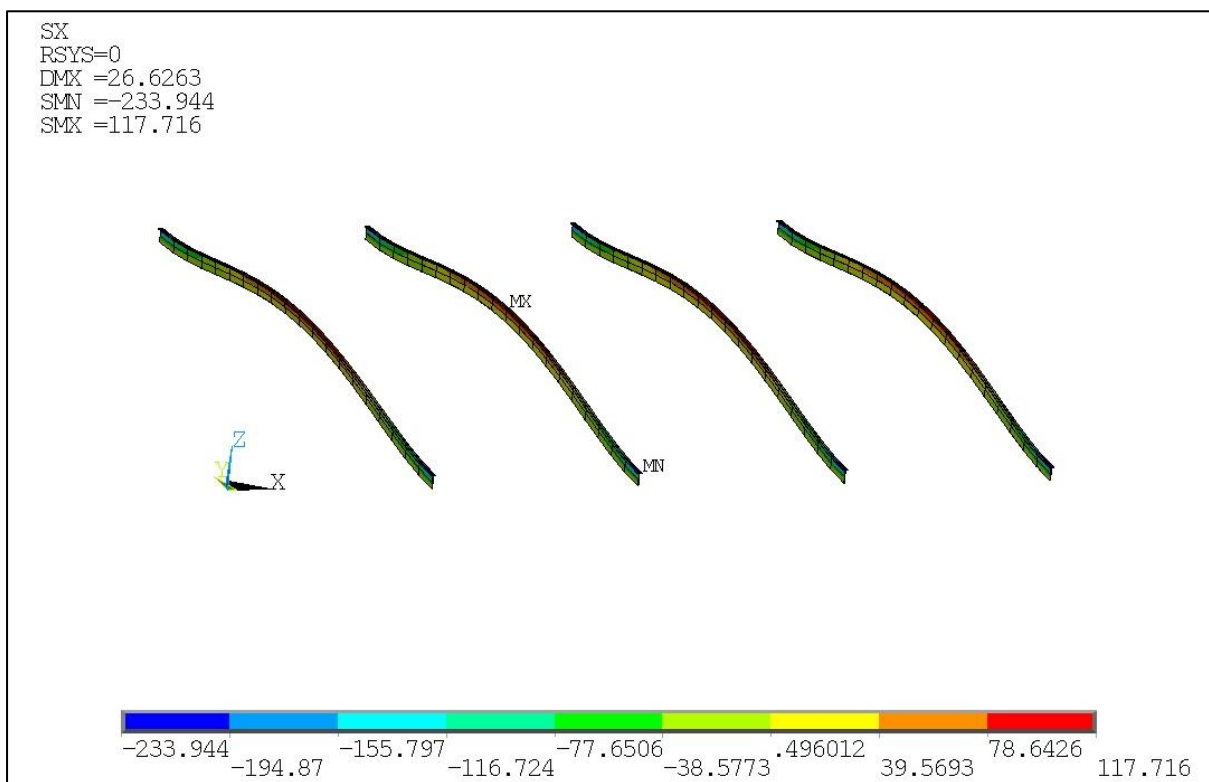


Figure 4.22: Contour plot of Sx Stress at Beam Elements (Transverses). Car Deck. Loading case: Pressure only // LOW

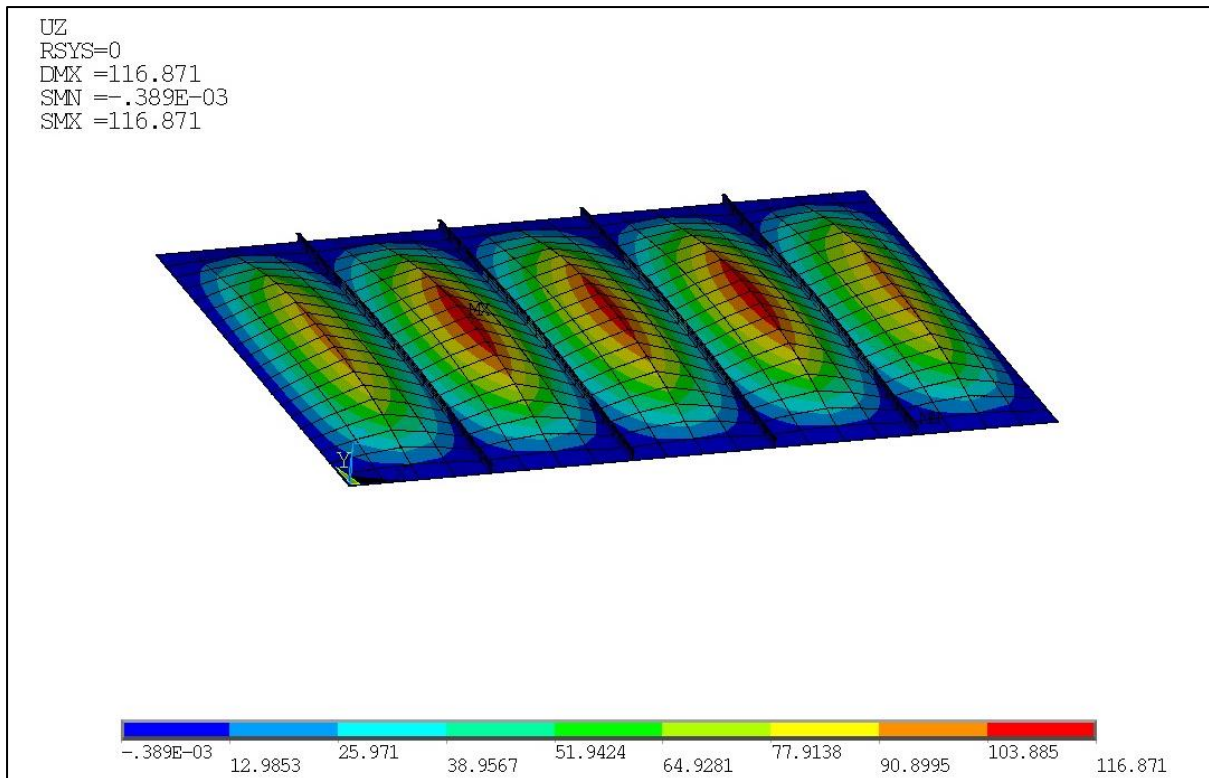


Figure 4.23: Contour plot of vertical Displacement (Uz). Car Deck. Loading case: Pressure only//  
LOW

### 1.2 Pressure only: MEDIUM

For this case the loading is  $p=2,5$  kPa

Table 4.8: Candidate points for Car Deck. Loading case: Pressure only// MEDIUM

Input Variables	Candidate point 1	Candidate point 2	Candidate point 3
<b>nx</b>	2	2	2
<b>ny</b>	4	4	4
<b>t_pl</b>	5	5	5
<b>Stif_type_long</b>	2	2	2
<b>Stif_type_trans</b>	2	2	2
<b>tw_x</b>	6	6	6
<b>hw_x</b>	130	131	131
<b>bf_x</b>	57	57	57
<b>tf_x</b>	10	10	10
<b>tw_y</b>	8	8	8
<b>hw_y</b>	248	248	249
<b>bf_y</b>	94	94	94
<b>tf_y</b>	7	7	7

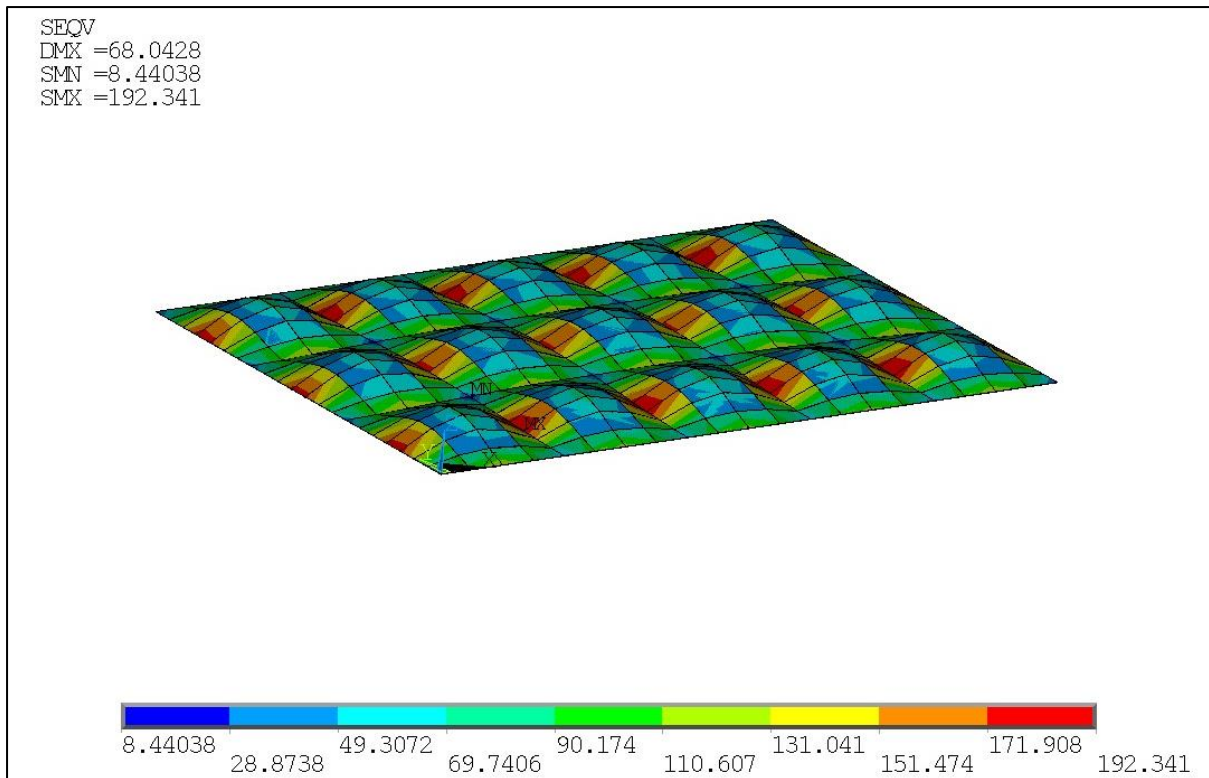


Figure 4.24: Contour plot of Von Mises Stress at Shell Elements. Car Deck. Loading case: Pressure only // MEDIUM

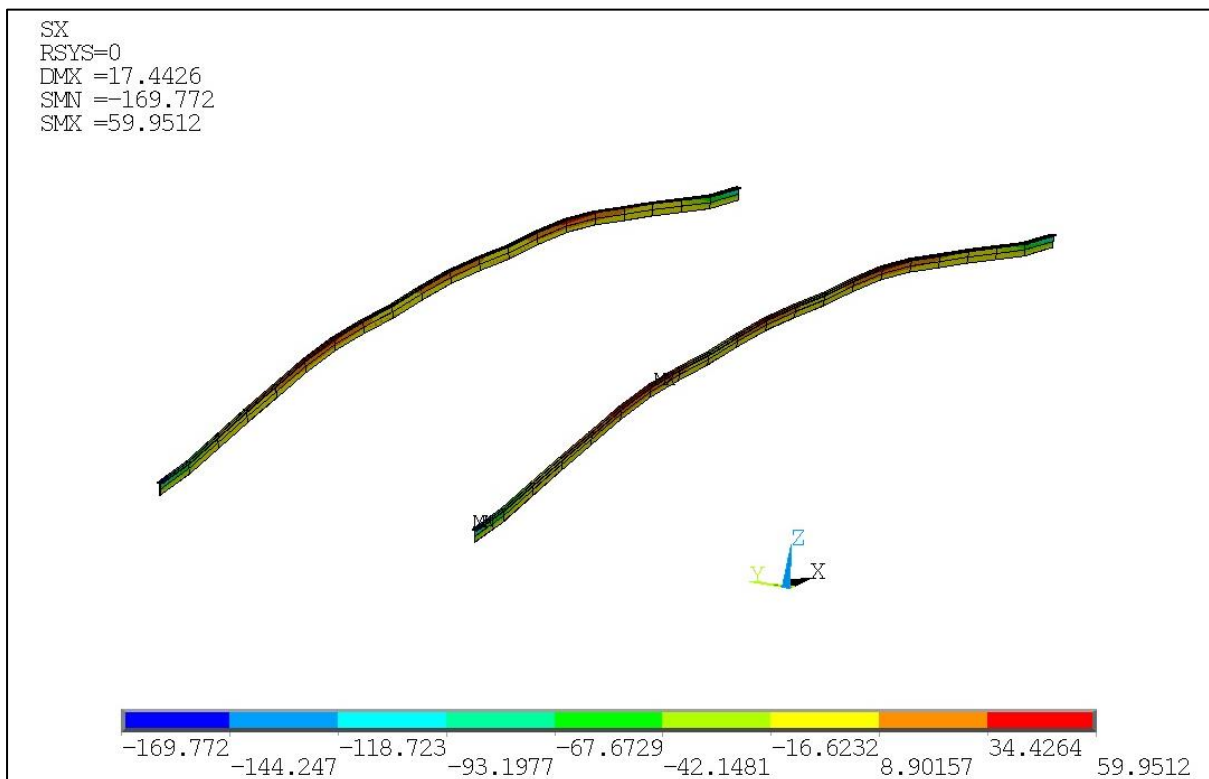


Figure 4.25: Contour plot of Sx Stress at Beam Elements (Longitudinals). Car Deck. Loading case: Pressure only// MEDIUM



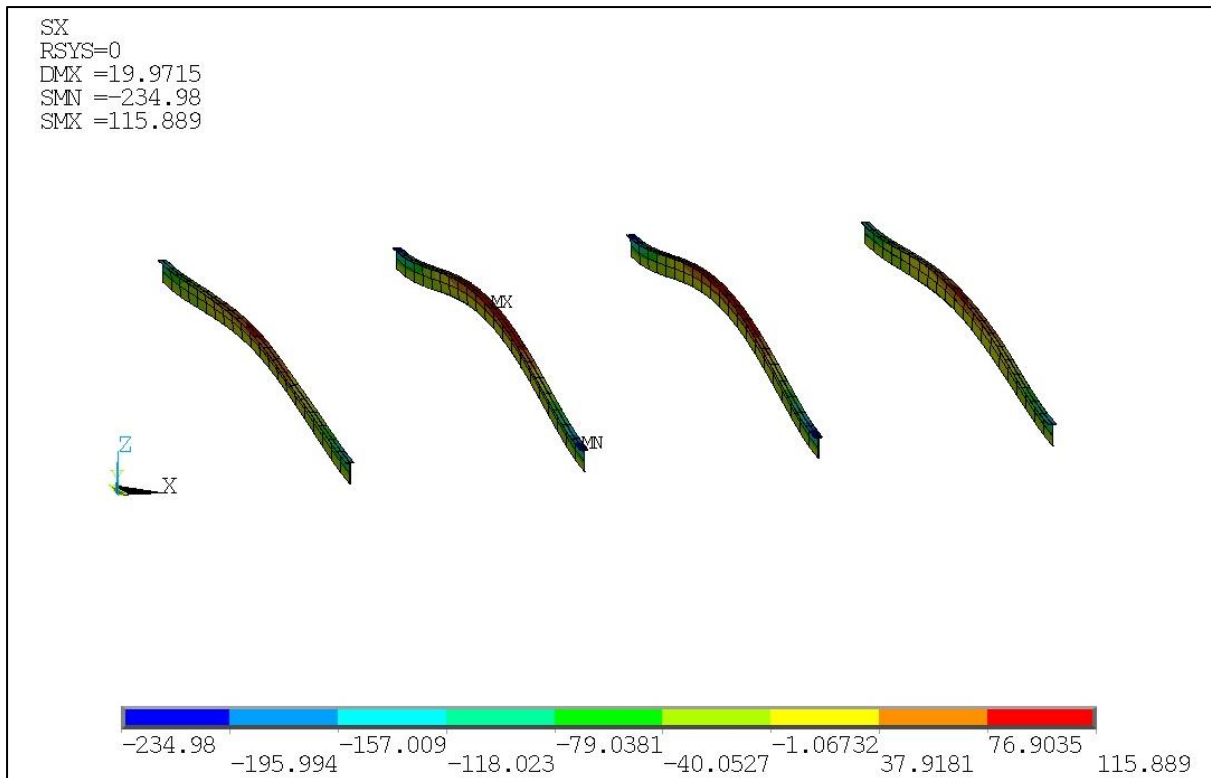


Figure 4.26: Contour plot of Sx Stress at Beam Elements (Transverses). Car Deck. Loading case: Pressure only// MEDIUM

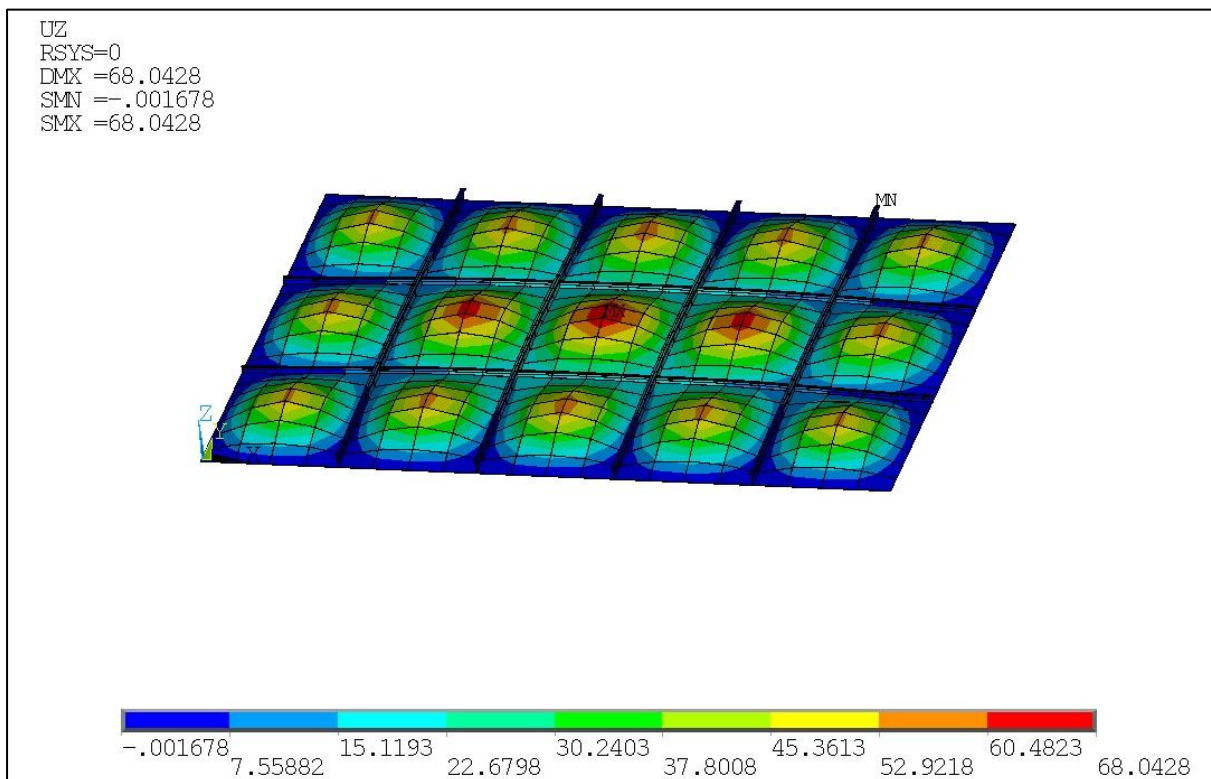


Figure 4.27: Contour plot of vertical Displacement (Uz). Car Deck. Loading case: Pressure only// MEDIUM

### 1.3 Pressure only: HIGH

For this case the loading is  $p=5$  kPa

Table 4.9: Candidate points for Car Deck. Loading case: Pressure only// HIGH

Input Variables	Candidate point 1	Candidate point 2	Candidate point 3
<b>nx</b>	3	3	3
<b>ny</b>	6	6	6
<b>t_pl</b>	5	5	5
<b>Stif_type_long</b>	2	2	2
<b>Stif_type_trans</b>	2	2	2
<b>tw_x</b>	9	9	9
<b>hw_x</b>	120	122	122
<b>bf_x</b>	84	81	82
<b>tf_x</b>	6	6	6
<b>tw_y</b>	6	6	6
<b>hw_y</b>	365	365	365
<b>bf_y</b>	67	67	67
<b>tf_y</b>	9	9	9

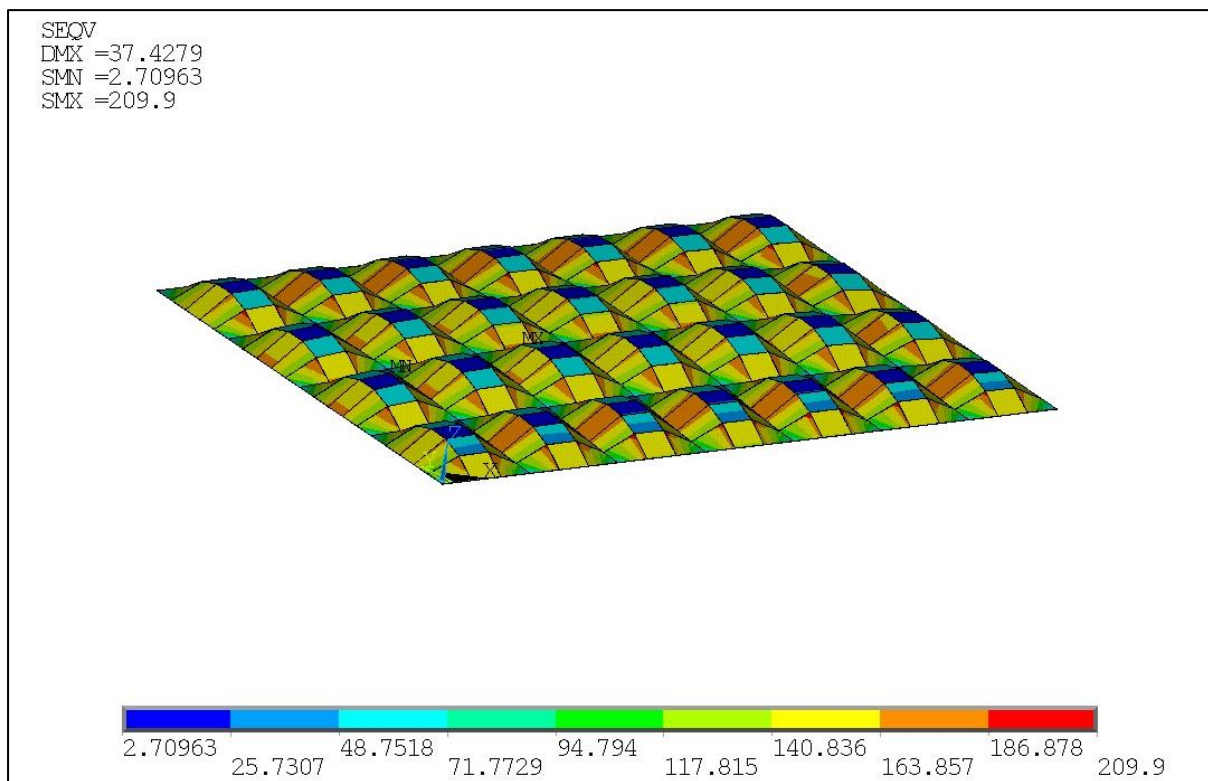


Figure 4.28: Contour plot of Von Mises Stress at Shell Elements. Car Deck. Loading case: Pressure only // HIGH

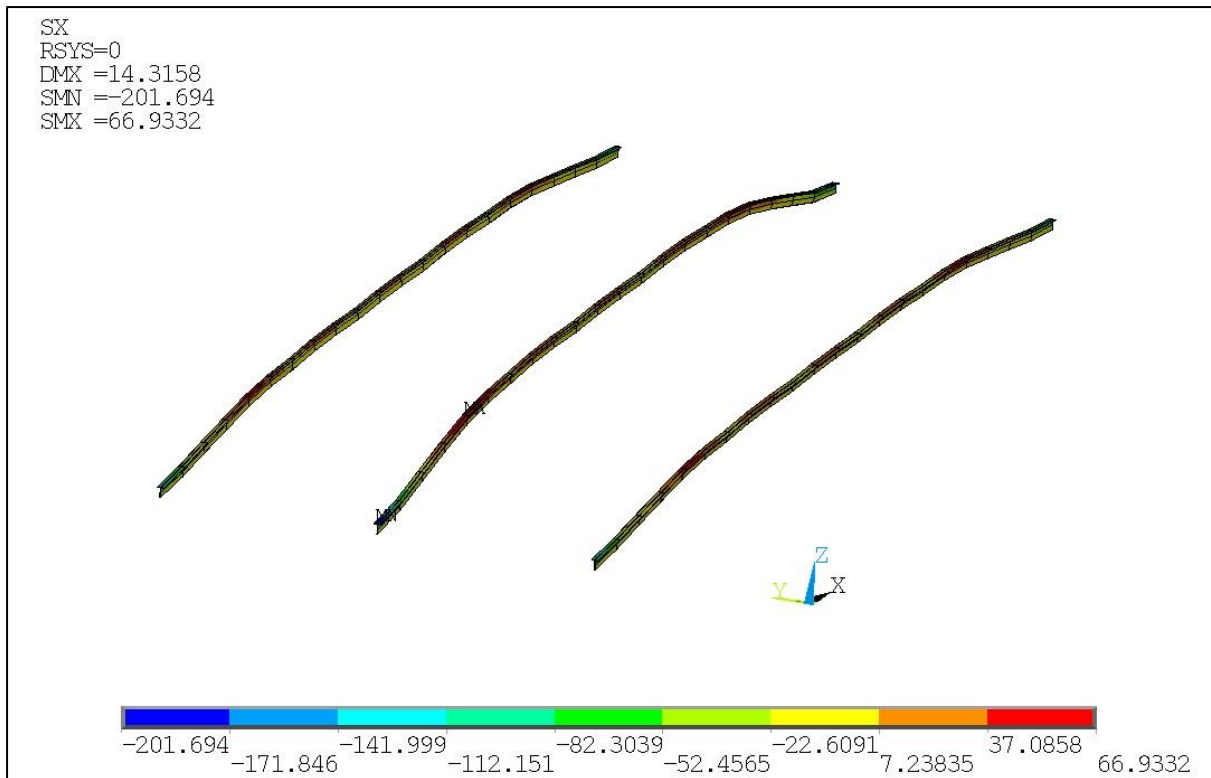


Figure 4.29: Contour plot of Sx Stress at Beam Elements (Longitudinals). Car Deck. Loading case: Pressure only// HIGH

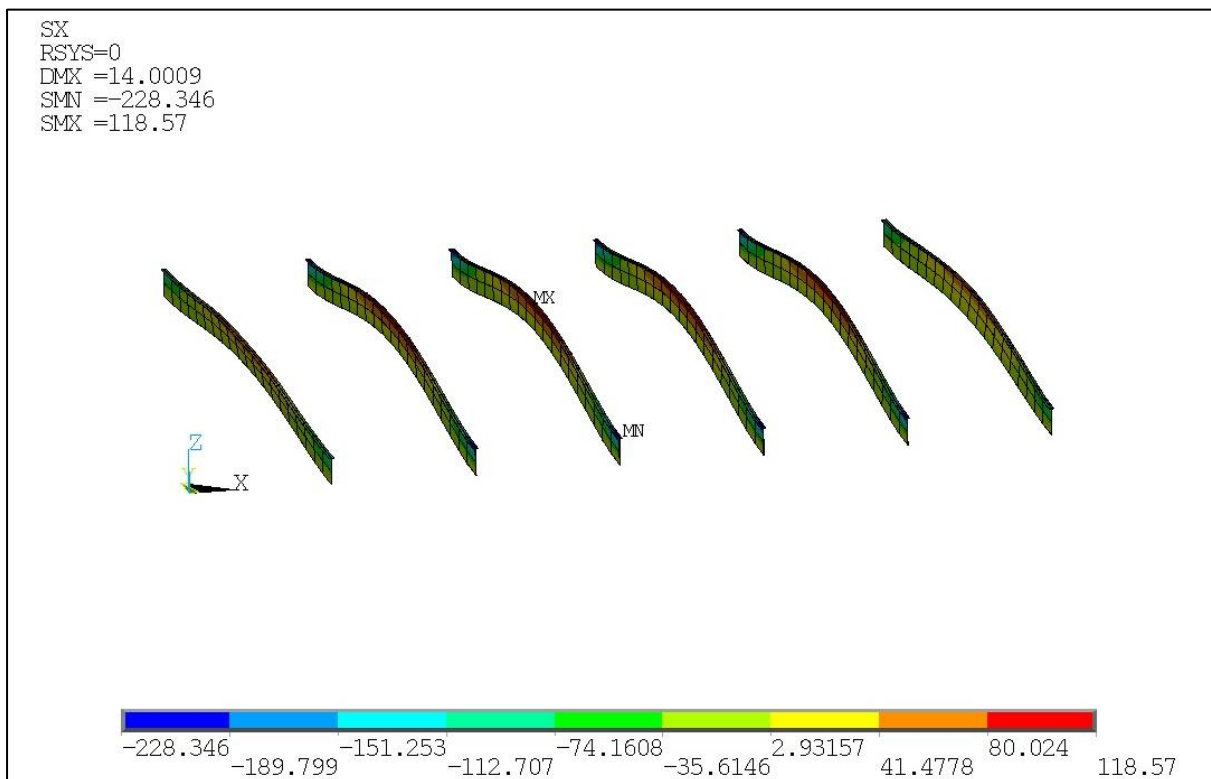


Figure 4.30: Contour plot of Sx Stress at Beam Elements (Transverses). Car Deck. Loading case: Pressure only// HIGH



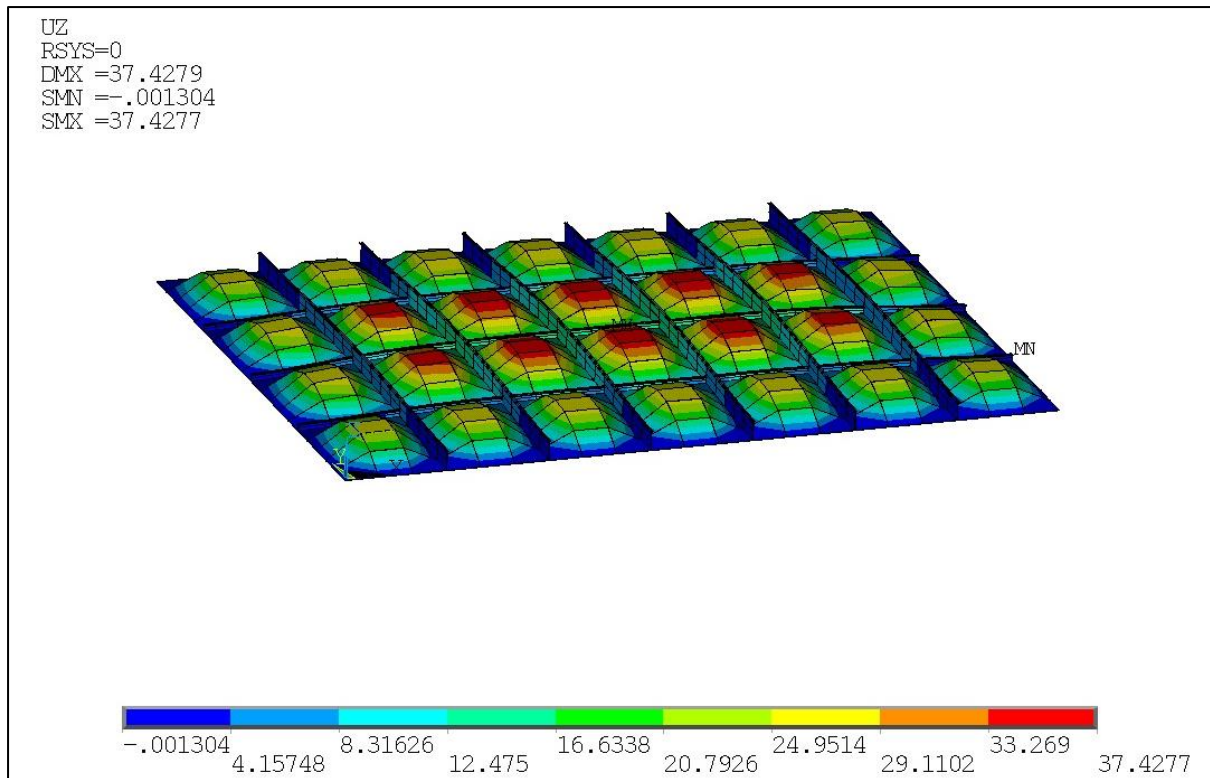


Figure 4.31: Contour plot of vertical Displacement (Uz). Car Deck. Loading case: Pressure only// HIGH

### 2.1 Pressure and stress: LOW

For this case the loading is  $p=1,25$  kPa and  $\sigma=30$  MPa

Table 4.10: Candidate points for Car Deck. Loading case: Pressure and Stress// LOW

Input Variables	Candidate point 1	Candidate point 2	Candidate point 3
<b>nx</b>	0	0	0
<b>ny</b>	4	4	4
<b>t_pl</b>	5	5	5
<b>Stif_type_long</b>	-	-	-
<b>Stif_type_trans</b>	2	2	2
<b>tw_x</b>	-	-	-
<b>hw_x</b>	-	-	-
<b>bf_x</b>	-	-	-
<b>tf_x</b>	-	-	-
<b>tw_y</b>	169	169	169
<b>hw_y</b>	78	68	69
<b>bf_y</b>	6	7	7
<b>tf_y</b>	1	1	1

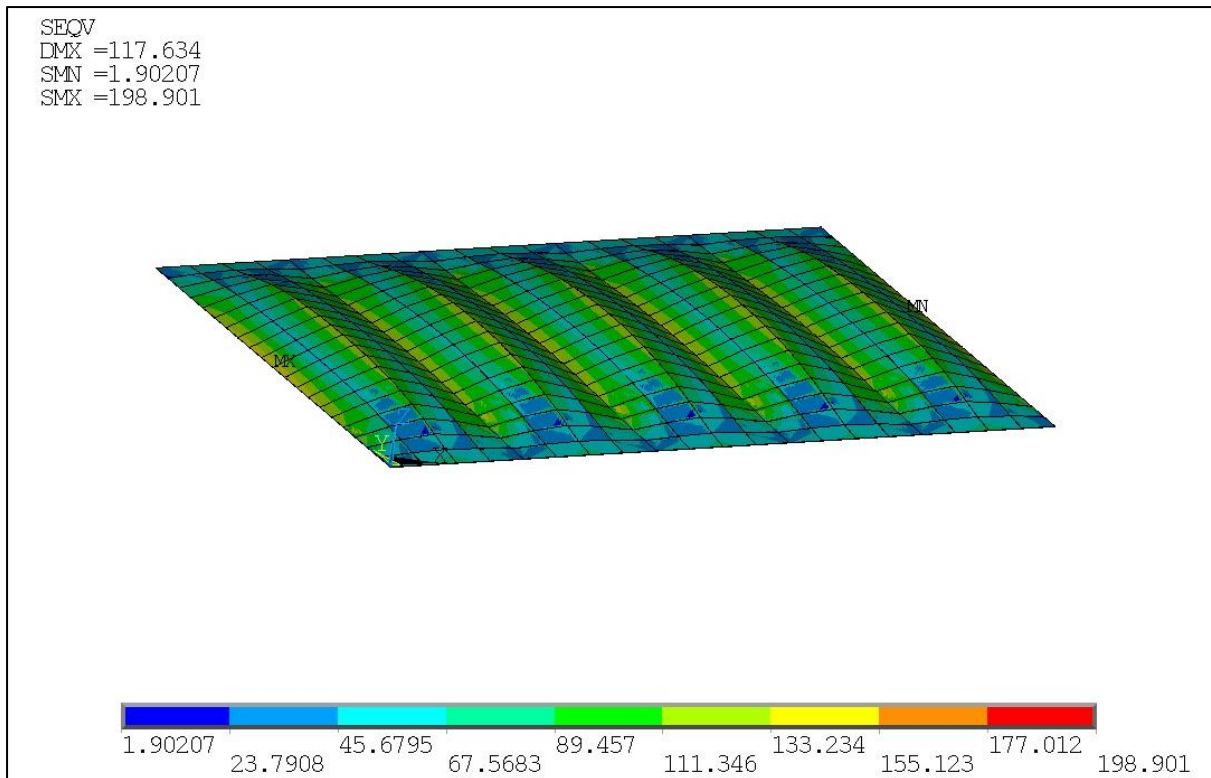


Figure 4.32: Contour plot of Von Mises Stress at Shell Elements. Car Deck. Loading case: Pressure and Stress // LOW

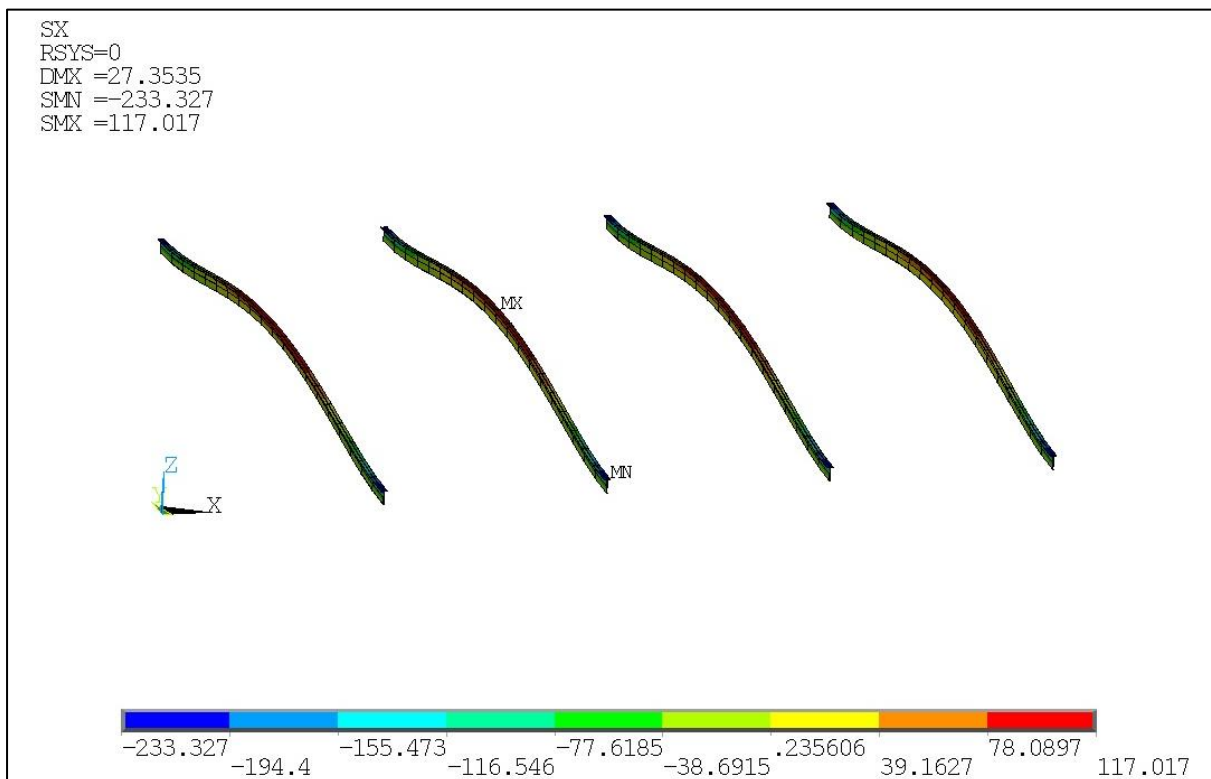


Figure 4.33: Contour plot of Sx Stress at Beam Elements (Transverses). Car Deck. Loading case: Pressure and Stress // LOW

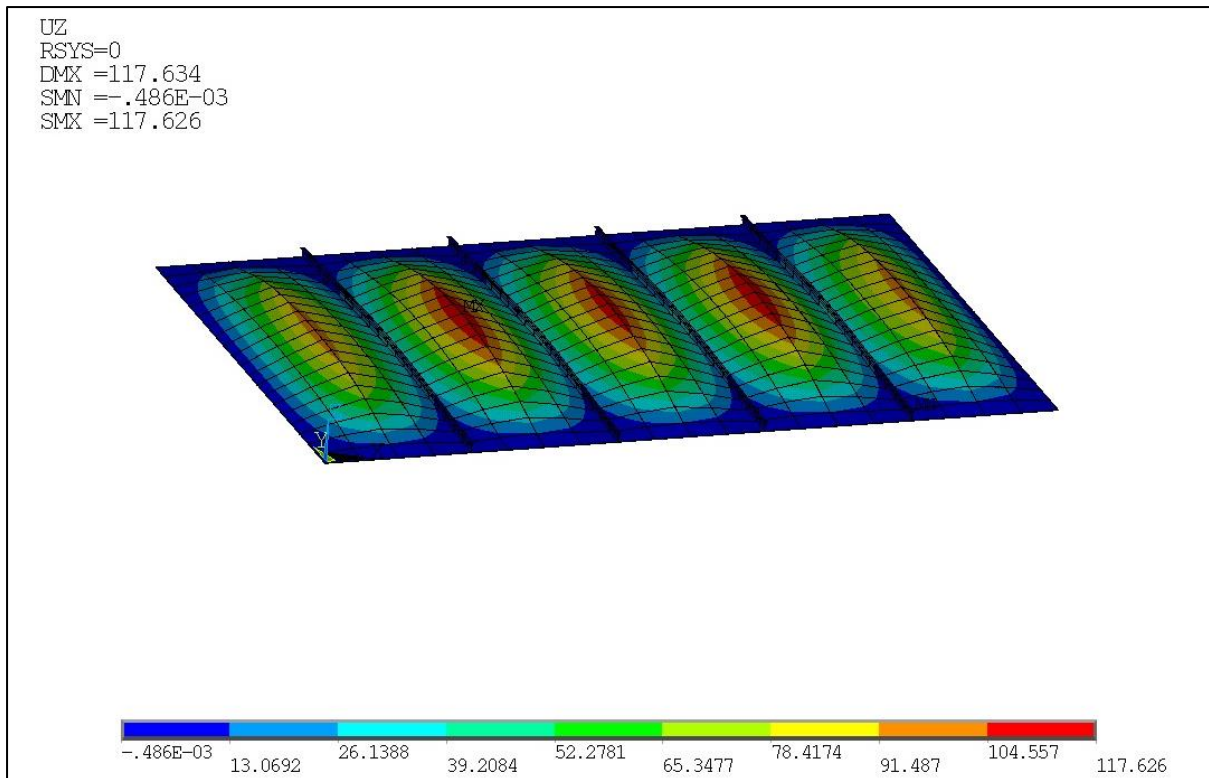


Figure 4.34: Contour plot of vertical Displacement (Uz). Car Deck. Loading case: Pressure and Stress  
// LOW

## 2.2 Pressure and stress: MEDIUM

For this case the loading is  $p=2,5$  kPa and  $\sigma=60$  MPa

Table 4.11: Candidate points for Car Deck. Loading case: Pressure and Stress// MEDIUM

Input Variables	Candidate point 1
<b>nx</b>	4
<b>ny</b>	4
<b>t_pl</b>	5
<b>Stif_type_long</b>	1
<b>Stif_type_trans</b>	2
<b>tw_x</b>	7
<b>hw_x</b>	113
<b>bf_x</b>	-
<b>tf_x</b>	-
<b>tw_y</b>	8
<b>hw_y</b>	190
<b>bf_y</b>	70
<b>tf_y</b>	19

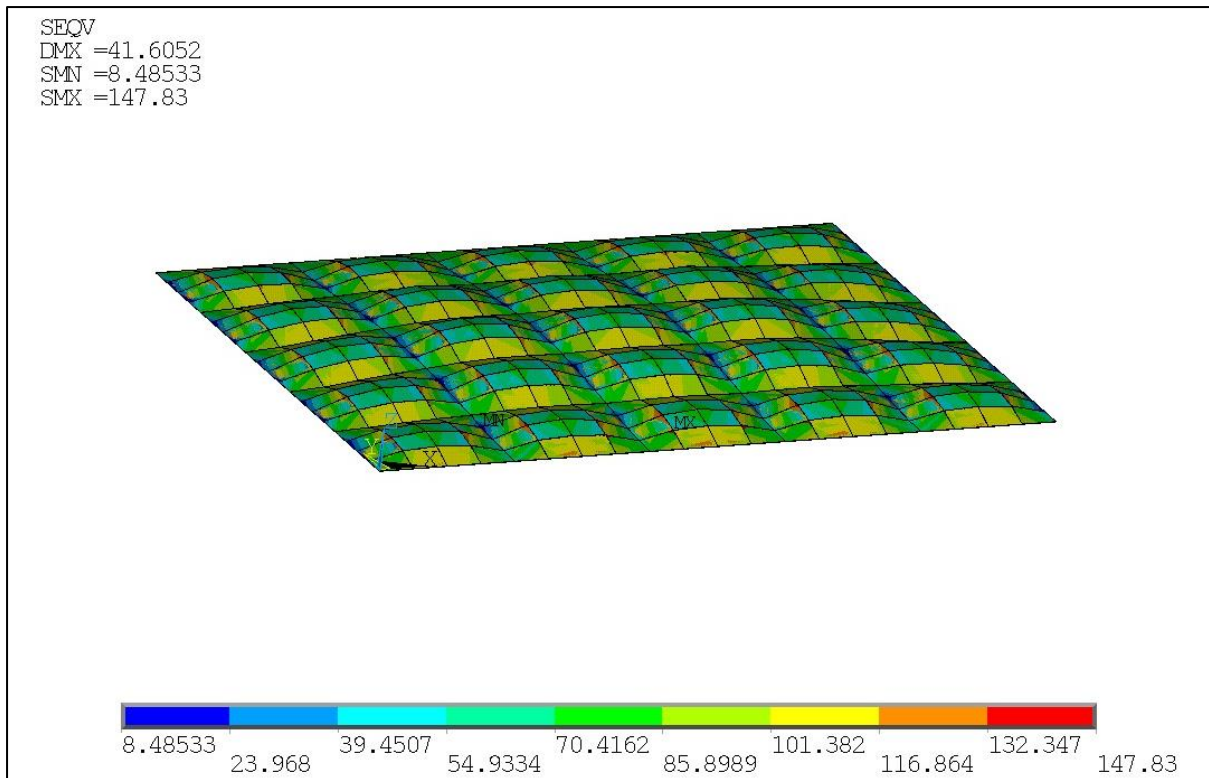


Figure 4.35: Contour plot of Von Mises Stress at Shell Elements. Car Deck. Loading case: Pressure and Stress // MEDIUM

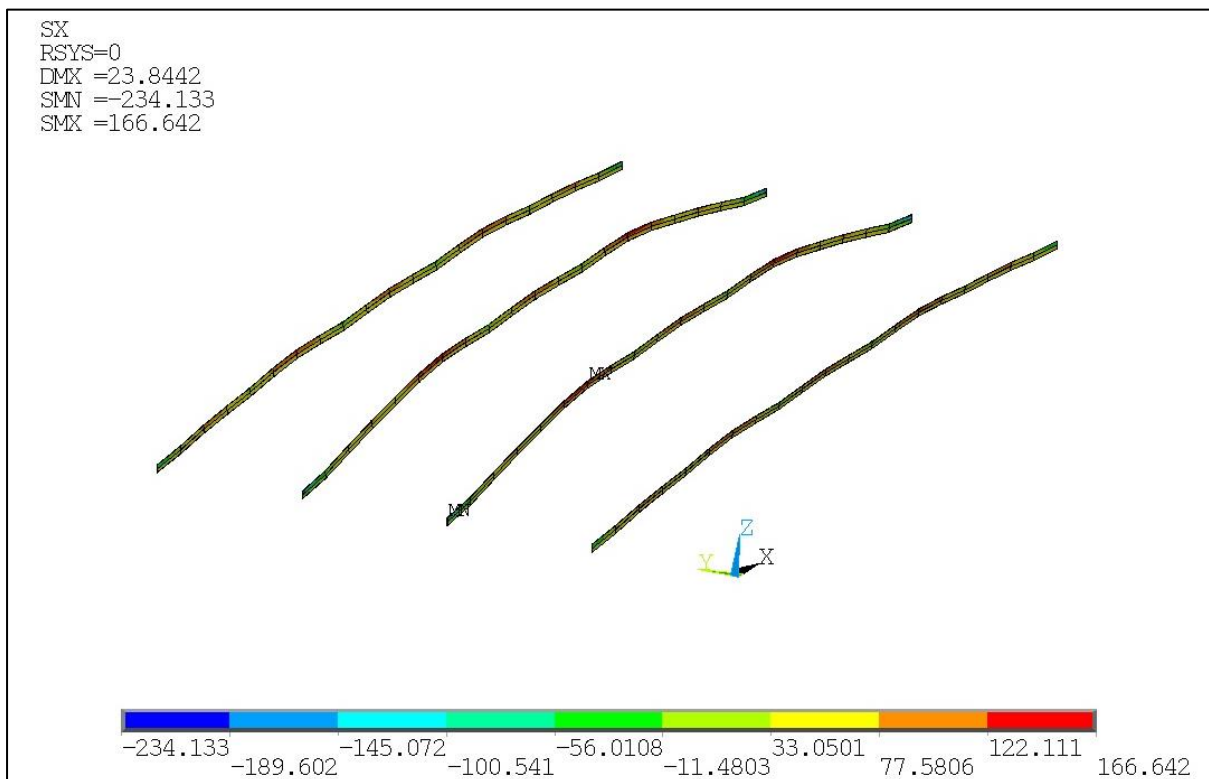


Figure 4.36: Contour plot of Sx Stress at Beam Elements (Longitudinals). Car Deck. Loading case: Pressure and Stress // MEDIUM

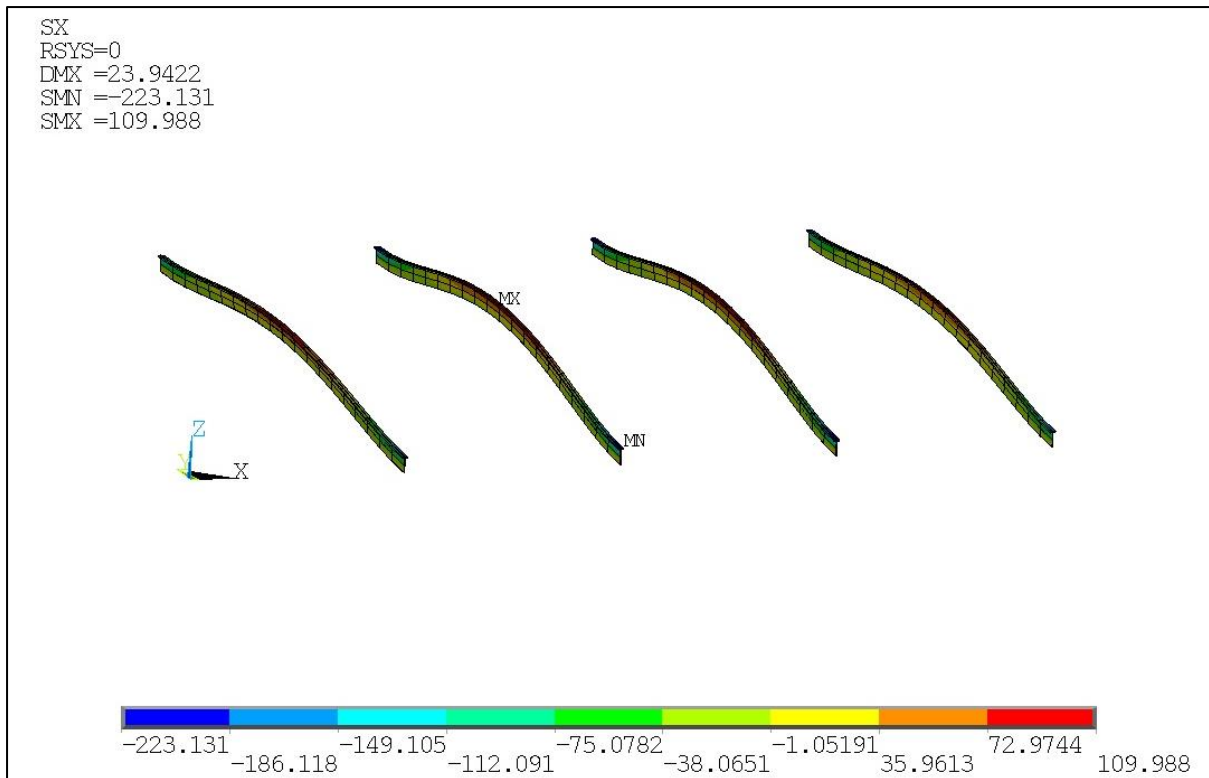


Figure 4.37: Contour plot of Sx Stress at Beam Elements (Transverses). Car Deck. Loading case: Pressure and Stress // MEDIUM

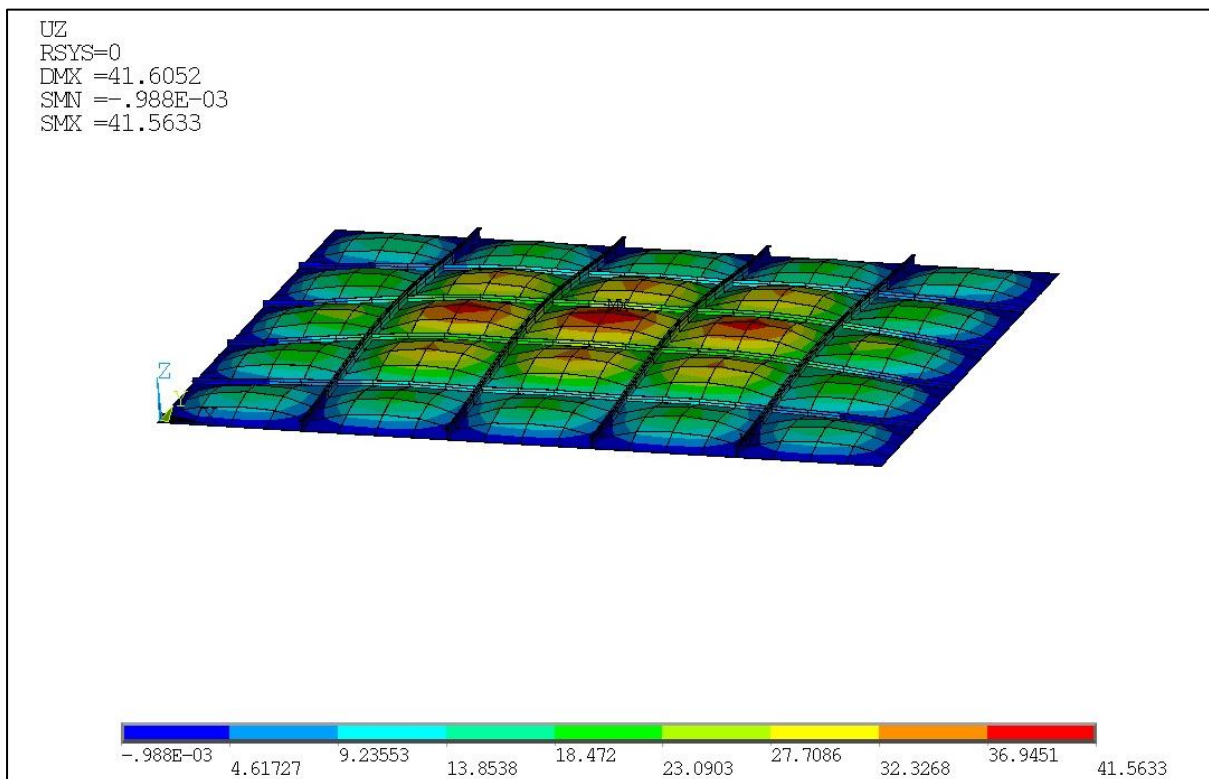


Figure 4.38: Contour plot of vertical Displacement (Uz). Car Deck. Loading case: Pressure and Stress // MEDIUM

### 2.3 Pressure and stress: HIGH

For this case the loading is  $p=5$  kPa and  $\sigma=120$  MPa

Table 4.12: Candidate points for Car Deck. Loading case: Pressure and Stress// HIGH

Input Variables	Candidate point 1	Candidate point 2	Candidate point 3
<b>nx</b>	0	0	0
<b>ny</b>	11	11	11
<b>t_pl</b>	5	5	5
<b>Stif_type_long</b>	-	-	-
<b>Stif_type_trans</b>	2	2	2
<b>tw_x</b>	-	-	-
<b>hw_x</b>	-	-	-
<b>bf_x</b>	-	-	-
<b>tf_x</b>	-	-	-
<b>tw_y</b>	9	9	10
<b>hw_y</b>	188	189	188
<b>bf_y</b>	51	51	51
<b>tf_y</b>	18	18	18

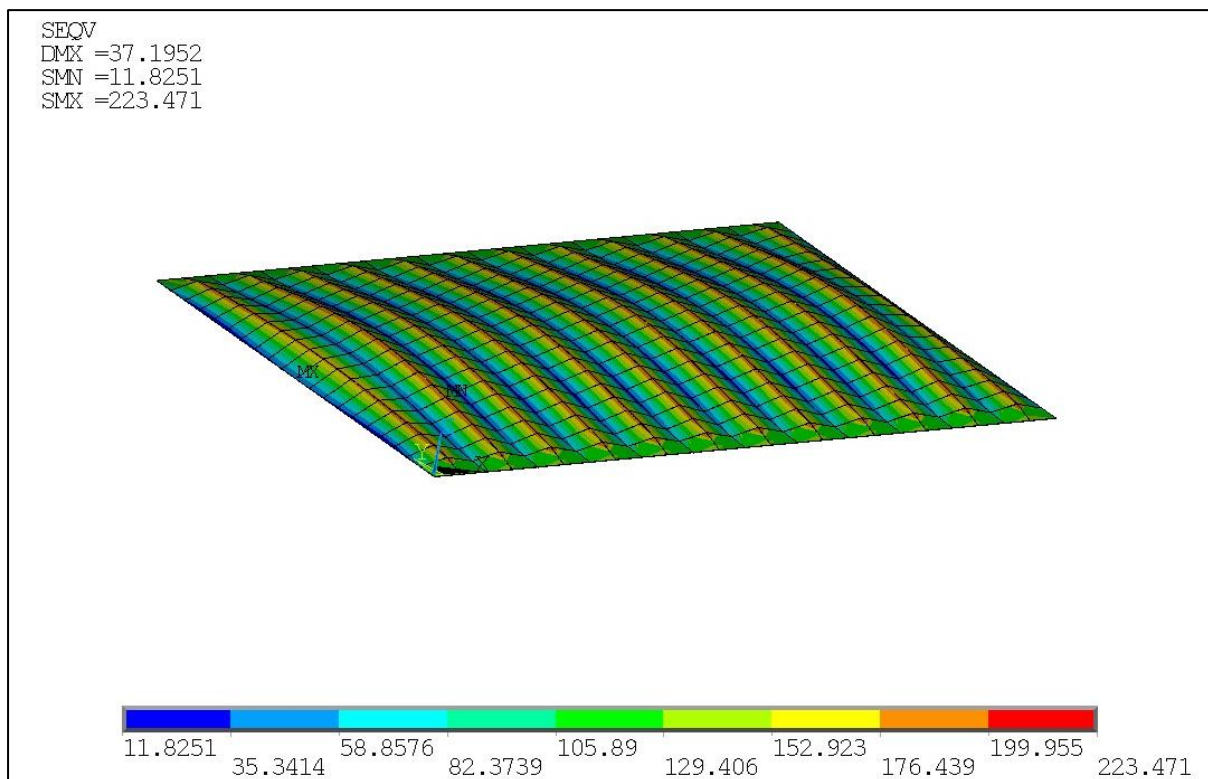


Figure 4.39: Contour plot of Von Mises Stress at Shell Elements. Car Deck. Loading case: Pressure and Stress // HIGH



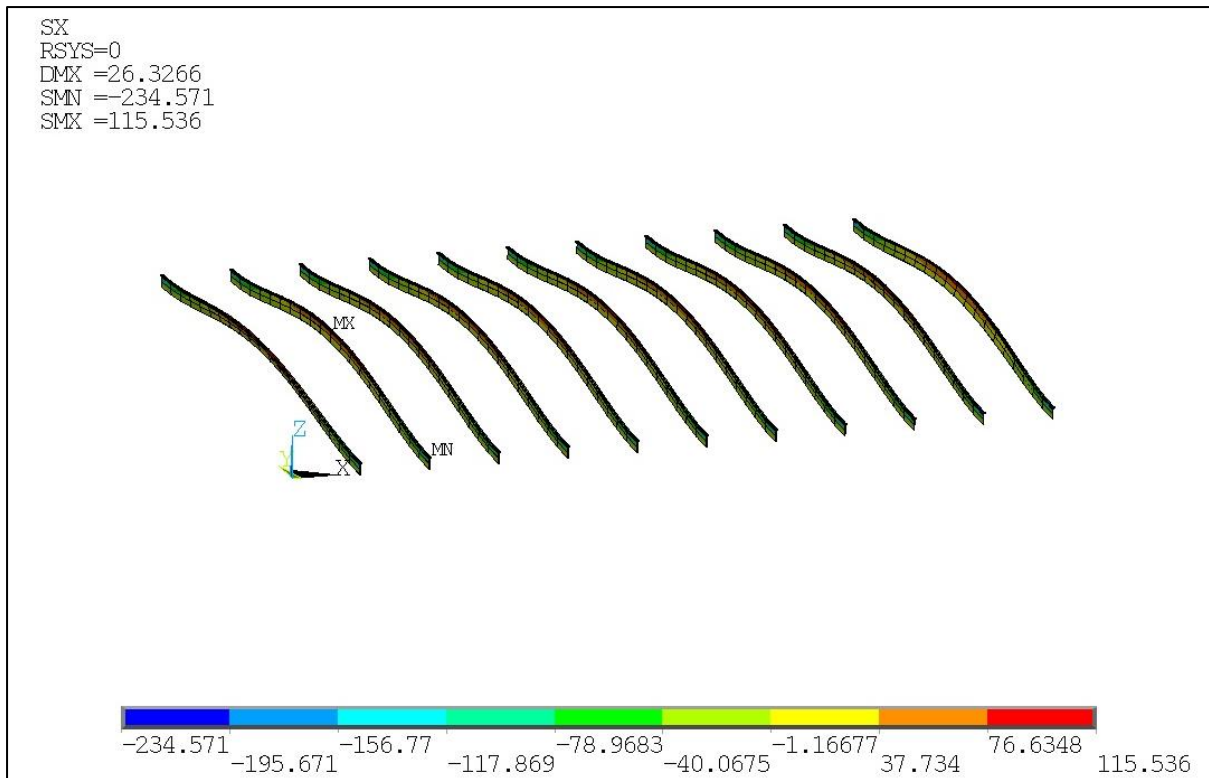


Figure 4.40: Contour plot of Sx Stress at Beam Elements (Transverses). Car Deck. Loading case: Pressure and Stress // HIGH

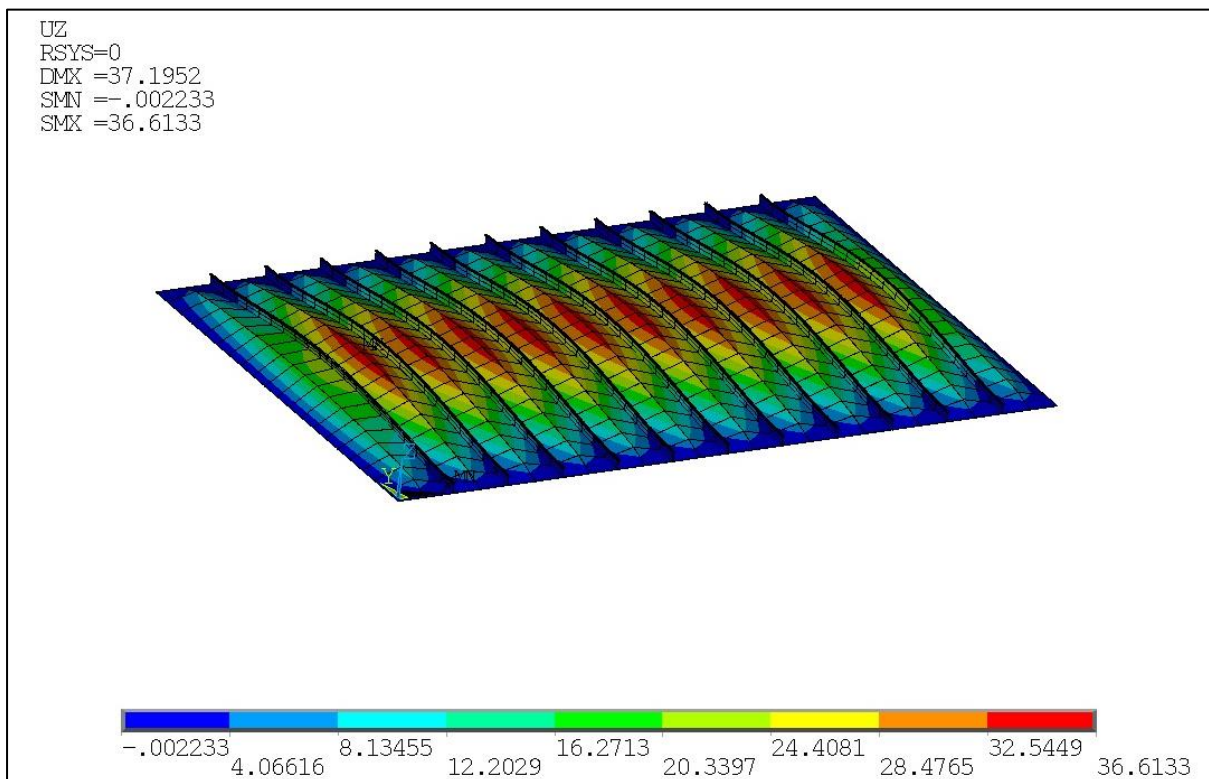


Figure 4.41: Contour plot of vertical Displacement (Uz). Car Deck. Loading case: Pressure and Stress // HIGH

## 5 Conclusions and Future Work

### 5.1 Conclusions

After having presented the optimization results, some comments and potentially valuable remarks towards the interpretation of the results are discussed in this chapter.

Regarding the Small stiffened panel (i.e. 1<sup>st</sup> case), as mentioned previously this is an area found in cargo ships which is traditionally single-stiffened and one would assume that this pattern would be kept during the optimization process as the scantlings and loads were similar to those found at this type of structures. This pattern was preserved at the low and midlevel of loading for example the loading cases *1.1*, *1.2*, *2.1* and *2.2*. Especially, the last case could represent a realistic loading scenario. However, the stiffening of the panels that received only uniform pressure was not along the x-axis (i.e. the axis that  $\sigma_x$  acts), but all the stiffeners were parallel to the y-axis. This could be attributed to the greater length of side b ( $a=2500\text{mm}<b=2850\text{mm}$ ), as if the plate is considered to be comprised of beams of elementary breadth, these beams have a greater unsupported length when being parallel to the y-axis than when being parallel to the x-axis. As, for the panels which received uniform pressure and tensile stress (low and medium levels of intensity), the reinforcement was along the x-axis, which confirms the initial assumption for the stiffeners' configuration. At the high levels of loading intensity ( $p$  and  $p+\sigma$ ), the panel is cross-stiffened as the magnitude of the loading imposes that. As for the section type selected for the stiffeners, it was mainly the flat bars and T-type chosen. Especially, in the high intensity cases, the T-type was chosen both times (i.e. "pressure only" scenario and "pressure and stress" scenario). In addition, at all the loading scenarios it was observed that the optimizer tended to choose a thinner plate design with more stiffeners to compensate for the lack of strength.

With regard to the car deck model (i.e. 2<sup>nd</sup> case), as previously stated this is an area often found in passenger ships which is traditionally cross-stiffened and also more lightly loaded in the vertical direction in comparison with the first case studied, as the pressure exerted by the water is greater than that exerted by vehicles. Due to the apparent bigger size of this plate in comparison with the first case studied, it was expected that the cross-stiffened pattern would be preserved and that expectation was partially confirmed. Except from the low loading scenarios (i.e. *1.1,2.1*) and the heaviest loading scenario (i.e. *2.3*), the latter of which was kind of unexpected, all the other cases of panels had stiffeners lying in both directions. As for the stiffener type mostly chosen, this was again the T-type, which kind of confirms the common design practice of implementing this type of stiffener in most ships of any type. As it is known from the beam theory, this type of stiffener has the greatest moment of inertia with respect to the horizontal axis (for a given sectional area) and that makes it really stiff against bending loads. Furthermore, as observed in the first case too, the optimizer tended to choose a thinner plate design, implementing a greater number of stiffeners in both directions.

Finally, although the model developed in this work was quite simplified, as the loads were chosen quite arbitrarily, no structural degradation was added to the model, etc., two things can be kept as conclusive remarks. The first one is that the T-type of stiffener was the most efficient one, as far as structural weight minimization and structural strength maximization are concerned. The second one is that the design of a cross-stiffened panel comprised of a thinner plate and more stiffeners seems to be more optimal for maximum performance. However, there are two limitations that have to be highlighted here. The first one is that enough thickness for corrosion concerns has to be considered. The second one is that the welding of such a panel requires some minimum thickness in order for the structure to be easily manufacturable and not too expensive.



## 5.2 Suggestions for Future works

In this work, a simple structural subset and particularly a cross-stiffened panel was modeled via the use of FE software, as part of a tool intended to implement structural optimization as a design technique. In future works, this method can be applied to larger and more complex structural assemblies such as a midship, a double-bottom or even to the entire ship. Furthermore, another possible idea could be the employment of different optimization methods and afterwards the comparison of the results produced by those methods regarding sanity of results, convergence and of course computing cost. Finally, another idea to reduce computing cost, which increases proportionately with the complexity of the structure, would be to implement surrogate modeling which would essentially reduce the problem's solution time and hence accelerate the optimization time.

## 6 References

- 1) Anyfantis, K. (2020). *Statics of Naval Structures*. Athens: NTUA.
- 2) Bathe, K.-J. (2014). *Finite Element Procedures (Second Edition ed.)*. Watertown: MA: K.J. Bathe.
- 3) Christensen, P., & Klarbring, A. (2009). *An Introduction to Structural Optimiaztion*. Springer.
- 4) Coello Coello, C., Lamont, G., & Van Veldhuizen, D. (2007). *Evolutionary Algorithms for Solving Multi-Objective Problems (2nd ed.)*. Springer.
- 5) Cook, R. D. (1995). *Finite Element Modeling for Stress Analysis*. John Wiley & Sons, Inc.
- 6) Cook, R. D., Malkus, D. S., Plesha, M. E., & Witt, R. J. (2003). *Concepts and applications of finite element analysis(4th ed.)*. John Wiley & Sons, Ltd.
- 7) Deb, K. (2001). *Multi-Objective Optimization Using Evolutionary Algorithms*. John Wiley & Sons, Inc.
- 8) Hiken, A. (2018, December). The Evolution of the Composite Fuselage: A Manufacturing Perspective. *SAE International Journal of Aerospace*.
- 9) Hughes, O., & Paik, J. (2010). *Ship Structural Analysis and Design*. Jersey City: NJ: The Society of Naval Architects and Marine Engineers.
- 10) IACS. (January 2021). *Common Structural Rules for Bulk Carriers and Oil Tankers*.
- 11) IACS. (Rev. 1 July 2018, July).
- 12) IMO. (2022, January). Retrieved from <https://www.imo.org/en/MediaCentre/HotTopics/Pages/Cutting-GHG-emissions.aspx>
- 13) Luo, Y. (2008). An Efficient 3D Timoshenko Beam Element with Consistent Shape Functions. *Advances in Theoretical and Applied Mechanics*, 3, p. 2.
- 14) Rao, S. (2020). *Engineering Optimization: Theory and Practice (5th ed.)*. John Wiley & Sons, Ltd.
- 15) Stamatelos, D., Labeas, G., & Tserpes, K. (n.d.). Analytical calculation of local buckling and post-buckling behavior of isotropic and orthotropic stiffened panels. *Thin-Walled Structures*.
- 16) Tutorials Point. (2022, February). Retrieved from [https://www.tutorialspoint.com/genetic\\_algorithms/index.htm](https://www.tutorialspoint.com/genetic_algorithms/index.htm)
- 17) Tuswan, T., Zubaydi, A., Budipriyanto, A., & Sujiantanti, S. (2018). Comparative Study on Ferry Ro-Ro's Car Deck Structural Strength by Means of Application of Sandwich Materials. *Proceedings of the 3rd International Conference on Marine Technology*.
- 18) Yu, Z., Amdahl, J., & Sha, Y. (2018). Large inelastic deformation resistance of stiffened panels subjected to lateral loading. *Marine Structures*, 59, p. 2.